Central GPR109A Mediates Neuronal Oxidative Stress and

Pressor Response in Conscious Rats

By

Samar Rezq

April 2016

Director of Dissertation: Dr. Abdel A. Abdel Rahman

Department of Pharmacology and Toxicology, Brody School of Medicine, East Carolina University

The primary goal of this study was to characterize the role of GPR109A in the rostral ventrolateral medulla (RVLM) in blood pressure (BP) regulation and to elucidate the mechanisms involved in the hypertensive response elicited by central GPR109A activation. The central hypothesis of this study was “central GPR109A activation causes neuronal oxidative stress and pressor response via local glutamate/prostaglandins release”. The data provide the first evidence for GPR109A expression in the RVLM, the major cardiovascular regulatory nucleus of the brainstem, and in pheochromocytoma cell line (PC12 cells), used as surrogates of the RVLM neurons. GPR109A co-localization was evident in tyrosine hydroxylase (TH)-expressing neurons and in PC12 cells. The anti-hyperlipidemic drug, nicotinic acid (NA) a known GPR109A agonist that activate the receptor and Ca^{2+}-dependently release prostaglandins (PGs), was used in the study. Our findings demonstrated that intra-RVLM activation of GPR109A receptors with NA produced a robust dose-dependent glutamate-like elevation in sympathetic tone and BP in normotensive conscious male

Sprague Dawley (SD) rats. The pressor response was abolished by prior blockade of the NMDA glutamate receptor (NMDAR) using 2-amino-5-phosphonopentanoic acid (AP5) or the prostanoid EP3 receptor (EP3R) using *N*-[(5-Bromo-2-methoxyphenyl) sulfonyl]-3-[2-(2-naphthalenylmethyl)phenyl]-2-propenamide (L-798106). Further, the NA pressor response was exacerbated by a prior application of the glutamate uptake inhibitor, L-trans-Pyrrolidine-2,4-dicarboxylic acid (PDC). *Ex vivo* studies revealed that intra-RVLM GPR109A activation (NA; 20μg) increased local prostaglandin E2 (PGE2) levels, enhanced RVLM ERK1/2 and nNOS phosphorylation and increased c-Fos immunoreactivity. Further, NA induced oxidative stress in the RVLM of NA-treated rats (increased ROS levels and NADPH oxidase activity and decreased catalase activity). Prior EP3R blockade (L-798106) abrogated the biochemical and the pressor response caused by intra-RVLM NA. NMDAR (AP5) or EP3R blockade similarly abolished NA-mediated pressor response, indicating the involvement of both glutamate and PGE2 in this effect. Selective inhibition of RVLM nNOS (N^{ω}-propyl-L-arginine; NPLA) abolished the intra-RVLM NA-evoked pressor response. Further, NPLA abrogated the GPR109A-mediated increases in RVLM nNOS phosphorylation and c-Fos and ROS levels. Our *in vitro* (PC12) studies supported and extended the in-vivo findings as NA increased Ca^{2+}, PGE2, L-glutamate and NO levels as well as ROS levels in cultured PC12 cells. The increase in L-glutamate level is likely mediated by PGE2/EP3R because L-798106 attenuated NA or PGE2-evoked L-glutamate release. The above-mentioned effects are mediated via GPR109A because the use of the inactive isomer, IsoNA failed to produce any hemodynamic or biochemical changes. Further, NA failed to increase Ca^{2+} or L-glutamate levels in PC12 cells following siRNA-evoked GPR109A knockdown. Collectively, these studies provide insight into identifying the role of central GPR109A activation in cardiovascular regulation in conscious animals and the potential mechanisms involved in this effect.

Central GPR109A Mediates Neuronal Oxidative Stress and Pressor Response in Conscious Rats

A Dissertation

Presented To

The Faculty of the Department of Pharmacology and Toxicology

The Brody School of Medicine at East Carolina University

In Partial Fulfillment

of the Requirements for the Degree of

Doctor of Philosophy in Pharmacology and Toxicology

By

Samar Rezq

April 2016

Central GPR109A Mediates Neuronal Oxidative Stress and

Pressor Response in Conscious Rats

By

Samar Rezq

APPROVED BY:

DIRECTOR OF DISSERTATION: _____

Abdel A. Abdel-Rahman, PhD

COMMITTEE MEMBER: _____

Jacques Robidoux, PhD

COMMITTEE MEMBER: _____

Jamie DeWitt, PhD

COMMITTEE MEMBER: _____

Rukiyah Van Dross-Anderson, PhD

COMMITTEE MEMBER: _____

Ethan J. Anderson, PhD

COMMITTEE MEMBER: _____

Qun Lu, PhD

CHAIR OF THE DEPARTMENT

OF PHARMACOLOGY & TOXICOLOGY: _____

David Taylor, PhD

DEAN OF THE GRADUATE SCHOOL: _____

Paul J. Gemperline, PhD

This work is dedicated to my parents, AbdelMeguid Rezq and Samia Assal and to my husband, Ahmed Nasr. Without your support, love and prayers I could not walk through my path.

ACKNOWLEDGEMENTS

When it comes to appreciation of people who helped me to be at this point of my life, words are not always enough. The idea of being a scientist is to give your expertise and knowledge to your crew and in back, you keep learning every day from their feedbacks and inputs. However, not every researcher is a successful scientist, it needs a lot of study, effort, time and most importantly priceless advice and supervision and this is what I got for being a student at Dr. Abdel A. Abdel-Rahman's lab. Thank you Dr. Abdel-Rahman for your help and support in the past 5 years of my life, starting from your support letter and finishing my papers to start my PhD in just perfect time and continuing to be an example of the perfect mentor whom I learned the scientific thinking and planning and the skilled writing and peer reviewing. Your trust in my abilities and your continuous encouragement was always my leader to continue and succeed, simply because it is hard to let down people who put trust in you.

I would like to thank the members of my committee: Dr. Qun Lu; Dr. Jacques Robidoux; Dr. Jamie DeWitt; Dr. Rukiyah Van Dross and Dr. Ethan Anderson. Your suggestions, inputs and advice are much appreciated.

I would also like to thank my fellow lab members who always gave me their support and answers to my questions and helped me learning the techniques and the hard animal work. Thank you Mrs. Kui Sun; Dr. Yao Fanrong and Dr. Rebecca Steagall for your precious support.

Special thanks to my fellow graduate students and to the faculty and staff in the department of Pharmacology and Toxicology for not hesitating to provide advice, support and expertise and for your open door lab policy. I really enjoyed being a student in this department

and I think I am lucky being surrounded by wonderful people with bright smiley faces who love each other as a family.

Finally, I want to thank my Husband, Ahmed for leaving his work back at home and choosing to be at my side. Without him, it would nearly impossible to get my degree. Grateful thanks to my parents for being the light that gives me kindness, warmness and prayers. Thank you Mom for taking care of my kids during my toughest periods in my study. I would like also to thank my friend Dr. Eman Soliman, and her Husband Dr. Ahmed El-Hassany for their support and help. Eman, I really appreciate your help in advancing my cell culture laboratory experience and sharing in critical thinking to solve cell culture related problem.

TABLE OF CONTENTS

LIST OF TABLES

LIST OF FIGURES

LIST OF SYMBOLS OR ABBREVIATIONS

ACSF: Artificial cerebrospinal fluid

ADN: Adiponectin

AP5: 2-amino-5-phosphonopentanoic acid

BP: Blood pressure

BRS: baroreflex sensitivity

cAMP: Cyclic adenosine monophosphate

CNS: Central nervous system

DAF-FM Diacetate: Difluorofluorescein diacetate

DCFH-DA: 2′, 7′-dichlorofluorescein diacetate

DHE: Dihydroethidium

DMSO: Dimethyl sulfoxide

eNOS: Endothelial nitric oxide synthase

EP3R: EP3 receptor

ICV: Intracerebroventricular

GPCR: G-protein coupled receptor

GPR109A: G-protein coupled receptor 109A

HR: Heart rate

HF: High frequency

iNOS: Inducible nitric oxide synthase

i.p.: Intraperitoneal

ir: Immunoreactive

IsoNA: Iso-nicotinic acid

i.v.: Intravenous

LF: Low frequency

MAP: Mean arterial pressure

MAPK: Mitogen activated protein kinase

NA: Nicotinic acid

MTS: 3-(4,5-dimethylthiazol-2-yl)-5-(3-carboxymethoxyphenyl)-2-(4-sulfophenyl)-2H-tetrazolium

nNOS: Neuronal nitric oxide synthase

NO: Nitric Oxide

NOX: NADPH oxidase

NPLA*:* N^{ω}-Propyl-L-arginine hydrochloride

PC12 cells: Pheochromocytoma cell line

pERK: Phosphorylated extracellular signal-regulated kinase

PGD2: Prostaglandin D2

PGE2: Prostaglandin E2

PGI2: Prostaglandin I2

PGs: Prostaglandins

PVN: Paraventricular nucleus

PKA: Protein kinase A

RRI: RR interval

RVLM: Rostral ventrolateral medulla

TH: Tyrosine hydroxylase

CHAPTER ONE-GENERAL INTRODUCTION

1.1. G-Protein Coupled Receptor 109A

GPR109A (also known as hydroxy-carboxylic acid receptor 2 (HCA_2), HM74a, or NIACR1) is a G protein coupled receptor (GPCR) of the Gi subtype. The receptor is the molecular target for nicotinic acid (NA). NA is taken as a dietary supplement (vitamin B3) or in high doses as anti-hyperlipidemic drug for treating hyperlipidemia and associated cardiovascular disorders (1975; Canner et al., 1986; Carlson, 2005).

1.1.1. Expression and Distribution of GPR109A

GPR109A is widely expressed in white and brown adipose tissue, keratinocytes and various immune cells including monocytes, macrophages, neutrophils and dendritic cells including Langerhans cells (Soga et al., 2003; Tunaru et al., 2003; Wise et al., 2003; Hanson et al., 2010), and likely in microglia (Penberthy, 2009).

1.1.2. GPR109A Ligands

GPR109A can be activated by either endogenous or exogenous ligands. D-ß-hydroxybutyrate (DHB) is the endogenous ligand of GPR109A. DHB reaches the µM-mM concentration range needed to activate GPR109A only under starvation condition to initiate survival homeostatic mechanisms that involves regulating its own production, preventing ketoacidosis, and regulating fat utilization (Taggart et al., 2005).

An increasing number of exogenous ligands for GPR109A receptor are now known among which NA, also known as niacin, is most clinically used. NA is prescribed as anti-hyperlipidemic

medication or as a vitamin supplement. Similar to DHB, NA only activates the receptor, when used in mega doses as anti-hyperlipidemic drug (Brown et al., 2001; Whitney et al., 2005). Representative structures of different GPR109A ligands and their chemical classes are included in **Fig. 1.1.**

Figure 1. 1. GPR109A ligands

Representative exogenous GPR109A ligands and their chemical classes, modified from (Blad et al., 2011).

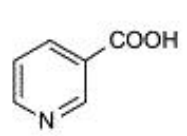

1 (Nicotinic acid)

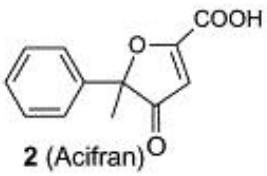

2 (Acifran)

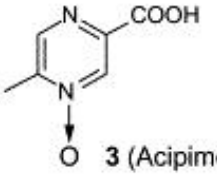

3 (Acipimox)

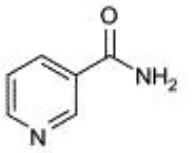

4 (Nicotinamide)

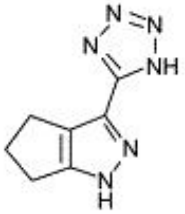

5 (MK-0354)

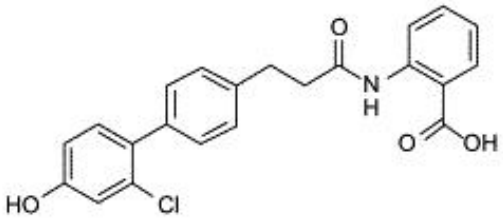

6 (Biphenyl anthranilic acid derivative)

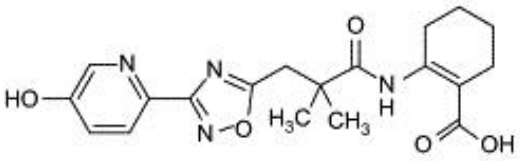

7 (MK-6892)

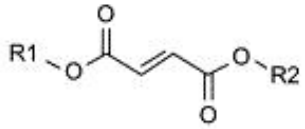

8 (Fumaric acid esters)
R1 = H, R2 = Me: MMF
R1 = H, R2 = Et: MEF

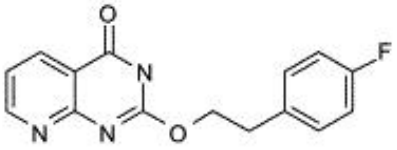

9 (Pyridopyrimidinones)

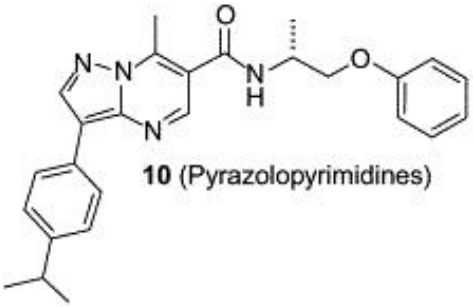

10 (Pyrazolopyrimidines)

1.1.3. Signaling Pathways Mediated Following GPR109A Activation

Activation of GPR109A by its agonist NA was reported to activate or inhibit versatile signaling pathways including but not limited to the reduction in cAMP levels, ERK phosphorylation, PLC/PKC activation and L-type Ca^{2+}channel opening as discussed below.

1.1.3.1. Increase of Intracellular Ca^{2+}

GPR109A receptor activation by its agonists was shown to increase the intracellular levels of Ca^{2+} in a number of cell types, in particular macrophages and epidermal Langerhans cells (Benyo et al., 2005; Benyo et al., 2006; Vanhorn et al., 2012; Gaidarov et al., 2013). This increase is associated with the activation of phospholipase A2 (PLA2) (Lin et al., 1992; Benyo et al., 2006) and subsequent production of different prostaglandins (PGs) including prostaglandin I_2 (PGI_2), prostaglandin E_2 (PGE_2), and prostaglandin D_2 (PGD_2) (Benyo et al., 2005).

1.1.3.2. Inhibition of Adenylyl Cyclase

GPR109A activation results in G_i/G_0 protein-mediated inhibition of adenylyl cyclase, leading to a decreased cAMP levels in a number of cell types (Soga et al., 2003; Tunaru et al., 2003; Zhang et al., 2005). This effect is particularly important in adipocytes as it leads to a reduced protein kinase A (PKA) activity and a decrease in hormone sensitive lipase activity resulting in an inhibition of lipolysis and this is the base of the clinical application of its agonist, NA, as anti-hyperlipidemic drug (Digby et al., 2009).

1.1.3.3. ERK1/2 Phosphorylation.

GPR109A activation by its agonists was reported to enhance ERK1/2 phosphorylation. Niacin or acifran produced this effect in stably transfected CHO-K1 cells in a pertussis toxin-sensitive way (Tunaru et al., 2003; Mahboubi et al., 2006; Tang et al., 2006). Further NA stimulated Gβγ-dependent ERK1/2 phosphorylation in different cell lines (Walters et al., 2009; Li et al., 2011).

1.1.4. NA Pharmacological Effects Mediated by GPR109A

Besides the anti-hyperlipidemic effect that is achieved with chronic NA therapy, a large number of clinical and animal studies reported NA versatile lipid independent beneficial effects. Interestingly, NA has an anti-inflammatory potential in a number of cells including adipocytes, macrophages/monocytes and endothelial cells, most likely due its ability to reduce ROS generation and pro-inflammatory cytokines expression in these preparations (Digby et al., 2009; Ganji et al., 2009; Tavintharan et al., 2009; Digby et al., 2010). Additionally, NA (via GPR109A) (Plaisance et al., 2009) can increase the levels of adiponectin, the cardiovascular protective hormone (Pischon et al., 2004; Schulze et al., 2005). Further, NA was reported to increase hemoxygenase-1 activity resulting in a vascular protective effect (Wu et al., 2012).

1.1.5. Flushing Reaction Associated with NA Therapy

As mentioned above GPR109A activation leads to higher intracellular Ca^{2+} levels that results in the activation of PLA2 and subsequent production of different PGs. PGs through activation of their own receptors, lead to the famous cutaneous flushing reaction associated with

NA therapy (Andersson et al., 1977; Morrow et al., 1989). A number of interventions are available to attenuate this flushing response either by inhibiting PGs synthesis with aspirin (Eklund et al., 1979) or by blocking their receptors using the selective PGD2 antagonist, laropiprant (Paolini et al., 2008).

1.2. Central Cardiovascular Regulation

The heart and blood vessels are subjects to both short and long-term central cardiovascular regulations. The reflex evoked responses from arterial baroreceptors, chemoreceptor or nociceptors contribute mainly to the short-term BP regulation, where's long-term BP control is mainly influenced by behavioral and disease state and usually involves hormonal imbalance, e.g the renin angiotensin system (Dampney et al., 2002). A number of brain areas are involved in central regulation of circulation and the maintenance of baseline arterial pressure. These areas contribute unequally to their effects on the sympathetic outflow to the peripheral system. The brainstem with its cardiovascular regulating nuclei is the principal regulatory site of central sympathetic outflow, among which the rostral ventrolateral medulla (RVLM) is the key regulator of basal BP activity.

1.3. Rostral Ventrolateral Medulla (RVLM) in Central Cardiovascular Regulation

The rostral ventrolateral medulla (RVLM) located in the ventral part of the brainstem, lateral to the inferior olive, caudal to the facial nucleus, and ventral to the nucleus ambiguous (Farlow et al., 1984; Dampney et al., 1987) is considered as the dominant source of excitatory input to the arterial system. It receives inputs from peripheral arterial baroreceptors and

peripheral chemoreceptors as well as from higher regions in the brain including periaqueductal gray, the paraventricular nucleus (PVN) and the caudal ventrolateral medulla (Guyenet et al., 1989; Kishi et al., 2001; Fisher and Paton, 2012). The RVLM contains both adrenergic and noradrenergic neurons (Hokfelt T. et al., 1984). The most important of the RVLM neurons, is a group of neurons called C1 neurons that synthesis adrenaline and release L-glutamate (DePuy et al., 2013). Further, C1 neurons modulate the sympathetic activity by sending excitatory discharges to the spinal cord and hence are involved in BP control (Dampney, 1994; Sved et al., 2003; Guyenet, 2006b).

1.3.1. Different Players that Modulate BP Control in the RVLM

1.3.1.1. Role of Ca^{2+} and Excitatory Amino Acids

L-glutamate is the major neurotransmitter in the cardiovascular nuclei involved in the neuronal control of the sympathetic drive and BP including the RVLM. In The CNS, higher intracellular Ca^{2+} levels can induce different neurotransmitters release including L-glutamate (Kish and Ueda, 1991; Berridge, 1998; Sudhof, 2004). L-glutamate activates fast-acting ionotropic receptors, including NMDA and AMPA receptors whose activation leads to elevations in intracellular Na^{+} and Ca^{2+} and increase nerve firing (Dingledine et al., 1999; Platt, 2007). The increased Ca^{2+} level may lead to excitotoxicity and oxidative stress (Lipton and Rosenberg, 1994). In addition, L-glutamate can competitively inhibit the uptake of cysteine, the precursor of glutathione (GSH), by inhibiting cystine/glutamate antiporter system leading to more oxidative stress (Albrecht et al., 2010). Further, L-glutamate activates metabotropic receptors, which trigger slower intracellular signaling pathways involving secondary messengers, protein kinases,

and phosphatases (Gabor and Leenen, 2012). Activation of both receptor types by locally injected L-glutamate or a glutamate analog leads to increased sympathetic nerve activity (SNA) and a pressor response (Ito et al., 2003). However, in the RVLM, the NMDA receptor-mediated fast and brief pressor response prevails (Kubo et al., 1993)

1.3.1.2. Impact of RVLM Oxidative Stress (Reactive Oxygen Species, ROS) on BP

A number of studies linked higher levels of ROS in the RVLM with hypertension (Zimmerman et al., 2004; Kishi et al., 2008; Koga et al., 2008). There are many triggers that can result in increased ROS levels including Ca^{2+} (Lipton and Rosenberg, 1994), angiotensin II (Zimmerman et al., 2004), increased NADPH oxidase (NOX) activity (Griendling et al., 2000; Bedard and Krause, 2007; Akki et al., 2009; Frey et al., 2009) and decreased activity or expression of superoxide dismutase or catalase (ROS scavenging enzymes) (Dieterich et al., 2000; Chan et al., 2006; Yoshitaka, 2008). The increase in ROS levels inhibits the activity of voltage-gated potassium channels, thereby enhancing action potential propagation and increasing neuronal activity and nerve firing leading to BP increase (Zimmerman et al., 2004; Zucker and Gao, 2005).

1.3.1.3. Role of RVLM ERK1/2-nNOS Pathway in BP Regulation

ERK1/2 activation of nNOS-NO signaling in the RVLM reduces GABA release and elicits sympathoexcitation (Chan et al., 2003; Martins-Pinge et al., 2007). There is also evidence that NO is involved in L-glutamate-mediated neurotransmission in different brain areas (Southam et al., 1991; Montague et al., 1994) including the RVLM (Martins-Pinge et al., 1999). Notably,

higher NO levels can contribute to RVLM oxidative stress via its interaction with elevated superoxide levels to produce peroxynitrite radical (Beckman et al., 1990), which causes dose-dependent transient excitatory responses when injected into the RVLM (Zanzinger, 2002). Conversely, others reported that intra-RVLM injection of NO precursor or donor decreases sympathetic nerve activity and BP (Kagiyama et al., 1997). The mechanisms of these discordant effects remain to be investigated.

1.3.1.4. Role of Prostaglandins

Higher levels of PGE2 in the CNS is shown to be sympathoexcitatory. Intracerebroventricular (ICV) or local PGE2 injection in the hypothalamic paraventricular nucleus is known to: (i) increase the sympathetic outflow/plasma catecholamines and BP in rats, which is not observed with other PGs (Ando et al., 1995; Ariumi et al., 2002; Murakami et al., 2002; Zhang et al., 2011); (ii) cause L-glutamate release in different CNS cell types (Bezzi et al., 1998; Wang et al., 2015); and (iii) induce ROS generation via activating NADPH Oxidase (NOX) activity (Wang et al., 2013a). Further, central (ICV) injection of PGE2 or misoprostol, the prostaglandin EP receptor agonist, increases c-Fos, a marker of neuronal activity (Bullitt, 1990; Morgan and Curran, 1991), expression in different brain areas (Lacroix et al., 1996; Zhang et al., 2011). Despite the critical involvement of the RVLM in central BP regulation, there are no reports on the cardiovascular role of PGs in RVLM.

1.4. Aims of Study

G protein-coupled receptor 109A (GPR109A) activation by its ligand nicotinic acid (NA) in immune cells increases Ca^{2+} and PGs levels (Benyo et al., 2005). Ca^{2+} and high prostaglandin E2 levels (PGE2) via EP3 receptor (EP3R) in the CNS induces L-glutamate release (Guemez-Gamboa et al., 2011; Wang et al., 2013a), and oxidative stress (Lipton and Rosenberg, 1994; Wang et al., 2013a) leading to sympathoexcitation and pressor response. Despite NA ability to reach the brain in appreciable levels following its peripheral administration in the dose range that is commonly prescribed for treating lipid disorders, the expression and function of its receptor GPR109A in the RVLM remains unknown and the cardiovascular consequences of possible central NA actions (via GPR109A activation) are not yet elucidated. Importantly, ROS generation in cardiovascular/sympathetic activity regulating neuronal pool, such as the rostral ventrolateral medulla (RVLM), increases sympathetic activity and BP. Therefore, the present studies tested the central hypothesis that **Ca^{2+}-dependent L-glutamate release and oxidative stress, triggered by NA activation of RVLM GPR109A, causes sympathoexcitation and a pressor response.** Additionally, the current study tested the corollary hypothesis that **RVLM PGE2 activation of EP3R plays a pivotal sympathoexcitatory role and serves intermediary role in the GPR109A-mediated glutamate release and the subsequent biochemical events in the RVLM that ultimately lead to the NA-evoked pressor response.** To test our hypotheses we followed a multi-level approach involving in vivo studies in conscious normotensive male rats along with molecular studies conducted *ex vivo*, and in PC12 cells (exhibit neuronal phenotype) (Okouchi et al., 2005) that were utilized as surrogates to RVLM neurons to perform

experiments that were unachievable in vivo due to limited tissue amounts obtained from the RVLM of treated and control rats**.**

Specific Aim 1: Experiments firstly examined the expression of GPR109A in the RVLM and in PC12 cells and its spatial distribution in relation to tyrosine hydroxylase immunoreactive (TH-ir) (pre-sympathetic) neurons. Second, the studies under this aim elucidated the cardiovascular function of RVLM GPR109A by testing the hypothesis that the NA-evoked pressor response is GPR109A-dependent.

Rationale: There are no reports on the expression of GPR109A protein in the brainstem cardiovascular regulating nuclei including the RVLM. Therefore, the first objective of the studies outlined under this aim was to determine whether GPR109A is expressed in the RVLM and in PC12 cells , and its spatial distribution in the RVLM relative to different cell types, particularly TH-ir neurons, which modulate the sympathetic activity and BP (Guyenet, 2006a; Kumagai et al., 2012). The preliminary hemodynamic studies have shown that activation of RVLM GPR109A leads to a pressor response associated with a decrease in the HR. Therefore, the studies under this aim investigated the dose dependent effect of NA on different hemodynamic and autonomic parameters that are involved in peripheral BP regulation by addressing the following questions:

1- Is GPR109A expressed within the RVLM and in PC12 cells?
2- What is the spatial distribution in the RVLM relative to different cell types (neuronal and glial cells), particularly TH-ir neurons?

3- Does intra-RVLM administration of the GPR109A ligand, NA, produce dose-dependent cardiovascular and autonomic effects that are GPR109A dependent?

Specific Aim 2: Studies under this aim tested the hypothesis that NA activation of RVLM GPR109A increases intracellular Ca^{2+} levels that lead to L-glutamate (NMDAR)-dependent oxidative stress and sympathoexcitation/pressor response.

Rationale: In the CNS, higher intracellular Ca^{2+} levels enhance neurotransmitters release, including L-glutamate (Kish and Ueda, 1991; Berridge, 1998; Sudhof, 2004). Our preliminary BP findings indicating a sharp L-glutamate-like increase in BP following intra-RVLM NA injection. Realizing that NA activation increases intracellular Ca^{2+} in other cell types (Benyo et al., 2006), it is likely that access of NA to central GPR109A might produce a similar effect and triggers L-glutamate release in the RVLM, which is Ca^{2+}-dependent (Tingley and Arneric, 1990). L-glutamate activation of fast-acting ionotropic receptors, including NMDA and AMPA receptors increases intracellular Na^{+} and Ca^{2+} as well as nerve firing (Dingledine et al., 1999). While the L-glutamate activation of the central ionotropic or the metabotropic receptors (Gabor and Leenen, 2012) causes sympathoexcitation and a pressor response (Ito et al., 2003), the NMDA receptor (NMDAR)-mediated fast and brief pressor response prevails in the RVLM (Kubo et al., 1993). Further, elevations in Ca^{2+} (Lipton and Rosenberg, 1994) and L-glutamate (Albrecht et al., 2010) levels lead to oxidative stress, and the occurrence of the latter in the RVLM leads to sympathoexcitation and pressor response (Nishihara et al., 2012). The studies under this aim are the first to elucidate the ability of NA to induce L-glutamate release associated with oxidative stress and sympathoexcitation in the RVLM following GPR109A activation by addressing the following questions:

1. Does NA increase Ca^{2+} levels in neuronal preparations? And is this effect GPR109A dependent?
2. Does NA induce L-glutamate release following GPR109A activation?
3. What is the effect of prior NMDA (AP5) and non NMDA L-glutamate receptors blockade (CNQX) or L-glutamate uptake inhibition (PDC) on GPR109A (NA)-mediated pressor response?
4. What is the role of ROS and NO in GPR109A (L-glutamate)-mediated pressor response?

Specific aim 3: The aim of these studies was to elucidate the role of PGs, in particular PGE2 via EP3R activation, in the molecular mechanisms for the RVLM GPR109A (NA) mediated pressor response in conscious rats, which focused on: NA-mediated increases in L-glutamate release, RVLM neuronal/sympathetic activity (c-Fos expression, p-ERK1/2 and p-nNOS levels), and oxidative stress (increased ROS levels, enhanced NOX activity and reduced catalase activity).

Rationale: The most common side effect of NA is the flushing reaction due to Ca^{2+}-dependent release of different PGs including prostaglandin I_2 (PGI_2), prostaglandin E_2 (PGE_2), and prostaglandin D_2 (PGD_2) (Benyo et al., 2005). Centrally, ICV or local PGE2 injection in the hypothalamic PVN increases the sympathetic outflow/plasma catecholamines and BP in rats, which is not observed with other PGs (Ando et al., 1995; Ariumi et al., 2002; Murakami et al., 2002; Zhang et al., 2011). PGE2 also causes L-glutamate release in different CNS cell types (Bezzi et al., 1998; Wang et al., 2015), and induces ROS generation via activating NADPH Oxidase (NOX) activity (Wang et al., 2013a). Further, central (ICV) injection of PGE2 or misoprostol, the prostaglandin EP receptor agonist, increases c-Fos, a marker of neuronal

activity, levels (Bullitt, 1990; Morgan and Curran, 1991) in different brain areas (Lacroix et al., 1996; Zhang et al., 2011). Four subtypes of prostanoid receptors (EP1, EP2, EP3, and EP4) are known to mediate the responses of PGE2 (Narumiya et al., 1999), among which EP_3 receptor (EP3R) mediates the central cardiovascular excitatory effects and renal sympathetic nerve activity of PGE_2 (Ariumi et al., 2002; Zhang et al., 2011). Notably, the reported EP3R-dependent activation of ERK1/2 (Chuang et al., 2006; Nicola et al., 2008) could be an important mediator of sympathetic excitation because ERK1/2 activation of nNOS-NO signaling in the RVLM reduces GABA release and elicits sympathoexcitation (Chan et al., 2003; Martins-Pinge et al., 2007). Despite this knowledge, the role of EP3R in RVLM BP regulation has not been yet investigated perhaps due lack of information on EP3R expression in the RVLM. Therefore, experiments under this aim determined, for the first time, if EP3R is expressed in the RVLM, its role in BP regulation and the possible intermediary role of released PGE_2 and the activation of RVLM EP3R in GPR109A (NA)-mediated sympathoexcitation and pressor response by addressing the following questions:

1- Is EP3R expressed in the RVLM and in its surrogate cell line (PC12 cells)? Does intra-RVLM GPR109A activation increase PGE2 levels in the RVLM and in PC12 cells?
2- Does intra-RVLM PGE2 increase BP via EP3R activation? Is this pathway implicated in NA-mediated pressor response?
3- Does RVLM GPR109A activation lead to PGE2/EPR3R-dependent increase in L-glutamate release, neuronal activity (c-Fos), oxidative stress (increased NOX activity and

decreased catalase activity)? Are these biochemical effects dependent on ERK1/2/nNOS phosphorylation?

4- Does nNOS inhibition using the selective nNOS inhibitor, N^{ω}-Propyl-L-arginine hydrochloride (NPLA) protect against NA-mediated adverse biochemical changes in the RVLM and the subsequent pressor response?

Collectively, the findings of the present study provide the first comprehensive in vivo and *ex vivo* evidence for the role of central GPR109A in central regulation of BP in conscious normotensive rats, elucidating the different molecular mechanisms implicated in this effect, and the clinical relevance of the findings. The latter is supported by identifying pharmacological interventions for mitigating the NA-evoked pressor response.

CHAPTER TWO-MATERIALS AND METHODS

2.1. Preparation of the Rats

Male Sprague Dawley (SD) rats (320–370 g; Charles River Laboratories, Raleigh, NC) were used in this study. Five days before the experiment, the animals were anesthetized using ketamine (9mg/100 g) and xylazine (1mg/100 g) mixture i.p. followed by femoral artery catheterization using a 5-cm PE-10 tube connected to PE-50 tubing filled with heparinized saline (heparin 200 units/ml) for measurement of blood pressure (BP) and heart rate (HR) as in our previous studies (Zhang and Abdel-Rahman, 2002b). Next unilateral stereotaxic insertion of a 23-guage stainless steel guide cannula (Small Parts, Miami, FL, USA) was performed to permit microinjection into the RVLM (posterior -2.8 mm, lateral $\pm$ 2.0 mm, dorsoventral -0.5 mm) (Paxinos and Watson, 2005). The cannula was secured to the skull with dental cement (Durelon; Thompson Dental Supply, Raleigh, NC, USA); pre- and post-operative buprenorphine (0.03 mg/kg) was used. At the end of the experiment, the position of the cannula was confirmed histologically following intra-RVLM injection of fast green dye (EM Sciences, Cherry Hill, NJ). These procedures are detailed in our recent study (Penumarti and Abdel-Rahman, 2014).

2.2. Blood pressure (BP) and heart rate (HR) measurements.

Blood pressure (BP) and heart rate (HR) measurements in conscious unrestrained rats were conducted using ML870 (PowerLab 8/30) system and displayed and analyzed by LabChart (v. 7) pro software (AD Instruments, Colorado Spring, CO) as in our reported studies (Ibrahim and Abdel-Rahman, 2011; Nassar et al., 2011; Penumarti and Abdel-Rahman, 2014). BP and HR were allowed to stabilize in the conscious unrestrained rats at baseline, for at least 30 min, followed by intra-RVLM microinjections of a constant volume (80nl) of different treatments

through a 30-guage stainless steel injector. At the end of BP recording period, animals were euthanized with a lethal dose of pentobarbital sodium (>100 mg/kg). For DHE ROS and immunofluorescence measurements, serial frozen brainstem sections (20 μm) containing the RVLM rostrally from -12.8 to -11.8 mm relative to bregma (Paxinos et al., 1980) were cut at −24°C with a microtome cryostat (HM 505 E; Microtome International GmbH, Walldorf, Germany). For other different biochemical measurements, a 0.75 micropunch instrument was used to collect micropunches (Stoelting Co., Wood Dale, IL) from the injected RVLM site (*n* = 4–5 each).

2.3. Cell Culture

Rat neuronal pheochromocytoma cell line (PC12 cells) was purchased from ATCC (Rockville, MD). Cells were grown in F12k medium supplemented with horse serum (15%), fetal bovine serum (2.5%), penicillin (100U/ml), and streptomycin (100U/ml) at 37°C in a humidified incubator with 95% air and 5% CO2. The cells were cultured on corning cell bind flasks for proper adherence followed by treatment with nerve growth factor (50ng/ml) until completely differentiated to the neuronal phenotype according to the protocol of the supplier. Passage was done every 3-5 days when cells reach confluence as in our previous studies (Zhang et al., 2001).

2.4. Immunofluorescence

Colocalization studies in the RVLM were conducted according to the protocol used in our previous reports (Wang and Abdel-Rahman, 2005; Ibrahim and Abdel-Rahman, 2012). Coronal

brainstem sections (20 μm) containing the RVLM from frozen brains of naïve untreated rats (*n* = 6) (rostrally from −12.8 to −11.8 mm relative to bregma) (Paxinos et al., 1980) were cut followed by fixation in 4% paraformaldehyde in PBS for 20 min. The sections were then washed with Tris-buffered saline (TBS) and incubated with blocking buffer (TBS buffer containing 0.2% Tween 20 and 0.2% triton-X (TBST) and 10% normal donkey serum) at 4 °C for 2 hrs then with mixtures of rabbit anti-GPR109A (1:200; Santa Cruz Biotechnology, CA, sc-134583) and one of the following antibodies: mouse anti-tyrosine hydroxylase (MAB318), mouse anti-GFAP (MAB360), mouse anti-NeuN (MAB377) (1:200; EMD Milipore, Temecula, CA) or mouse anti-CD11b/c (1:200; Abcam, Cambridge, MA, ab1211) for 48 hrs at 4°C. Dual-labeling immunofluorescence was revealed by incubation for 2 h in a mixture of fluorescein isothiocyanate-conjugated donkey anti-rabbit and Cy5-conjugated donkey anti-mouse (1:200; Jackson Immunoresearch Laboratories Inc., West Grove, PA). For TH-ir and c-Fos-ir neurons colocalization studies, sections from frozen brains of rats received different treatment (*n* = 5-7) were incubated for 48 h hrs at 4°C in a mixture of mouse anti-TH (1:200; EMD Milipore, Temecula, CA) and rabbit polyclonal anti-c-Fos antibody (1:200; Santa Cruz Biotechnology, CA). Dual-labeling immunofluorescence was revealed by incubating the sections for 2 h in a mixture of Cy3-conjugated donkey anti-mouse and fluorescein isothiocyanate-conjugated donkey anti-rabbit (1:200; Jackson Immunoresearch Laboratories Inc., West Grove, PA). Negative controls (leaving out the primary or secondary antibody) as well as single labeled controls were used to confirm the lack of nonspecific staining. Four to six sections per animal at the level of RVLM were examined.

PC12 cells were cultured on coverslips, washed with cold PBS and fixed with 4% paraformaldehyde for 30 min, incubated with permeabilization buffer (0.1% Triton X-100 in 1xPBS) for 10 min, and then blocked with blocking buffer (1X TBS + 1% Bovine serum albumin + 5% normal donkey serum+ 0.2% Tween20) for 2 hrs. The blocked cells were then incubated with a mixture of rabbit anti-GPR109A (1:200; Santa Cruz Biotechnology, CA) and mouse anti-tyrosine hydroxylase (1:200; EMD Milipore, Temecula, CA) for 24 hrs at 4°C. Immunofluorescence was revealed by incubation for 2 hrs in a mixture of fluorescein isothiocyanate-conjugated donkey anti-mouse and Cy3-conjugated donkey anti-rabbit (1:200; Jackson Immunoresearch Laboratories Inc., West Grove, PA). A Zeiss LSM 510 confocal microscope (Carl Zeiss Inc., Thornwood, New York) was used for the visualization, and acquisition of the images at the same brightness and contrast settings. Zen Lite 2011 software was used for quantification of protein co-localization as in our previous studies (Ibrahim and Abdel-Rahman, 2011).

2.5. Western Blot Analysis

Animals received a lethal dose of ketamine-xylazine mixture (i.p.), brains were removed, flash frozen in 2-methylbutane on dry ice, and stored at -80°C until use. Brains were equilibrated to -20°C and coronal sections containing the RVLM were obtained with a cryostat (HM 505E; Microm International GmbH, Waldorf, Germany) according to atlas coordinates (Paxinos and Watson, 2005). Tissues from the RVLM were collected bilaterally using a 0.75 mm punch instrument as described in other studies (Ibrahim and Abdel-Rahman, 2011; Penumarti and Abdel-Rahman, 2014) from approximately -12.8 to -11.8 mm relative to bregma (Paxinos and

Watson, 2005). Tissues were homogenized on ice by sonication in cell lysis buffer (20 mM Tris pH 7.5, 150 mM NaCl, 1 mM EDTA, 1 mM EGTA, 1% Triton X-100, 2.5 mM sodium pyrophosphate, 1 mM β-glycerolphosphate, 1 mM activated sodium orthovanadate) containing a protease inhibitor cocktail (Roche Diagnostics, Indianapolis, IN). PC12 cells freshly subcultured in 6-well plates were lysed using the same cell lysis buffer used for brain tissues and the total cell lysates were used for the assay. Protein concentration in samples was quantified using a standard Bio-Rad protein assay system (Bio-Rad Laboratories, Hercules, CA). Protein extracts (20 μg per lane) were denatured at 97°C for 5 minutes, separated on NuPAGE Novex Bis-Tris 4 to 12% SDS-PAGE gels (Invitrogen, Carlsbad, CA) using MOPS NuPAGE running buffer, and electroblotted to nitrocellulose membranes using standard procedures. Nonspecific binding sites on the membranes were blocked at room temperature in Odyssey blocking buffer (Li-Cor, Lincoln, NE). For GPR109A receptor expression, membranes containing proteins from RVLM, PC12 cells, liver (negative control) and spleen (positive control) were incubated overnight with rabbit anti-GPR109A (1:500; Santa Cruz Biotechnology, CA) and mouse anti-GAPDH (1: 10,000; Abcam, Inc., MA) at 4°C. For EP3R expression, membranes containing proteins from RVLM, PC12 cells and kidney (positive control) were incubated with anti EP3R polyclonal antibody (1:500; Cayman, Ann Arbor, MI) and mouse anti-βactin (1:500; Abcam, Inc., MA) at 4°C overnight. The band was verified using EP3R antibody blocking peptide (1:500; Cayman, Ann Arbor, MI). For ERK1/2 and nNOS measurements, membranes containing equal amounts of RVLM protein from rats received different treatments were incubated overnight at 4°C with a mixture of rabbit anti-phospho-nNOS (Ser1417) antibody (1:500; Thermo Fisher Scientific, Waltham, MA) or rabbit anti-ERK1/2 (1:500; Cell Signaling, Danvers, MA) and mouse

polyclonal anti-nNOS antibody (1:500; BD Biosciences, San Jose, CA) or mouse anti-p-ERK1/2 (1:500; Cell Signaling, Danvers, MA). Membranes were washed four times with phosphate-buffered saline (PBS) containing 0.1% Tween 20 then incubated for 60 min with mixture containing IRDye680-conjugated goat anti-mouse and IRDye800-conjugated goat anti-rabbit (1:10000; LI-COR Biosciences). Bands representing phosphorylated and total protein were detected simultaneously by using Odyssey Infrared Imager and analyzed with Odyssey application software version (LI-COR Biosciences). Data represent mean values of integrated density of different bands normalized to GAPDH or β-actin. For ERK1/2 and nNOS phosphorylation, the ratio of p-nNOS or p-ERK1/2 were normalized to the corresponding total nNOS (t-nNOS) or total ERK1/2 (t-ERK1/2), respectively.

2.6. $(Ca^{2+})i$ Measurements

PC12 cells (150,000/ml) were cultured in 96 wells plate for 48 h, loaded for 30 min in the dark at room temperature with cell permeant fura-2 AM (1 μM ; Molecular Probes, Invitrogen) in HEPES-buffered saline solution (HBSS) (110 mM NaCl, 2.6 mM KCl, 1 mM MgSO4, 1 mM $CaCl_2$, 25 mM HEPES, 11 mM glucose, pH 7.4), after that the cells were washed, and incubated for additional 30 min in HBSS alone. Fluorescence measurement (Ex λ: 340, 380 nm, Em λ: 510 nm) was done at 30 seconds, 2 and 4 min following different treatments. $(Ca^{2+})_i$ was determined following the ratio method described by Grynkiewicz et al. (Grynkiewicz et al., 1985) and using the equation, $(Ca^{2+})_i = K_d[(R-R_{min})/(R_{max}-R)] \times (S_{f2}/S_{b2})$; where R_{max} is the 340/380 nm ratio during Ca^{2+} saturation condition obtained by using Titon-X 100 (0.1%) in regular HBSS, and R_{min} is the 340/380 nm ratio during Ca^{2+}-free conditions obtained by using EGTA (4 mM) in Ca^{2+} free

HBSS buffer. S_{f2} and S_{b2} are the emission intensities at 380 nm excitation during Ca^{2+}-free and Ca^{2+}-saturating conditions, respectively. Fura-2 K_d was set at 224 nM. Results are reported as mean $(Ca^{2+})_i$ µM ± standard error of the mean (S.E.M).

2.7. L-glutamate Measurement

PC12 cells (150,000 cells/ml) were seeded in 12 wells plates with phenol red free F12k media with serum for 48 hrs. On the day of experiment, the media was replaced with HBSS. Different interventions were applied and the release of L-glutamate from PC12 cells in the buffer was measured using Amplex Red kit (Molecular Probes, Invitrogen) following the manufacturer instructions and reported studies (Drake et al., 2005; Medina-Ceja et al., 2015).

2.8. PGE2 Measurement

PGE2 level in RVLM homogenates (10 µg protein/sample) or the culture media of PC12 cells was measured using rat ELISA kits (Cayman, Ann Arbor, MI) according to the manufacturer's instructions. The absorbance was detected at 420 nm. A standard curve was established using serial dilutions of PGE2 standard. PGE2 level in different samples was calculated from the standard curve equation.

2.9. Quantification of Reactive Oxygen and Nitrogen Species

2.9.1. Dihydroethidium (DHE) Staining for ROS Detection.

Fresh unfixed brain sections with the RVLM (rostrally from -12.8 to -11.8 mm relative to bregma) (Paxinos et al., 1980) were cut followed by incubation with 10 µM dihydroethidium

(DHE) (Molecular Probes, Grand Island, NY) at 37°C in the presence of 5% CO2 in a moist chamber for 30 min. Images were visualized with a Zeiss LSM 510 microscope. Three to five images were acquired from four brainstem sections for each experimental condition. Fluorescence intensity was quantified using Zen Lite 2011 software (Penumarti and Abdel-Rahman, 2014).

2.9.2. Measurement of Reactive Oxygen Species by DCFH-DA.

PC12 cells (150,000/ml) were cultured in 96 wells plate for 48 hrs. 2′,7′-Dichlorofluorescein diacetate (DCFH-DA) (Molecular Probes, Grand Island, NY) was dissolved in methanol (20 mM) and kept at −20°C in the dark. Shortly before the experiment, it was freshly diluted (1mM) with serum free cell culture media and incubated with the cells in the dark at 37°C for 30 min. The solution was discarded and the cells were washed twice with HBSS. The treatments were then performed in serum free media. RVLM specimen from treated or control rats were homogenized in phosphate-buffered saline (50 mM, pH 7.4) followed by centrifugation (14,000 rpm, 20 min) and protein quantification of the supernatant using a Bio-Rad protein assay system. Next, 150 μM freshly diluted DCFH-DA with phosphate buffer working solution was added to RVLM homogenate supernatant (10 μl) in a 96-well plate for a final concentration of 25 μM DCFH-DA. 2′,7′-Dichlorofluorescein (DCF) was used to generate the standard curve. Quantification was conducted by measuring fluorescence intensity using a microplate fluorescence reader at excitation 485 nm/emission 530 nm. Kinetic readings were recorded for 60 min at 37°C. Reactive oxygen species (ROS) level was calculated as fold increase of DCF

fluorescence of control as in our reported studies (McGee and Abdel-Rahman, 2012; Penumarti and Abdel-Rahman, 2014).

2.9.3. Measurement of Nitric Oxide Level

PC12 cells (150,000/ml) were cultured in black 96 wells plates for 48 hrs. Cells were incubated with 2 μM 2′,7′-Dichlorofluorescein diacetate (DAF-FM) in serum free medium for 30 min at 37°C in the dark. The cells were washed with HBSS to remove excess probe and then incubated for an additional 15–30 min with HBSS to allow complete de-esterification of the intracellular diacetate followed by the addition of different treatments. The fluorescence intensity was quantified immediately using a microplate fluorescence reader with excitation wavelength at 495 nm and emission wavelength at 512 nm. NO levels are expressed as mean DAF-FM fluorescence as in reported studies (Cortese-Krott et al., 2012).

2.10. Quantification of Catalase Activity

RVLM punches from injected sites were homogenized in 35 μl lysis buffer (20 mM Tris, pH 7.5, 150 mM NaCl, 1 mM EDTA, 1 mM EGTA, 1% Triton X-100, 2.5 mM sodium pyrophosphate, 1 mM β-glycerol-phosphate, 1 mM activated sodium orthovanadate, and 1 ug/ml leupeptin) with protease inhibitor cocktail (Roche Diagnostics, Indianapolis, IN) followed by centrifugation at 2,700 *g* for 4 min at 4°C. The supernatant was separated and assayed for protein content (Bradford assay, Bio-Rad). Catalase activity was determined colorimetrically in 10 μg protein using the Catalase Assay Kit (catalog no. CAT-100, Sigma-Aldrich, St. Louis, MO) according to the manufacturer's instructions.

2.11. Quantification of NADPH Oxidase Activity

NADPH oxidase (NOX) Activity was measured according to (La Favor et al., 2013) with modification. For this assay, 30 µl of homogenate was added to 180 µl of a cocktail containing 10 µM Amplex Red (Molecular Probes, OR), 2.0 U/ml horseradish peroxidase, 30 U/ml superoxide dismutase, and 100 µM NADPH (Sigma Aldrich, St. Louis, MO) in PBS. Fluorescence intensity (530 nM ex/590 nM em) was measured continuously with a microplate fluorescence reader at 37°C at 5 min intervals for 30 min, total NADPH-dependent H_2O_2 generated in the sample was used as an index of NOX activity. Activity was normalized to total protein content, as determined by Bradford assay (Bio-Rad).

2.12. siRNA Knockdown of GPR109A in PC12 Cells.

PC12 cells in suspension (150,000 cells/ml) were transfected with 2.5 µg GPR109A siRNA Flexitube Gene Solution or Allstars negative control siRNA (Qiagen, KY) using 12 µl HiPerFect transfection reagent (Qiagen, KY) in 6 wells plates for 24 hrs according to the manufacturer's protocol. A substantial (≈70%) reduction in GPR109A expression (western blot) validated the adopted siRNA knockdown strategy.

2.13. MTS Cell Viability Assay

PC12 cells were plated in 96-well plates and cultured for 48 hrs (100,000 cells/ml). Different treatments were performed in serum free medium. In one experiment, the cells were incubated with NA (100µm, 1mM and 10mM) or IsoNA (10mM) for 24 hrs. In another experiment, cells were treated with NA (1mM) or PGE2 (10µM) with or without 30 min prior

incubation with the EP3R blocker, L-798106 for 24 hrs. Twenty microliters of MTS reagent (Promega, Madison, WI) was then added to each well following the manufacturer instructions and absorbance which represents viable cells was measured at 495 nm.

CHAPTER THREE - Central GPR109A Activation Mediates Glutamate-Dependent Pressor Response in Conscious Rats

3.1. Abstract

G protein-coupled receptor 109A (GPR109A) activation by its ligand nicotinic acid (NA) in immune cells increases Ca^{2+} levels, and Ca^{2+} induces glutamate release, and oxidative stress in central blood pressure (BP) regulating nuclei e.g. the rostral ventrolateral medulla (RVLM) leading to sympathoexcitation. Despite NA ability to reach the brain, the expression and function of its receptor GPR109A in the RVLM remains unknown. We hypothesized that NA activation of RVLM GPR109A causes Ca^{2+} dependent L-glutamate release, and subsequently increases neuronal oxidative stress, sympathetic activity, and BP. To test this hypothesis, we adopted a multilevel approach, which included pharmacological in vivo studies along with *ex vivo* and *in vitro* molecular studies in PC12 cells (exhibit neuronal phenotype). We present the first evidence for GPR109A expression in the RVLM and in PC12 cells. Next, we showed that RVLM GPR109A activation (NA) caused pressor and bradycardic responses in conscious rats. The resemblance of these responses to those caused by intra-RVLM glutamate, and their attenuation by NMDA receptor (NMDAR) blockade (2-amino-5-phosphonopentanoic acid; AP5) and enhancement by L-glutamate uptake inhibition (L-trans-Pyrrolidine-2,4-dicarboxylic acid; PDC) supported our hypothesis. NA increased Ca^{2+}, glutamate, nitric oxide (NO) and reactive oxygen species (ROS) levels in PC12 cells and increased RVLM ROS levels. The inactive NA analog iso-nicotinic acid (IsoNA) failed to replicate the cardiovascular and biochemical effects of NA. Further, GPR109A knockdown (siRNA) abrogated the biochemical effects of NA in PC12 cells. These novel findings yield new insight into the role of RVLM GPR109A in central BP control.

3.2. Introduction

The recently identified G protein coupled receptor 109A (GPR109A) is now recognized as the molecular target that mediates the long established anti-hyperlipidemic effect of nicotinic acid (NA) (Canner et al., 1986; Carlson, 2005). The most common side effect of NA is the prostaglandins-dependent flushing reaction (Andersson et al., 1977; Morrow et al., 1989). The latter involves intracellular Ca^{2+} elevation and subsequent activation of phospholipase A2 (Lin et al., 1992; Benyo et al., 2006). In the CNS, higher intracellular Ca^{2+} levels enhance neurotransmitters release, including glutamate (Kish and Ueda, 1991; Berridge, 1998; Sudhof, 2004).

GPR109A is widely expressed in white and brown adipose tissue, keratinocytes and various immune cells including monocytes, macrophages, neutrophils and dendritic cells including Langerhans cells (Soga et al., 2003; Tunaru et al., 2003; Wise et al., 2003; Hanson et al., 2010), and likely in microglia (Penberthy, 2009). Despite NA ability to enter the brain (Spector, 1979), there are no reports on the expression or function of GPR109A in cardiovascular regulating nuclei including the RVLM. The latter sends excitatory input to the sympathetic preganglionic neurons, and regulate the sympathetic nervous system and peripheral cardiovascular activity (Ciriello et al., 1986; Chapp et al., 2014).

Realizing that NA activation increases intracellular Ca^{2+} in other cell types (Benyo et al., 2006), it is likely that access of NA to central GPR109A might produce a similar effect and triggers L-glutamate release in the RVLM, which is Ca^{2+}-dependent (Tingley and Arneric, 1990). L-glutamate activation of fast-acting ionotropic receptors, including NMDA and AMPA receptors increases intracellular Na^{+} and Ca^{2+} as well as nerve firing (Dingledine et al., 1999). While the L-glutamate activation of

the central ionotropic or the metabotropic receptors (Gabor and Leenen, 2012) causes sympathoexcitation and a pressor response (Ito et al., 2003), the NMDA receptor (NMDAR)-mediated fast and brief pressor response prevails in the RVLM (Kubo et al., 1993). Further, elevations in Ca^{2+} (Lipton and Rosenberg, 1994) and L-glutamate (Albrecht et al., 2010) levels lead to oxidative stress, and the occurrence of the latter in the RVLM leads to sympathoexcitation and pressor response (Nishihara et al., 2012).

In the present study, we tested the hypothesis that Ca^{2+}-dependent L-glutamate release and oxidative stress, triggered by NA activation of RVLM GPR109A, causes sympathoexcitation and a pressor response. We adopted a multilevel approach, which included pharmacological cardiovascular studies in conscious rats complemented with *ex vivo* and *in vitro* molecular studies. We conducted the detailed molecular studies *in vitro*, because the tissue scarcity and the rapid onset of the NA-evoked pressor response precluded conducting detailed *ex vivo* studies on RVLM tissue. Importantly, differentiated PC12 cells, used in these studies, exhibit a sympathetic-neuron-like phenotype (Greene, 1978; Penugonda et al., 2005). Following the first demonstration of GPR109A expression in the RVLM and in PC12 cells, we investigated the effects of intra-RVLM NA, or its inactive isomer iso-nicotinic acid (IsoNA), on BP and heart rate (HR) in conscious rats. Additional in vivo studies were conducted in the presence of NMDAR blockade (2-amino-5-phosphonopentanoic acid; AP5), non-NMDAR (AMPA/Kainate) blockade (6-cyano-7-nitroquinoxaline-2,3-dione; CNQX) or L-glutamate uptake inhibition (L-trans-Pyrrolidine-2,4-dicarboxylic acid; PDC) in the RVLM. The effects of these pharmacological interventions or GPR109A knockdown (siRNA) on the GPR109A

(NA)-mediated biochemical responses were also investigated in PC12 cells to complement, and to mechanistically explain, the in vivo findings.

3.3. Materials and Methods

3.3.1. Animal Preparation.

Male Sprague Dawley (SD) rats (320–370 g; Charles River Laboratories, Raleigh, NC) were used in this study. All rats were housed two per cage in a room with a controlled environment at a constant temperature of 23 ± 1°C, humidity of 50% ± 10%, and a 12-hour light/dark cycle. Food (Prolab Rodent Chow, Prolab RMH 3000; Granville Milling, Creedmoor, NC) and water were provided ad libitum. All surgical, postoperative care, and experimental procedures were performed in accordance with, and approved by the Institutional Animal Care and Use Committee and in accordance with the *Guide for the Care and Use of Laboratory Animals* (Institute for Laboratory Animal Research, 2011). Surgical procedures, BP and HR measurements were performed as reported in our recent study (Penumarti and Abdel-Rahman, 2014), and as detailed in chapter 2.

3.3.2. Cell Culture

Rat neuronal pheochromocytoma cell line (PC12 cells) was purchased from ATCC (Rockville, MD). Cells were grown in F12k medium supplemented with horse serum (15%), fetal bovine serum (2.5%), penicillin (100U/ml), and streptomycin (100U/ml) at 37°C in a humidified incubator with 95% air and 5% CO_2. The cells were cultured on corning cell bind flasks for proper adherence followed by treatment with nerve growth factor (50ng/ml) till

completely differentiated to the neuronal phenotype according to the protocol of the supplier. Passage was done every 3-5 days when cells reach confluence as in our previous studies (Zhang et al., 2001).

3.3.3. Western Blot Analysis and Immunofluorescence.

We followed the protocols described in chapter 2 and in our previous studies (Ibrahim and Abdel-Rahman, 2012; Penumarti and Abdel-Rahman, 2014).

3.3.4. $(Ca^{2+})_i$, Glutamate, and NO Measurements.

$(Ca^{2+})_i$ was measured in PC12 cells using cell permeant fura-2 AM (1 μM) (Molecular Probes, Invitrogen) as detailed in chapter 2. For L-glutamate measurement, Amplex Red kit was used (Molecular Probes, Invitrogen) following the manufacturer instructions and reported studies (Medina-Ceja et al., 2015) as provided in chapter 2. NO was measured using 4-amino-5-methylamino-2′,7′-difluorofluorescein diacetate (DAF-FM Diacetate) (Molecular Probes, Grand Island, NY) according to the manufacturer instructions and reported studies (Cortese-Krott et al., 2012) as described under methods in chapter 2.

3.3.5. Measurement of Oxidative Stress.

We used 2′,7′-Dichlorofluorescein diacetate (DCFH-DA) (Molecular Probes, Grand Island, NY), a general detector of oxidative species, to measure oxidative stress in PC12 cells and in RVLM specimens taken from animals that received NA or its vehicle. Further, the dihydroethidium (DHE) staining method, which is more superoxide anion selective (Bindokas et

al., 1996; Robinson et al., 2006) was used for ROS measurements in RVLM sections of animals that received the different treatments described below. The methods and protocols used are detailed in our previous studies (Penumarti and Abdel-Rahman, 2014) and described in chapter 2.

3.3.6. siRNA Knockdown of GPR109A in PC12 Cells.

PC12 cells in suspension (150,000 cells/ml) were transfected with 2.5 µg GPR109A siRNA Flexitube Gene Solution or Allstars negative control siRNA (Qiagen, KY) using 12 µl HiPerFect transfection reagent (Qiagen, KY) in 6-wells plates for 24 h according to the manufacturer's protocol. A substantial (≈70%) reduction in GPR109A expression (western blot) validated the adopted siRNA knockdown strategy.

3.4. Experimental Groups and Protocol

3.4.1. Experiment 1: Expression of GPR109A in the RVLM and PC12 Cells.

The objective of this experiment was to determine if GPR109A is expressed in the RVLM and in PC12 cells, and its spatial distribution in the RVLM relative to different cell types, particularly tyrosine hydroxylase (TH) immunoreactive (ir) neurons, which modulate the sympathetic activity and BP (Guyenet, 2006a; Kumagai et al., 2012). First, western blot (WB) analysis was conducted to detect GPR109A in PC12 cell lysate, and in punches taken from the RVLM of naïve rats (n = 3). Tissues rich in (spleen), or devoid of (liver) GPR109A (Soudijn et al., 2007) were used as positive and negative controls, respectively, in these studies. Second, dual labeled immunofluorescence (IF) was conducted in post-fixed sections from rat frozen brains and

PC12 cells. Neuronal and glial cell markers including the neuronal marker, NeuN, the astrocyte marker, GFAP, and the microglia marker, CD11b/c were used to investigate the spatial distribution of GPR109A in different cell types in the RVLM. Further the expression of GPR109A relative to TH-ir neurons was investigated by using an anti-tyrosine hydroxylase antibody. We followed methods described in our previous studies (Ibrahim and Abdel-Rahman, 2011; Penumarti and Abdel-Rahman, 2014) and detailed in chapter 2.

3.4.2. Experiment 2: Functional Role of RVLM GPR109A in BP and HR Regulation.

As there are no reported studies on intra-RVLM NA, a preliminary study was conducted to determine the optimal NA dose to be used throughout the study based on estimated penetration of systemic NA into the CNS (Spector, 1979). Two groups of conscious unrestrained SD rats (n = 4-7), instrumented for BP and HR measurements and RVLM microinjections as detailed under methods, received intra-RVLM NA (5, 10 and 20 µg/animal) or the vehicle, artificial cerebrospinal fluid (ACSF). The 20 µg NA dose, which produced consistent pressor response, was used in subsequent studies. There are currently no GPR109A antagonists. Therefore, to ensure that the NA-evoked pressor response was GPR109A mediated, the same dose (20 µg/animal) of the NA inactive isomer, IsoNA, was microinjected into the RVLM of a third group of rats (n = 6).

3.4.3. Experiment 3: Effect of NMDAR, non-NMDAR Blockade or L-glutamate Uptake Inhibition on the Cardiovascular Effects of NA.

The role of L-glutamate in NA-induced pressor response was investigated using different pharmacological interventions in conscious male SD rats instrumented for measurements of BP and HR and RVLM microinjections as detailed under *methods*. Four groups of rats (n = 5-7) received the NMDAR blocker, AP5 (2 nmol/100nl) (Zhang and Abdel-Rahman, 2002a), the non-NMDAR blocker, CNQX (200 pmol) (Wang et al., 2007), the glutamate uptake inhibitor, PDC (1 µM) (Montiel et al., 2005) or ACSF 10 min before NA (20 µg/animal) microinjection.

3.4.4. Experiment 4: GPR109A-dependent Biochemical Effects of NA.

The objective of this experiment was to obtain direct biochemical evidence that GPR109A mediates elevations in L-glutamate release, intracellular Ca^{2+} and reactive oxygen species (ROS), which are implicated in sympathoexcitation and BP elevation (Lipton and Rosenberg, 1994; Ito et al., 2003; Nishihara et al., 2012). PC12 cells, used as surrogates of RVLM neurons, were incubated with NA (10 µM, 100 µM or 1mM) in the absence or the presence of the pharmacological interventions used in vivo (experiment 3). This model system permitted rapid (0.5-1 min) biochemical measurements after NA addition, a timeframe consistent with the rapid onset of the pressor response caused by intra-RVLM NA. The dependence of the biochemical effects of NA on GPR109A activation was verified in PC12 cells by: (i) replacing NA with its inactive isomer, IsoNA (Maciejewski-Lenoir et al., 2006) (1 mM); (ii) the addition of NA (1 mM) to PC12 following GPR109A knockdown with siRNA (see methods). The pharmacological interventions incubated with PC12 cells in the absence or the presence of NA (1 mM) included:

(i) L-glutamate in a concentration (100 nM) that was achieved 1 min after NA (1 mM) addition to PC12 (preliminary experiment); (ii) the glutamate uptake inhibitor, PDC (0.1 mM) for 1 h (Pepponi et al., 2009); (iii) the NMDAR blocker, AP5 (100 μM) for 10 min (Reigada et al., 2006). For *ex vivo* ROS measurements, brain tissues were collected from animals (n = 4–5 rats) that received the different treatments following euthanasia with a lethal dose of pentobarbital sodium (>100 mg/kg) at the end of BP recording period. Fresh unfixed brainstem sections (20 μm) sections were taken followed by collecting micropunches from the injected RVLM side using a 0.75 micropunch instrument (Stoelting Co., Wood Dale, IL), using the following coordinates 12.6 to -11.8 mm relative to bregma as in reported studies including ours (Paxinos et al., 1980; Ibrahim and Abdel-Rahman, 2015).

3.4.5. Drugs.

NA, L-glutamate, and PDC were purchased from Sigma-Aldrich (St. Louis, MO), and DL-AP5 and CNQX from Tocris Bioscience (Ellisville, MO). Sterile saline was purchased from B. Braun Medical (Irvine, CA). IsoNA acid was purchased from TCI America (Portland, OR).

3.5. Data Analysis and Statistics

Animal studies data (n = 3-7) and *in vitro* data from three independent experiments are expressed as mean ± standard error of mean (S.E.M). Analysis of Variance (ANOVA) or repeated-measures analysis of variance followed by Bonferroni's post hoc test and Student's *t*-test were carried out using GraphPad Prism to state differences between groups.

3.6. Results

3.6.1. GPR109A Co-expression with Tyrosine Hydroxylase in the RVLM and in PC12 Cells.

WB analysis revealed and verified the expression GPR109A in the RVLM and PC12 cells, when compared to tissues rich in (spleen) or devoid of (liver) GPR109A expression (Fig. 3.1A). Further, dual-labeled IF findings in PC12 cells showed co-expression of GPR109A and TH (Fig. 3.1B). Cell type specific labeling (Fig. 3.2 A-D), and quantitative comparisons of cell types (Fig. 3.2E), showed that GPR109A is expressed in much greater percentage (approx. 70%) in neuronal than in non-neuronal cells (astrocytes and microglia) (30%) of the counted cells in the RVLM sections. Further, the majority (>90%) of the RVLM TH-ir neurons also expressed GPR109A (Fig. 3.2E).

3.6.2. Activation of RVLM GPR109A Causes Glutamate-like Pressor Response and Neuronal Oxidative Stress.

BP and HR values before intra-RVLM microinjection of NA in the absence or presence of pharmacologic interventions, indicated below, were not significantly different (Table 1). Intra-RVLM NA (5, 10, 20 µg) caused dose-dependent pressor response and bradycardia in conscious rats (Fig. 3.3). These cardiovascular responses resembled the responses elicited by intra-RVLM L-glutamate (1 nmol; 169 ng) (Fig. 3.3A). Importantly, the inactive NA isomer, IsoNA (20 µg), failed to influence BP or HR (Fig. 3.4, A and B). *Ex vivo* studies revealed higher ROS levels in NA (20 µg)-treated RVLM, but not following the same dose of IsoNA (Fig. 3.5).

3.6.3. Selective NMDAR Blockade and Glutamate Uptake Inhibition Abrogates and Enhances, Respectively, the Intra-RVLM NA-Evoked Oxidative Stress and Pressor Response.

Prior RVLM NMDAR (AP5; 2 nmol), but not non-NMDAR (CNQX; 200 pmol) blockade abrogated ($P < 0.05$) the pressor and bradycardic responses (Fig. 3.4, C, D and E), and abolished the increase in ROS (Fig. 3.5B) caused by subsequent intra-RVLM NA (20 µg). On the other hand, prior L-glutamate uptake inhibition with intra-RVLM PDC (1 µM) significantly ($P < 0.05$) increased the magnitude and duration (presented as area under the curve, AUC) of the pressor response (Fig. 3.4, C and E) and exacerbated the elevation in RVLM ROS (Fig. 3.5B) caused by subsequent intra-RVLM NA (20 µg) microinjection. None of these intervention changed BP or HR from the corresponding baseline values (Table 3.1).

3.6.4. GPR109A Activation Increases L-glutamate, Ca^{2+} and NO levels and Produces NMDAR-Dependent Oxidative Stress in PC12 cells.

The rapid onset (approx. 1 min) of the pressor response caused by intra-RVLM NA precluded measurements of RVLM L-glutamate, Ca^{2+} and NO levels during this timeframe. Therefore, such measurements were made in differentiated PC12 cells, which exhibit neuronal phenotype and express GPR109A (Fig. 3.1, A and B). NA (100 µM or 1mM) significantly ($P < 0.05$) increased Ca^{2+} (Fig. 3.6A), L-glutamate (Fig. 3.6B), and NO (Fig. 3.6C) levels 30-60 sec after NA addition to the incubation medium. Pre-incubating PC12 cells with the L-glutamate uptake inhibitor PDC (0.1 mM/1 h) significantly ($P < 0.05$) enhanced NA-evoked glutamate release (Fig. 3.6B). These biochemical responses were associated with significant ($P < 0.05$) increases in ROS levels (Fig. 3.7A). Notably, L-glutamate, in a concentration (100 nM), detected

after NA (1 mM) addition to incubation medium (preliminary), significantly (P <0.05) increased ROS level (Fig. 3.7B). Similar to *ex vivo* findings on RVLM (Fig. 3.5), the NA-induced oxidative stress was circumvented by prior NMDAR blockade with AP5 (100 μM) (Fig. 3.7B). Further, the inactive NA isomer, IsoNA (1 mM), had no effect on Ca^{2+}, glutamate, NO (Fig. 3.6, A, B and C) or ROS (Fig. 3.7A) levels.

3.6.5. GPR109A Knockdown Abolishes NA Induced Ca^{2+} and Glutamate Release in PC12 Cells.

There are no available GPR109A antagonists. Therefore, we used siRNA knockdown strategy to validate the involvement of GPR109A in the NA-evoked biochemical responses in PC12 cells, described above. The GPR109A targeting siRNA significantly (P < 0.05) reduced GPR109A expression (Fig. 3.8A). In PC12 cells pretreated with the negative siRNA control (scrambled siRNA), NA (1 mM) significantly (P < 0.05) increased Ca2+(Fig. 8B) and glutamate (Fig. 3.8C) levels. However, in PC12 cells, which exhibited significant (P < 0.05) siRNA-induced reduction in GPR109A expression (Fig. 3.8A), NA (1 mM) failed to produce these biochemical responses (Fig. 3.8, B and C).

Table 3. 1. Mean arterial pressure (MAP, mm Hg) and heart rate (HR, beats/min) values immediately before intra-RVLM treatment with the indicated intervention or the vehicle (ACSF).

Pretreatment/Treatment	Rats per group (n)	MAP (mmHg)	HR (beats/min)
ACSF	7	126.1 ± 5.501	341.7 ± 12.36
IsoNA	6	133.7 ± 4.219	336.3 ± 6.224
ACSF/Nicotinic acid	7	122.6 ± 5.086	353.7 ± 18.19
AP5/Nicotinic acid	5	127.2 ± 6.258	379.3 ± 26.75
PDC/Nicotinic acid	7	125.0 ± 3.070	326.7 ± 30.92
CNQX/Nicotinic acid	5	126.8 ± 4.737	340.2 ± 24.97

Figure 3.1. Expression of GPR109A in the rat RVLM and PC12 cells

(**A**) Expression of GPR109A (42 kDa) in the rat RVLM or PC12 cells compared with expression in the spleen (positive control) and liver (negative control). Data are presented as integrated density ratio of GPR109A to the corresponding GAPDH values (n = 3) and expressed as mean ± S.E.M. **(B)** Dual-labeled IF of PC12 cells showing co-expression of GPR109A and TH.

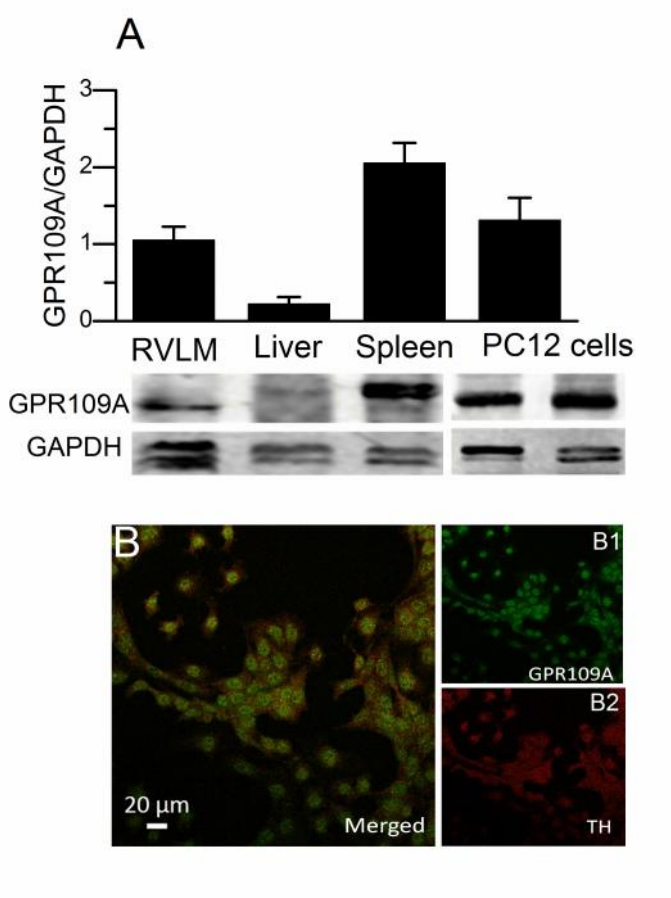
A
GPR109A/GAPDH
3
2
1
0
RVLM
Liver
Spleen
PC12 cells
GPR109A
GAPDH
B
B1
GPR109A
B2
TH
20 μm
Merged

Figure 3.2. Spatial distribution of GPR109A in the RVLM

Confocal dual-labeled IF of post-fixed RVLM sections (n = 4-6) from naïve rats (n = 6) showing the spatial distribution of GPR109A in neurons, TH-ir neurons, astrocytes and microglia. Dual-channel images showing GPR109A (green) and one of the following markers (red): NeuN **(A)**, TH **(B)**, GFAP **(C)** or CD11b/c (**D**). In general, the 3 images for each section (A, B, C or D) show the same field at different magnifications where the two smaller images showing staining for different markers (e.g. A2 and A3) while the larger image (e.g. A1) shows the merged staining for these two markers. The arrows illustrate co-labeled cells. Scale bar, 20 µm. **(E)** quantitative analysis of A, B, C and D. Bar graph represents the total number of cells expressing different markers (white) and the number of co-labeled cells of GPR109A with each marker (black) in the examined RVLM sections (mean ± S.E.M). CD11b/c: microglia marker; GFAP: astrocytes marker; NeuN: neurons marker; IF: immunofluorescence; RVLM: the rostral ventrolateral medulla; TH: tyrosine hydroxylase.

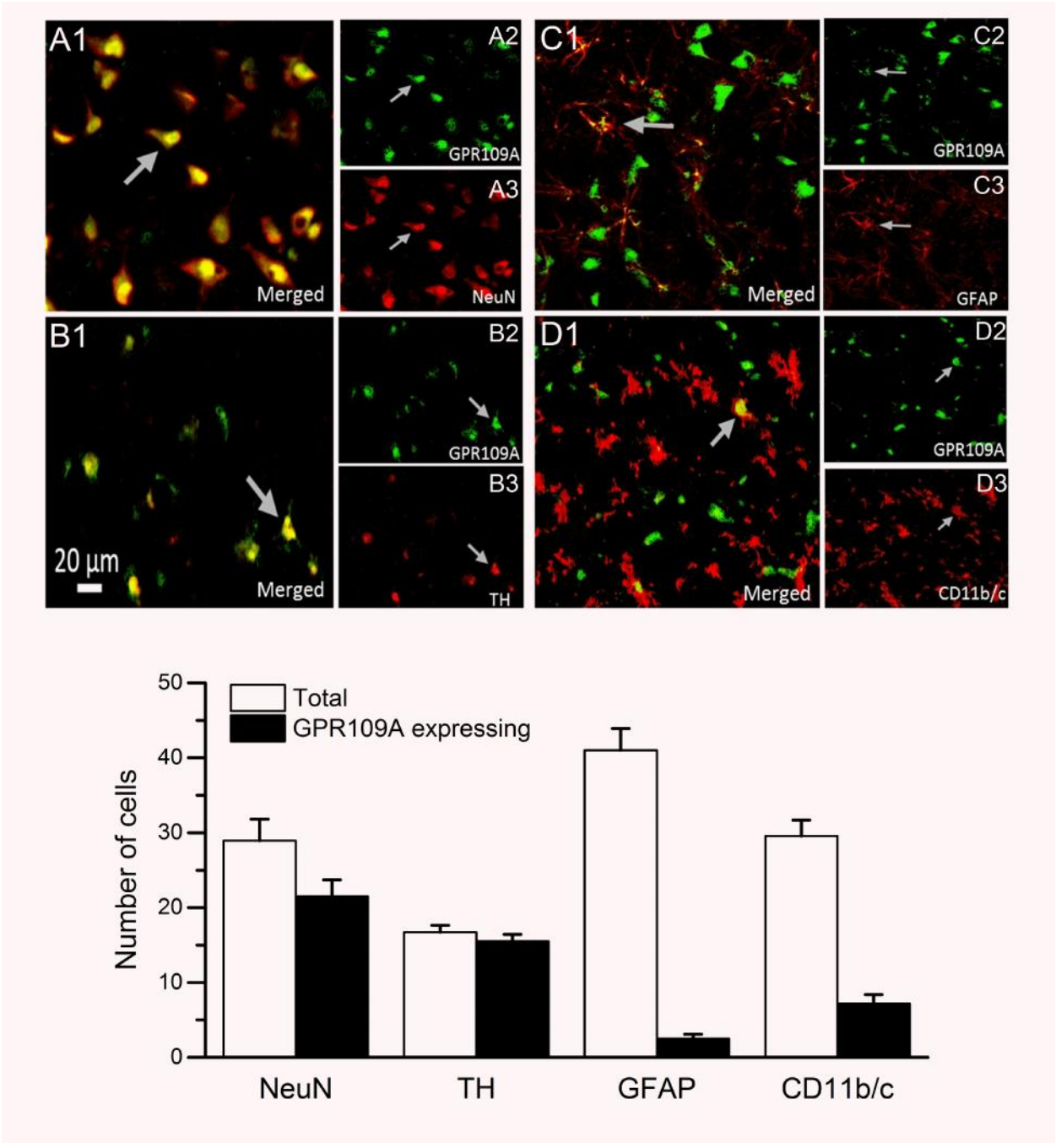
A1
A2
GPR109A
A3
NeuN
Merged
C1
C2
GPR109A
C3
GFAP
Merged
B1
B2
GPR109A
B3
TH
20 µm
Merged
D1
D2
GPR109A
D3
CD11b/c
Merged
Total
GPR109A expressing
Number of cells
50
40
30
20
10
0
NeuN
TH
GFAP
CD11b/c

Figure 3.3. Effect of intra-RVLM NA on MAP and HR in conscious male rats

Representative mean arterial pressure (MAP) and heart rate (HR) responses caused by intra-RVLM NA (20µg) or L-glutamate (169 ng) **(A)**. Effect of intra-RVLM NA (5, 10, or 20 μg) on MAP **(B)** and HR **(C)** in conscious male rats. Values are mean change from base line ± S.E.M, (n = 4-7). *P < 0.05 vs. ACSF. ACSF: artificial cerebrospinal fluid; ΔHR: change in HR; ΔMAP: change in mean arterial pressure; RVLM: the rostral ventrolateral medulla.

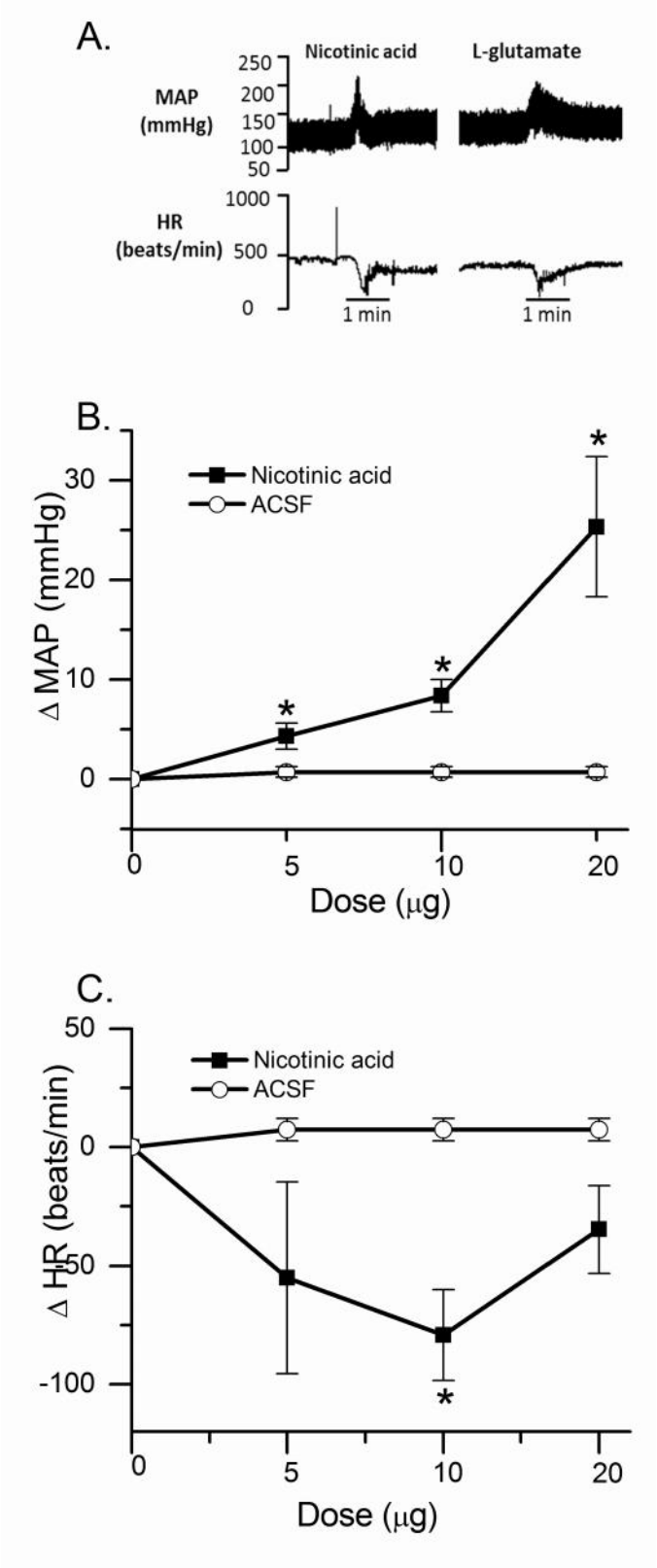
A.
Nicotinic acid
L-glutamate
MAP
(mmHg)
250
200
150
100
50
HR
(beats/min)
1000
500
0
1 min
1 min
B.
Nicotinic acid
ACSF
Δ MAP (mmHg)
30
20
10
0
*
*
*
0
5
10
20
Dose (μg)
C.
Nicotinic acid
ACSF
Δ HR (beats/min)
50
0
-50
-100
*
0
5
10
20
Dose (μg)

Figure 3.4. Effect of NMDAR blockade or glutamate uptake inhibition on NA pressor response

Time-course changes in mean arterial pressure (ΔMAP) **(A)** and heart rate (ΔHR) **(B)** evoked by intra-RVLM NA or IsoNA (20 µg) compared with equal volume of ACSF in conscious male rats. **(C, D)**: time-course changes in ΔMAP and ΔHR evoked by intra-RVLM NA (20 µg) in conscious male rats pretreated, 10 min earlier, with ACSF, NMDA receptor blocker (AP5, 2 nmol/100nl) or L-glutamate uptake inhibitor (PDC, 1 µM). **(E)** The area under the curve (AUC) data generated from 20 min BP time-course values for different treatments. Data from AP5 (2 nmol/100nl) or PDC (1 µM) treated rats were not significantly different from the control values, and are not shown for clarity. Values are mean change from base line ± S.E.M (n = 5-7). *P < 0.05 vs. ACSF values; $^{\#}P$ < 0.05 vs. NA. ACSF: artificial cerebrospinal fluid; BP: blood pressure; IsoNA: iso-nicotinic acid; RVLM: the rostral ventrolateral medulla.

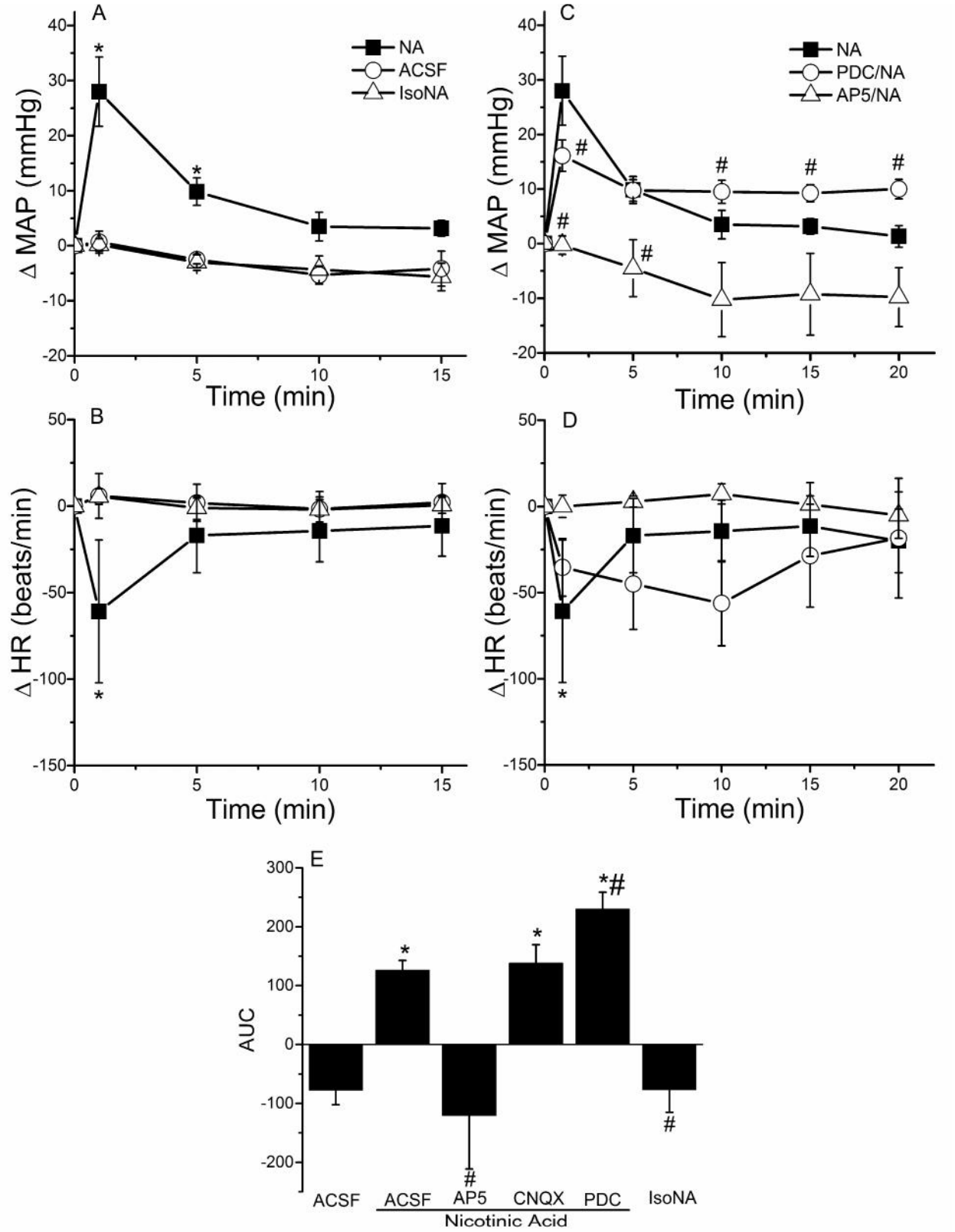
A
NA
ACSF
IsoNA
Δ MAP (mmHg)
Time (min)
B
Δ HR (beats/min)
Time (min)
C
NA
PDC/NA
AP5/NA
Δ MAP (mmHg)
Time (min)
D
Δ HR (beats/min)
Time (min)
E
AUC
ACSF
ACSF
AP5
CNQX
PDC
IsoNA
Nicotinic Acid

Figure 3.5. Effect of GPR109A activation on RVLM ROS levels and the impact of NMDAR blockade or glutamate uptake inhibition in this response.

(A) DCFH-DA measured ROS levels in terms of relative fluorescence units (RFU) of produced DCF in the RVLM after ACSF or NA (20 μg) injection. **(B)** Effect of ACSF, NA (20 μg), AP5 (2 nmol)/NA (20 μg), CNQx (200 pmol)/NA (20 μg), PDC (1 µM)/NA (20 μg) and isoNA (20 μg) on RVLM ROS levels detected by DHE staining (visualized with confocal microscopy and quantified using Zen Lite 2011 software). Values are mean ± S.E.M. (n = 4-5 rats). *P < 0.05 vs. ACSF values; $^{\#}P$ < 0.05 vs. NA. ACSF: artificial cerebrospinal fluid; IsoNA: iso-nicotinic acid; NA: nicotinic acid; RVLM: the rostral ventrolateral medulla.

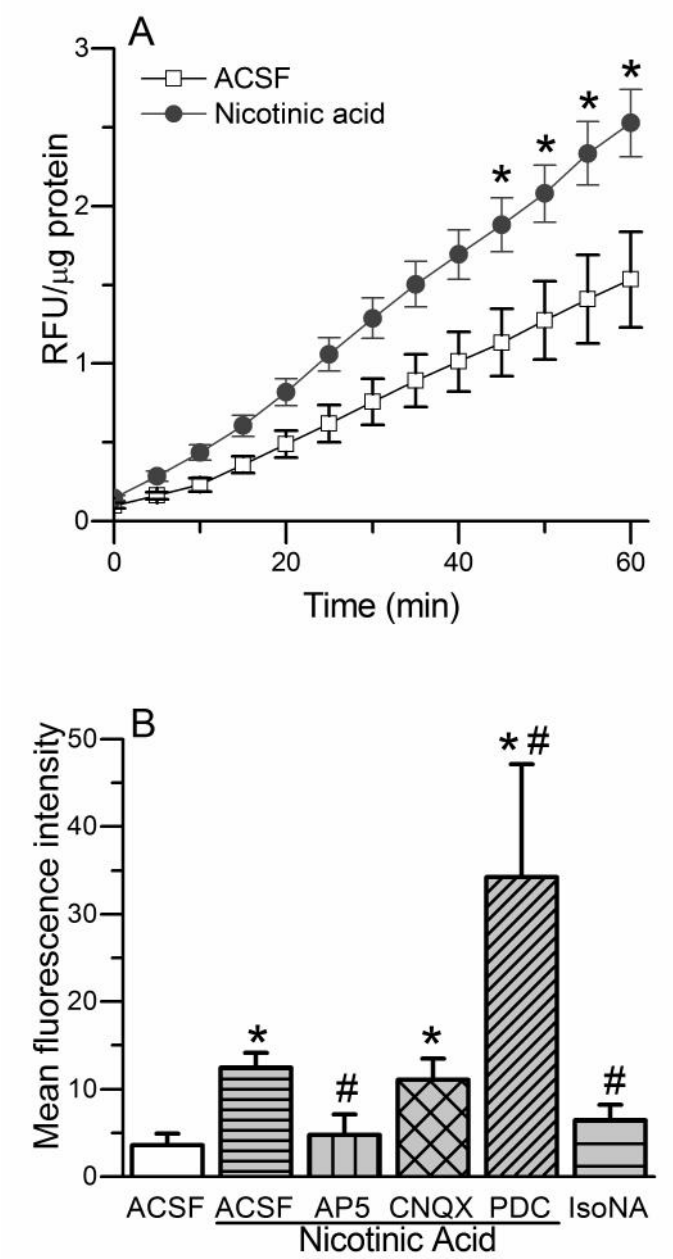
A
ACSF
Nicotinic acid
RFU/μg protein
Time (min)
0
1
2
3
0
20
40
60
*
B
Mean fluorescence intensity
0
10
20
30
40
50
ACSF
ACSF
AP5
CNQX
PDC
IsoNA
Nicotinic Acid
*
#

Figure 3.6. Effect of NA on Ca^{2+}, L-glutamate and NO levels in PC12 Cells

(A) Effect of NA (10 µM, 100 µM, and 1mM), or IsoNA (1mM) on Ca^{2+} levels in PC12 cells. Measurements were done 30 secs, 2 and 4 min incubation time. Data representing Ca^{2+} concentration (µM) is expressed as mean ± S.E.M. **(B)** Effect of 1 min exposure of PC12 cells to NA or IsoNA (1mM) on L-glutamate levels (folds increase of control) with or without 1 h prior incubation with PDC (0.1 mM). **(C)** NO DAF-FM fluorescence intensity in PC12 cells incubated with NA (10 µM, 100 µM, 1mM) or IsoNA (1mM) for 1 min. Data are expressed as mean ± S.E.M. $^{*}P < 0.05$ vs. control values; $^{\#}P < 0.05$ vs. PDC; $^{\wedge}P < 0.05$ vs. NA. IsoNA: iso-nicotinic acid; NA: nicotinic acid; NO: nitric oxide.

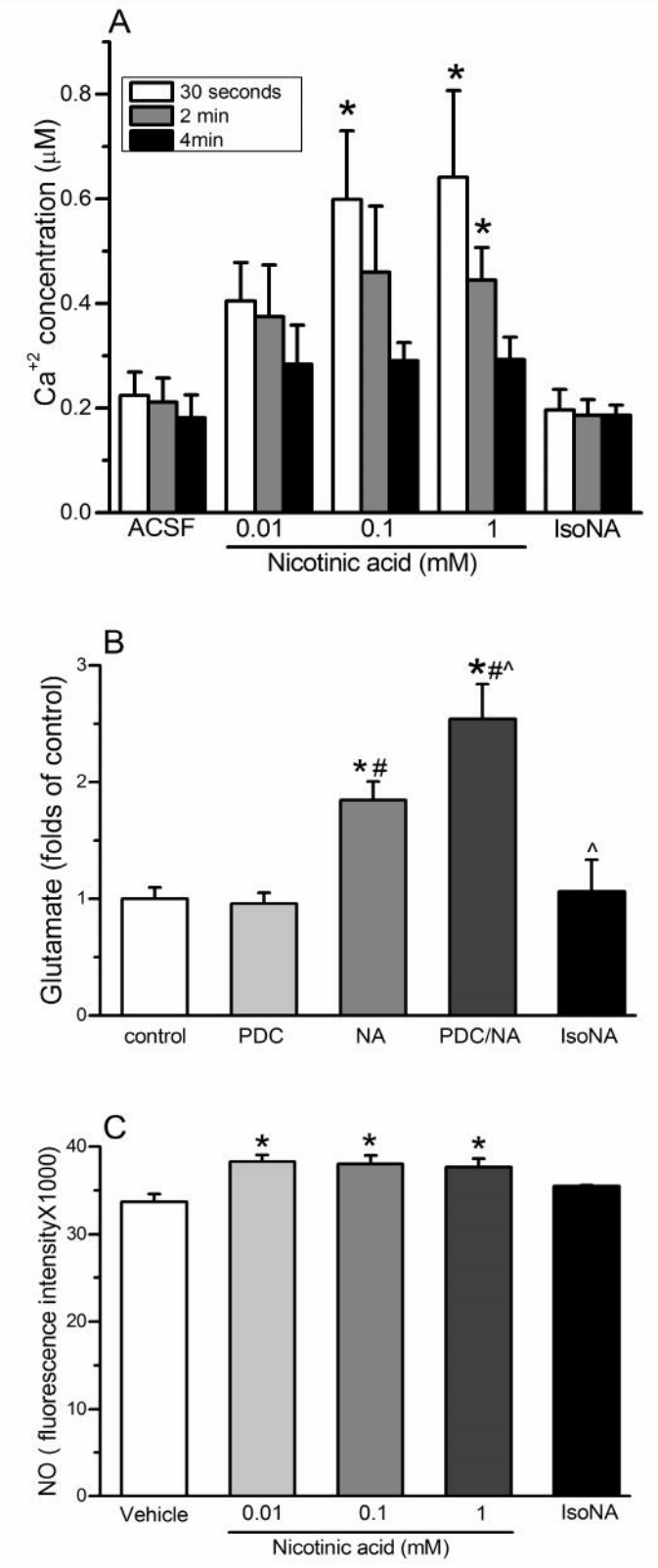
A
30 seconds
2 min
4min
Ca+2 concentration (μM)
0.0
0.2
0.4
0.6
0.8
*
*
*
ACSF
0.01
0.1
1
IsoNA
Nicotinic acid (mM)
B
Glutamate (folds of control)
0
1
2
3
*#
*#^
^
control
PDC
NA
PDC/NA
IsoNA
C
NO (fluorescence intensityX1000)
0
10
20
30
40
*
*
*
Vehicle
0.01
0.1
1
IsoNA
Nicotinic acid (mM)

Figure 3.7. Role of glutamate in NA-mediated ROS generation in PC12 cells

Effect of NA (10 µM, 100 µM, and 1mM), or IsoNA (1mM) on DCFH-DA measured ROS generation in PC12 cells (folds increase from control). **(B)** Effect of NA (1mM) on DCFH-DA measured ROS generation compared to glutamate (100nM) with or without 1 h or 10 min prior incubation with PDC (0.1 mM), or AP5 (100 µM), respectively. Kinetic measurements were recorded for 30 min following different treatments. Data are expressed as mean ± S.E.M. *P < 0.05 vs. control. IsoNA: iso-nicotinic acid; L-glut.: L-glutamate; NA: nicotinic acid.

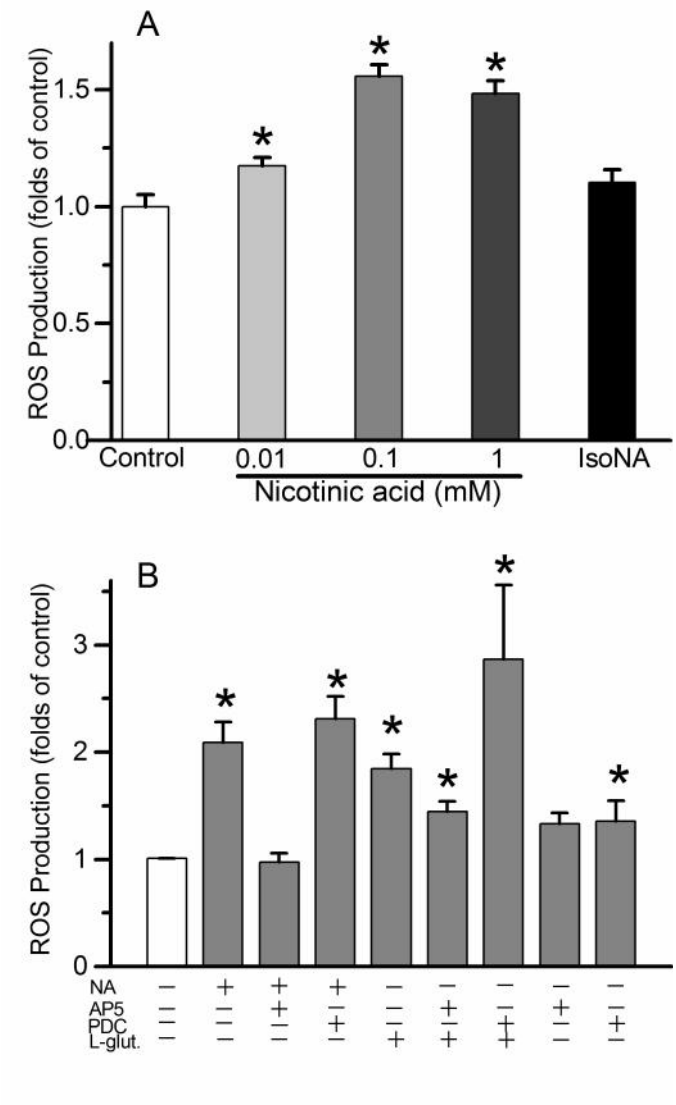
A
ROS Production (folds of control)
1.5
1.0
0.5
0.0
Control
0.01
0.1
1
IsoNA
Nicotinic acid (mM)
B
ROS Production (folds of control)
3
2
1
0
NA
AP5
PDC
L-glut.

Figure 3.8. Effect of GPR109A knockdown on NA-mediated increase in and glutamate levels in PC12 cells

Western blot for GPR109A in siRNA transfected cells compared to control (n = 3). Data are presented as integrated density ratio of GPR109A to the corresponding β-actin values, and expressed as mean ± S.E.M. Effect of vehicle or NA (1mM) on Ca^{2+} **(B)** and glutamate **(C)** levels in PC12 cells pre-incubated for 24 hrs with either scrambled or GPR109A siRNA. Measurements were done at 30 secs and 1 min incubation times for the measurements of Ca^{2+} and glutamate, respectively, and represented as fold increase from corresponding control. Data are expressed as mean ± S.E.M. *$P < 0.05$ vs. control values. NA: nicotinic acid.

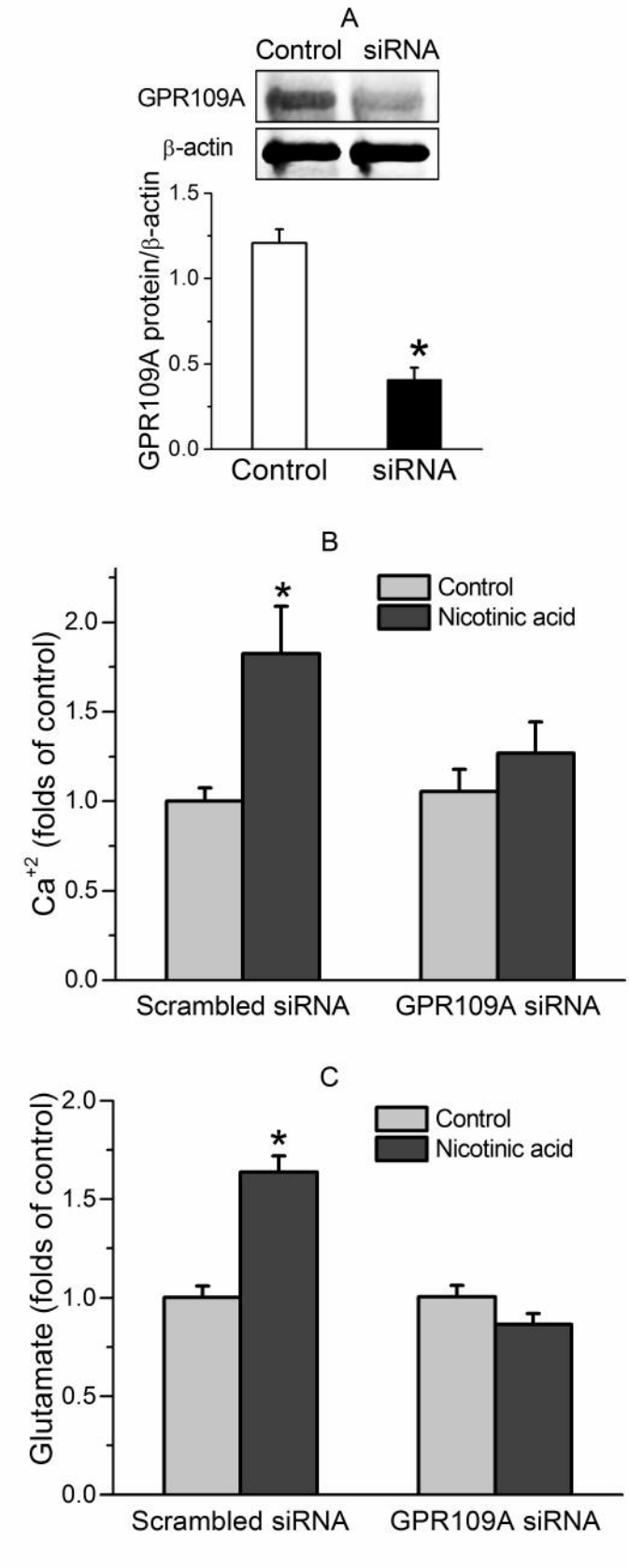
A
Control
siRNA
GPR109A
β-actin
GPR109A protein/β-actin
1.5
1.0
0.5
0.0
*
Control
siRNA
B
Control
Nicotinic acid
Ca+2 (folds of control)
2.0
1.5
1.0
0.5
0.0
*
Scrambled siRNA
GPR109A siRNA
C
Control
Nicotinic acid
Glutamate (folds of control)
2.0
1.5
1.0
0.5
0.0
*
Scrambled siRNA
GPR109A siRNA

3.7. Discussion

In this study we tested the hypothesis that NA activation of RVLM GPR109A induces L-glutamate (NMDAR)-dependent oxidative stress and sympathoexcitation/pressor response. We focused on the RVLM because it mediates L-glutamate-dependent increases in sympathetic activity and BP, and tonically regulates the peripheral vascular activity (Ciriello et al., 1986; Bazil and Gordon, 1993; Chapp et al., 2014).

Our most important findings are: (i) the majority of RVLM neurons, and particularly the TH-ir neurons, express GPR109A; (ii) intra-RVLM injection of the GPR109A agonist NA, but not its inactive isomer (IsoNA) caused elevations in RVLM oxidative stress and BP, which resembled glutamate-evoked responses; (iii) NMDAR blockade (AP5) and L-glutamate uptake inhibition (PDC) abrogated and exacerbated, respectively, the NA-evoked increases in BP and RVLM oxidative stress; (iv) NA, but not IsoNA, increased Ca^{2+}, NO, glutamate, and ROS levels in PC12 cells; (v) GPR109A knockdown (siRNA) abrogated the NA-evoked biochemical responses in PC12 cells.

GPR109A, which serves as a receptor for NA (Soga et al., 2003; Tunaru et al., 2003), is expressed in adipose tissue and immune cells (Soga et al., 2003; Maciejewski-Lenoir et al., 2006; Penberthy, 2009). Under normal physiological conditions, the levels of the endogenous agonist (β-hydroxybutyrate) or exogenous agonist (NA), when taken as a vitamin, might be lower than the μM-mM concentration range needed to activate GPR109A (Taggart et al., 2005). However, when used in much higher doses as anti-hyperlipidemic drug (Brown et al., 2001; Whitney et al., 2005), such NA concentrations might be achieved. Further, despite evidence that NA is

transported into the brain in appreciable concentrations following systemic administration (Spector, 1979), there are no reports on GPR109A expression or function in neuronal structures, which regulates sympathetic outflow and BP (e.g. RVLM). Here, we present the first evidence that GPR109A is expressed in RVLM neurons, including the TH expressing neurons (Fig. 3.2, A and B); the latter modulate the sympathetic activity and BP (Guyenet, 2006a; Kumagai et al., 2012). These findings, which infer a cardiovascular role for GPR109A, were confirmed by observing dose-related increases in BP following intra-RVLM NA microinjection in conscious rats (Fig. 3.3B). The rapid onset of the NA-induced pressor response along with the associated bradycardia were reminiscent of cardiovascular responses elicited by L-glutamate microinjection into the same neuronal pool observed in a separate group of rats (Fig. 3.3A), and in reported studies including ours (Bachelard et al., 1990; Mao and Abdel-Rahman, 1994). While the rapid onset of the pressor response (Fig. 3.3A) precluded investigation of NA effect on RVLM L-glutamate release, we adopted pharmacological approaches in vivo and direct biochemical measurements in PC12 cells to support L-glutamate involvement in the NA-evoked cardiovascular responses. It is imperative, nonetheless, to note that these cardiovascular responses were mediated via NA activation of RVLM GPR109A because the inactive NA isomer, IsoNA, failed to produce similar cardiovascular effects (Fig. 3.4, A and B).

We hypothesized that NA activation of GPR109A in the RVLM leads to Ca^{2+}-dependent L-glutamate release because: (i) NA (10 µM-3 mM) mediates GPR109A dependent increase in intracellular Ca^{2+} levels in macrophages and epidermal Langerhans cells (Benyo et al., 2005; Benyo et al., 2006; Vanhorn et al., 2012; Gaidarov et al., 2013), (ii) Ca^{2+} triggers L-glutamate

release (Kish and Ueda, 1991; Berridge, 1998; Sudhof, 2004), and (iii) elevated L-glutamate levels cause oxidative stress (Wang et al., 2013b; Yang et al., 2014), sympathoexcitation (Chapp et al., 2014), and ultimately BP elevation (Iwata et al., 1987; Bazil and Gordon, 1993). Therefore, the RVLM GPR109A most likely mediates a glutamate-dependent sympathoexcitation. Although the origin of NA-induced glutamate release in the RVLM remains uncertain, the RVLM presympathetic neurons contribute, at least partly to this process because they exhibit the highest GPR109A level in the RVLM (Fig. 3.2E), and their axonal varicosities contain the glutamate transporter VGLUT2, and release glutamate (DePuy et al., 2013). Our in vivo and *ex vivo* findings supported the L-glutamate hypothesis because local NMDAR blockade (AP5) abrogated, while glutamate uptake inhibition (PDC) exacerbated, the pressor response (Fig. 3.4) and RVLM oxidative stress (Fig. 3.5) caused by intra-RVLM NA.

Next, we leveraged the biological phenotype resemblance of the differentiated PC12 cells and RVLM neurons (Separovic et al., 1997; Zhang et al., 2001) to obtain direct evidence that NA activation of GPR109A leads to L-glutamate and Ca^{2+} release. However, in the absence of any reports on GPR109A expression in PC12 cells, it was important to determine if, similar to the RVLM neurons, the receptor is expressed, and is spatially associated with TH, in this cell line. Our WB and dual labeling IF (Fig. 3.1, A and B) confirmed our assumptions, and validated the use of differentiated PC12 cells as an appropriate model system for studying the biochemical events triggered by NA activation of GPR109A. We showed that NA causes increases in Ca^{2+} and L-glutamate levels in PC12 cells (Fig. 3.6, A and B) along with oxidative stress (Fig. 3.7A).

It was important to determine if the GPR109A-mediated increase in glutamate release (Fig. 3.6B) accounts for the oxidative stress (Fig. 3.7A) because the latter is implicated in sympathoexcitation as discussed above. Our findings support this view because: (i) NA (1 mM) and L-glutamate, in a concentration (100 nM) similar to that released by NA (1 mM), produced comparable increases in oxidative stress in PC12 cells (Fig. 3.7B); (ii) L-glutamate uptake inhibition augmented the NA-induced glutamate release (Fig. 3.6B). Although no GPR109A antagonists are currently available, these effects are most likely GPR109A-dependent because the inactive NA isomer IsoNA, whose microinjection into the RVLM had no effect on BP or RVLM redox state (Figs. 3.4 and 3.5), also failed to reproduce NA-evoked biochemical effects in PC12 cells (Figs. 3.6 and 3.7). The latter findings agree with reported studies in other model systems (Maciejewski-Lenoir et al., 2006; Gaidarov et al., 2013). Equally important, NA failed to increase Ca^{2+} or glutamate levels in PC12 cells following siRNA-evoked GPR109A knockdown (Fig. 3.8), which provided direct evidence for GPR109A mediation of NA actions, and support the in vivo findings, discussed above.

It is important to comment on the role of the NMDAR in mediating the biochemical and pressor responses caused by NA activation of GPR109A. As discussed above, NA activation of GPR109A leads to the release of L-glutamate, which activates ionotropic and metabotropic glutamate receptors (Gabor and Leenen, 2012). The rapid onset of the NA-evoked pressor response is consistent with L-glutamate activation of the NMDAR ionotropic receptors in the RVLM (Kubo et al., 1993). This assumption was confirmed by the ability of the NMDAR blocker AP5 (Fig. 3.4C), but not the non-NMDAR blocker CNQX (Fig. 3.4E), to abrogate the

NA-evoked pressor response as well as oxidative stress (Fig. 3.5B). Further, NMDAR activation by L-glutamate mediates a Ca^{2+}/calmodulin-dependent nNOS-derived NO generation and neurotoxicity (Garthwaite et al., 1988; Dawson et al., 1993). There is also evidence that NO is involved in glutamate-mediated neurotransmission in different brain areas (Southam et al., 1991; Montague et al., 1994) including the RVLM (Martins-Pinge et al., 1999). Additionally, the nNOS-derived NO in the RVLM causes sympathoexcitation in reported studies including ours (Martins-Pinge et al., 2007; Ibrahim and Abdel-Rahman, 2012). Therefore, It is likely that the increased levels of NO by NA (0.01-1mM) in PC12 cells (Fig. 3.6C) levels, which agrees with a reported finding in cultured endothelial cells treated with similar (0.5-2mM) NA concentrations (Huang et al., 2012), is probably due to the activation of NMDAR, via GPR109A mediated glutamate release. Notably, higher NO levels can contribute to RVLM oxidative stress via its interaction with elevated superoxide levels, detected by DHE staining in the RVLM of NA treated rats (Fig. 3.5B), to produce peroxynitrite radical (Beckman et al., 1990), which causes dose-dependent transient excitatory responses when injected into the RVLM (Zanzinger, 2002). Conversely, others reported that intra-RVLM injection of NO precursor or donor decreases sympathetic nerve activity and BP (Kagiyama et al., 1997). Therefore, the possibility must be considered that the GPR109A-mediated increase in NO levels could either contribute to, or oppose, the pressor effect of intra-RVLM NA.

In conclusion, the present study presents the first evidence for GPR109A expression in the RVLM, and its mediation of sympathoexcitation and elevation of BP via glutamate/NMDAR-dependent mechanisms (Fig. 3.9). The complementary pharmacologic and

biochemical findings clearly implicate the GPR109A in the observed responses. The present pharmacological findings might have clinical relevance in situations where high doses of NA are prescribed for the treatment of hyperlipidemia. Further, the present findings might have pathophysiological ramifications, particularly in hypertension for two reasons. First, there is a clear link between an exacerbated RVLM neuronal oxidative stress and the elevated BP in hypertension (Wu et al., 2014). Second, compared to normotensive controls, activation of RVLM NMDAR causes greater elevation in BP in spontaneously hypertensive rats (Lin et al., 1995). Collectively, the present findings, along with these reported studies, highlight central GPR109A as molecular target for the development of novel antihypertensive medications.

Figure 3.9. Proposed GPR109A signaling in the RVLM

Suggested mechanisms for the GPR109A-mediated pressor response caused by nicotinic acid (NA) microinjection into the RVLM. The sequence of events is based on the findings that: (i) Intra-RVLM GPR109A activation (NA) increased blood pressure in conscious freely moving rats (Fig. 3.3), and increased RVLM ROS levels (Fig. 3.5); (ii) NA increased Ca^{2+}, glutamate NO and ROS levels (Figs. 3.6 and 3.7) in PC12 cells, which exhibit a neuronal phenotype. The dashed arrows indicate proposed signaling (see text for details).

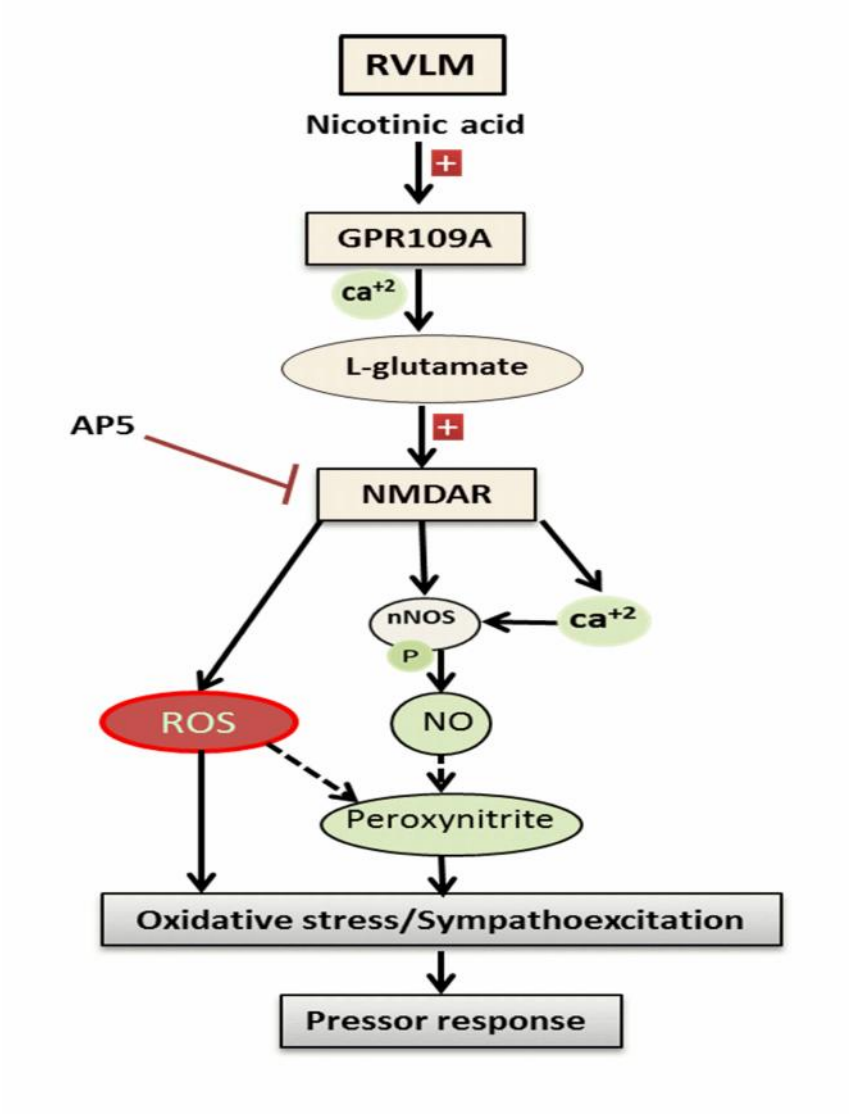
RVLM
Nicotinic acid
GPR109A
ca+2
L-glutamate
AP5
NMDAR
nNOS
P
ca+2
ROS
NO
Peroxynitrite
Oxidative stress/Sympathoexcitation
Pressor response

CHAPTER FOUR - PGE2-EP3 RECEPTOR SIGNALING IS CRITICAL FOR THE CENTRAL GPR109A-MEDIATED PRESSOR RESPONSE IN CONSCIOUS RATS

4.1. Abstract

Nicotinic acid (NA) activation of the G protein-coupled receptor 109A (GPR109A) in immune cells releases prostaglandins (PGs), and prostaglandin E2 (PGE2) activation of its EP3 receptor (EP3R) in the CNS increases sympathetic activity and blood pressure (BP). Despite NA ability to reach the brain, it is not known if PGE2 release and its activation of EP3R in the rostral ventrolateral medulla (RVLM) contribute to the centrally-mediated pressor effect of NA observed in our recent study. To test this hypothesis, we determined if the EP3R is expressed in the RVLM, and if PGE2 release in the RVLM is involved in the pressor and autonomic (sympathoexcitatory) responses elicited by intra-RVLM NA in conscious rats. Biochemical measurements showed higher PGE2 levels, c-Fos expression, ERK1/2 and nNOS phosphorylation along with oxidative stress in the RVLM of NA-treated rats. Further, PGE2 increased L-glutamate release in cultured PC12 cells. Selective pharmacological inhibition of nNOS (N^{ω}-propyl-l-arginine, NPLA) abolished the pressor response and the associated oxidative stress caused by intra-RVLM NA. We present the first evidence that EP3R is expressed in the RVLM and that the selective EP3R blocker L-798106 attenuated the NA-evoked pressor response and the associated biochemical responses. These findings suggest an intermediary role for PGE2-EP3R signaling in the GPR109A-mediated elevations of RVLM neuronal activity and BP. Further, the findings yield new insight into the sympathoexcitatory role of RVLM EP3R.

4.2. Introduction

Nicotinic acid (NA) is used for the treatment of dyslipidemia and prevention of clinical cardiovascular diseases partly via a recently identified receptor, GPR109A. The most common side effect of NA is the flushing reaction due to Ca^{2+}-dependent release of different prostaglandins (PGs) including prostaglandin I_2 (PGI_2), prostaglandin E_2 (PGE_2), and prostaglandin D_2 (PGD_2) (Benyo et al., 2005). Intracerebroventricular (ICV) or PGE2 microinjection into the hypothalamic paraventricular nucleus (PVN) increases the sympathetic outflow/plasma catecholamines and BP in rats, and these effects are not observed with other PGs (Ando et al., 1995; Ariumi et al., 2002; Murakami et al., 2002; Zhang et al., 2011). PGE2 also causes L-glutamate release in different CNS cell types (Bezzi et al., 1998; Wang et al., 2015), and induces reactive oxygen species (ROS) generation via activating NADPH Oxidase (NOX) (Wang et al., 2013a). Further, central (ICV) injection of PGE2 or misoprostol, the prostaglandin EP receptor agonist, increases c-Fos, a marker of neuronal activity, levels (Bullitt, 1990; Morgan and Curran, 1991) in different brain areas (Lacroix et al., 1996; Zhang et al., 2011). However, there is currently no information on the expression and function of EP receptors in one of the major cardiovascular regulating nuclei, the RVLM.

Our previous findings (Rezq and Abdel-Rahman, 2015) showed that GPR109A is expressed in tyrosine hydroxylase immunoreactive neurons (TH-ir) in the RVLM, and that its activation by NA causes a pressor response in conscious rats. Pharmacologic and mechanistic studies in PC12 cell line, which exhibits neuronal phenotype (Separovic et al., 1997), suggest

local L-glutamate release in the robust pressor response caused by intra-RVLM NA in our previous study (Rezq and Abdel-Rahman, 2015). However, it is not known if local PGE2 serves an intermediary role in the GPR109A (via NA)-mediated L-glutamate release in the RVLM and the subsequently elicited pressor response.

Four subtypes of prostanoid receptors (EP1, EP2, EP3, and EP4) are known to mediate the responses of PGE2 (Narumiya et al., 1999), among which EP3 receptor (EP3R) mediates the central cardiovascular excitatory effects and renal sympathetic nerve activity of PGE2 (Ariumi et al., 2002; Zhang et al., 2011). Notably, the reported EP3R-dependent activation of ERK1/2 (Chuang et al., 2006; Nicola et al., 2008) could be an important mediator of sympathetic excitation because ERK1/2 activation of nNOS-NO signaling in the RVLM reduces GABA release and elicits sympathoexcitation (Chan et al., 2003; Martins-Pinge et al., 2007). Despite this knowledge, the role of EP3R in central RVLM BP regulation has not been investigated perhaps due lack of information on EP3R expression in the RVLM.

In the present study we tested the hypothesis that local PGE2 activation of EP3R plays a pivotal role in the GPR109A-mediated glutamate release and the subsequent biochemical events in the RVLM that ultimately produce the NA-evoked pressor response. To test our hypothesis, it was important to determine if the EP3R is expressed in the RVLM and in PC12 cells before conducting the pharmacological and molecular studies. In vivo studies in conscious rats included investigations of the cardiovascular function of RVLM EP3R, and the effect of its blockade (L-798106, 0.1 nmol/100nl), on the BP and autonomic responses elicited by intra-RVLM NA (20 µg/rat). Molecular studies were conducted *ex vivo*,

and in PC12 cells, to elucidate the roles of PGE2/EP3R-dependent increases in glutamate release, RVLM neuronal/sympathetic activity (c-Fos expression, p-ERK1/2 and p-nNOS levels), and oxidative stress (enhanced NOX and reduced catalase activities) as molecular mechanisms for the RVLM GPR109A (NA)-mediated pressor response in conscious rats. Parallel molecular studies on tissues collected following treatment with the inactive NA isomer, IsoNA, were conducted to confirm the dependence of the observed molecular events on GPR109A activation.

4.3. Materials and Methods

4.3.1. Animal Preparation.

Male Sprague Dawley (SD) rats (300–360 g; 12-13 weeks old; Charles River Laboratories, Raleigh, NC) housed two per cage were used in this study. The rats were kept in a controlled environment at a constant temperature of 23 ± 1°C, humidity of 50% ± 10%, and a 12-hour light/dark cycle with food (Prolab Rodent Chow, Prolab RMH 3000; Granville Milling, Creedmoor, NC) and water provided ad libitum. Surgical and experimental procedures were performed in accordance with, and approved by the Institutional Animal Care and Use Committee and in accordance with the *Guide for the Care and Use of Laboratory Animals* (Institute for Laboratory Animal Research, 2011).

4.3.2. Surgical procedure.

Femoral artery catheterization and stereotaxic implantation of RVLM guide cannula were performed under anesthesia (ketamine, 9 mg/100 g and xylazine 1 mg/100 g, i.p.) and

appropriate analgesia (buprenorphine, 0.03 mg/kg) as detailed in our recent study (Rezq and Abdel-Rahman, 2015). Histological verification of the RVLM position was done via intra-RVLM injection of fast green dye (EM Sciences, Cherry Hill, NJ).

4.3.3. Blood Pressure and Heart Rate Measurements.

Five days after the surgical procedures, ML870 (PowerLab 8/30) system was utilized to measure blood pressure (BP) and heart rate (HR) in conscious unrestrained rats. The data were analyzed and displayed using LabChart (v. 7) pro software (AD Instruments, Colorado Spring, CO) as in our reported studies (Ibrahim and Abdel-Rahman, 2011; Nassar et al., 2011; Penumarti and Abdel-Rahman, 2014).

4.3.4. Spectral Analysis and Heart Rate Variability Analysis.

Spontaneous baroreflex sensitivity (BRS) was measured by the frequency domain analysis method as in reported studies including ours (Parati et al., 1995; Shaltout and Abdel-Rahman, 2005) using Nevrokard SA-BRS software package (Nevrokard SA-BRS; Medistar, Ljubljana, Slovenia) for small animals. The Power of RR interval (RRI) and spectral density oscillations computed for the two specific frequency bands, low frequency (LF, 0.25–0.75 Hz) and high frequency (HF, 0.75–3 Hz) domains, which reflect changes in sympathetic and vagal activity, respectively (Malliani et al., 1991) were used as indices for spontaneous BRS while the sympathovagal balance index (LF_{RRI}/HF_{RRI}) was used as an index of heart rate variability (HRV).

4.3.5. Cell Culture.

Rat neuronal pheochromocytoma cell line (PC12 cells) purchased from ATCC (Rockville, MD) was used according to the protocol detailed in our recent study (Rezq and Abdel-Rahman, 2015).

4.3.6. Western Blot.

Protocols from our recent study (Rezq and Abdel-Rahman, 2015) were followed. For EP3R expression, membranes were incubated with anti EP3R polyclonal antibody (1:500; Cayman, Ann Arbor, MI) at 4°C overnight. The band was verified using EP3R blocking peptide (Cayman, Ann Arbor, MI). For ERK1/2 and nNOS measurements, membranes were incubated overnight at 4°C with a mixture of rabbit anti-phospho-nNOS (Ser1417) antibody (1:500; Thermo Fisher Scientific, Waltham, MA) or rabbit anti-ERK1/2 (1:500; Cell Signaling, Danvers, MA) and mouse polyclonal anti-nNOS antibody (1:500; BD Biosciences, San Jose, CA) or mouse anti-pERK1/2 (1:500; Cell Signaling, Danvers, MA). Membranes were washed four times with phosphate-buffered saline (PBS) containing 0.1% Tween 20 then incubated for 60 min with mixture containing IRDye680-conjugated goat anti-mouse and IRDye800-conjugated goat anti-rabbit (1:5000; LI-COR Biosciences). Bands representing phosphorylated and total protein were detected simultaneously by using Odyssey Infrared Imager and analyzed with Odyssey application software version .3 (LI-COR Biosciences). Data represent mean values of integrated density ratio of p-nNOS or p-ERK1/2 normalized to the corresponding total nNOS (t-nNOS) or total ERK1/2 (t-ERK1/2), respectively.

4.3.7. Immunofluorescence.

The protocol used in our recent report (Rezq and Abdel-Rahman, 2015) was used for TH-ir neurons and c-Fos-ir neurons colocalization studies in coronal sections containing the RVLM, rostrally from -12.8 to -11.8 mm relative to bregma (Paxinos et al., 1980). Frozen sections from brains of treated and control rats (n = 5-7) were incubated for 48 h at 4°C in a mixture of mouse anti-TH (1:200; EMD Milipore, Temecula, CA) and rabbit polyclonal anti-c-Fos antibody (1:200; Santa Cruz Biotechnology, CA). The sections then were incubated for 2 h in a mixture of Cy3-conjugated donkey anti-mouse and fluorescein isothiocyanate-conjugated donkey anti-rabbit (1:200; Jackson Immunoresearch Laboratories Inc., West Grove, PA). A Zeiss LSM 510 confocal microscope (Carl Zeiss Inc., Thornwood, New York) was used for the visualization, acquisition, and quantification of colocalization. Four to six sections per animal at the level of RVLM were examined. Fluorescence intensity was quantified using Zen Lite 2011 software.

4.3.8. Measurement of PGE2.

PGE2 level in RVLM homogenates (10 µg protein/sample) or the culture media of PC12 cells was measured using rat PGE2 ELISA kit (Cayman, Ann Arbor, MI) according to the manufacturer's instructions. The absorbance was detected at 420 nm. A standard curve was established using serial dilutions of PGE2 standard. Different samples PGE2 levels were calculated from the standard curve equation.

4.3.9. NOX Activity.

NOX activity was measured according to reported protocols (La Favor et al., 2013) with modification. For this assay, 30 µl of homogenate was added to 180 µl of a cocktail containing 10 µM Amplex Red (Molecular Probes, OR), 2.0 U/ml horseradish peroxidase, 30 U/ml superoxide dismutase, and 100 µM NADPH (Sigma Aldrich, St. Louis, MO) in PBS. Fluorescence intensity (530 nM ex/590 nM em) was measured continuously with a microplate fluorescence reader at 37°C at 5 min intervals for 30 min, total NADPH-dependent H_2O_2 generated in the sample was used as an index of NOX activity. Activity was normalized to total protein content, as determined by Bradford assay (Bio-Rad).

4.3.10. Catalase Activity.

RVLM punches from injected sites were homogenized in 35 µl lysis buffer (20 mM Tris, pH 7.5, 150 mM NaCl, 1 mM EDTA, 1 mM EGTA, 1% Triton X-100, 2.5 mM sodium pyrophosphate, 1 mM β-glycerol-phosphate, 1 mM activated sodium orthovanadate, and 1 µg/ml leupeptin) with protease inhibitor cocktail (Roche Diagnostics, Indianapolis, IN) followed by centrifugation at 14,000 rpm for 20 min at 4°C. The supernatant was separated and assayed for protein content (Bradford assay, Bio-Rad). Catalase activity was determined colorimetrically in 10 µg protein using the Catalase Assay Kit (catalog no. CAT-100, Sigma-Aldrich, St. Louis, MO) according to the manufacturer's instructions.

4.3.11. DCFH-DA.

A 20 mM stock solution of 2′,7′-Dichlorofluorescein diacetate (DCFH-DA) (Molecular Probes, Grand Island, NY) in methanol was prepared and kept at -20°C in the dark. RVLM homogenate in PBS (50 mM, pH 7.4) from different groups was centrifuged at 14,000 rpm for 20 min at 4°C. The protein in the supernatant was quantified using a Bio-Rad protein assay system. Shortly before the experiment, DCFH-DA stock solution was freshly diluted with PBS to 150 μM working solution. The reaction started by adding 10 μl RVLM homogenate supernatant in a 96-well plate for a final concentration of 25 μM DCFH-DA to generate fluorescent 2′,7′-Dichlorofluorescein (DCF) followed by measuring fluorescence intensity using a microplate fluorescence reader at excitation 485 nm/emission 530 nm for 60 min at 37°C . DCF was used to generate the standard curve. Reactive oxygen species (ROS) level was expressed in terms of relative fluorescence units (RFU) of produced DCF as detailed in our recent study (Rezq and Abdel-Rahman, 2015).

4.3.12. L-glutamate Measurement

L-glutamate release in cultured PC12 cells was measured using Amplex Red kit (Molecular Probes, Invitrogen) following the manufacturer instructions and as detailed in our recent study (Rezq and Abdel-Rahman, 2015).

4.3.13. Protocols and Experimental Groups.

We investigated the effects of prior RVLM EP3R blockade (L-798106, 0.1 nmol) on BP, HR and autonomic responses elicited by intra-RVLM NA (20 µg). It was important to determine,

for the first time, the dose of L-798106 that optimally block the RVLM EP3R in a pilot study (*n* = 3). The selected intra-RVLM PGE2 dose (0.2 nmol), which produced pressor response when injected into the hypothalamus (Zhang et al., 2011), also produced pressor response that was abolished by the selected L-798106 dose in our pilot study. Conscious unrestrained SD rats (*n* = 5-8 each), pre-instrumented with intra-RVLM and intra-arterial cannulas as indicated under methods, were used. BP and HR were allowed to stabilize at baseline, for at least 30 min, before intra-RVLM microinjections started. All injections (100 nl) were made unilaterally into the RVLM according to established protocol in our lab (Penumarti and Abdel-Rahman, 2014). Control rats received 100 nl of the artificial cerebrospinal fluid (ACSF) that was used as a vehicle. Treatment groups received L-798106 or the vehicle followed 10 min later by 100 nl of NA (20 µg) or ACSF. To investigate the role of nNOS in NA-mediated pressor response, the selective nNOS blocker, N^{ω}-propyl-l-arginine (NPLA, 250 pmol) was injected in a separate group of rats followed by NA (20 µg) or equal volume of ACSF (n = 5 each). The selected NPLA dose was used in our previous studies (Ibrahim and Abdel-Rahman, 2012). At the end of BP recording period, animals were euthanized with a lethal dose of pentobarbital sodium (100 mg/kg), and their brains were rapidly removed and stored at -80°C. For the different biochemical measurements detailed above, a 0.75 micropunch instrument was used to collect unilateral micropunches (Stoelting Co., Wood Dale, IL) at -12.8 to -11.8 mm relative to bregma (Paxinos et al., 1980) from the injected RVLM site (*n* = 5-8). For *in vitro* EP3R expression (WB), PGE2 and glutamate measurements, neuronal PC12 cells were used as surrogates of RVLM neurons. PGE2 ELISA measurement was performed in the media of cells treated with NA (1mM) for 5 min. The effect of NA (1 mM) or PGE2 (10 µM) on glutamate release in treated

cells was investigated with or without 30 min prior incubation with L-798106 (10 μM). To investigate the role of nNOS in NA mediated L-glutamate release, PC12 cells were pretreated with NPLA (1 μM) for 30 min according to reported protocol (Filpa et al., 2015). For each experiment, IsoNA (20 μg in rats or 1mM in cells), the inactive isomer of NA that lack GPR109A activity (Maciejewski-Lenoir et al., 2006), was used to verify the dependence of the effect on GPR109A. The tissues used for *ex vivo* biochemical measurements following intra-RVLM IsoNA (20 μg) came from rats used in our recent study (Rezq and Abdel-Rahman, 2015).

4.4. Drugs

NA and L-798106 were purchased from Sigma-Aldrich (St. Louis, MO). PGE2 was purchased from Cayman (Ann Arbor, MI). Sterile saline was purchased from B. Braun Medical (Irvine, CA). IsoNA acid was purchased from TCI America (Portland, OR). NPLA was purchased from Abcam (Cambridge, MA).

4.5. Statistical Analysis

In vitro data were collected from three independent experiments, and in vivo data were collected from 3-8 rats per group. Data are expressed as mean ± standard error of mean (S.E.M). Analysis Of Variance (ANOVA) or repeated-measures ANOVA followed by Bonferroni's post hoc test and Student's *t*-test were carried out using GraphPad Prism to state differences between groups.

4.6. Results

4.6.1. EP3R is Expressed in the RVLM and PC12 Cells.

EP3R was expressed in the RVLM and in PC12 cells (Fig. 4.1A), and the bands were verified using EP3R blocking peptide (Fig. 4.1B) as well as by including blot from the kidney as positive control (Kotani et al., 1995). Notably, the molecular weight of EP3R varies from 53-98 kDa (Fig. 4.1A) according to the degree of its posttranslational modification, and whether the receptor is expressed as monomer or dimer (Osborne et al., 2009).

4.6.2. GPR109A Activation via NA Increases PGE2 Levels in the RVLM and in PC12 Cells.

Although a number of studies reported NA to increase PGE2 levels by activating peripheral GPR109A receptor, there is no evidence for NA ability to produce a similar effect centrally. Therefore, PGE2 measurements were done in the RVLM of NA-treated rats (20 µg, n = 6-8) and in PC12 cells incubated with NA (1 mM, n = 3). NA caused approximately two-fold increase in PGE2 levels, compared to vehicle treatment in both preparations (Fig. 4.1C, D). This effect is likely GPR109A receptor-dependent because the inactive NA isomer, IsoNA, did not change PGE2 levels in both preparations (Fig. 4.1C, D).

4.6.3. Central PGE2/EP3R Signaling Mediates the Pressor and Autonomic Responses Elicited by Intra-RVLM NA.

Due to the lack of data on the cardiovascular effects of intra-RVLM PGE2 or the EP3R blocker, we used a PGE2 dose (0.2 nmol), which produced sympathoexcitation following

microinjection into the hypothalamus (Zhang et al., 2011), in the absence or presence of the EP3R antagonist, L-798106 (0.1 nmol). Intra-RVLM PGE2 caused modest but significant ($P < 0.05$; n=3) increase in BP, which was fully abrogated by prior EP3R blockade by L-798106 (0.1 nmol/100nl; $n = 5$) (Fig. 4.2A). Similarly, prior EP3R blockade significantly ($P < 0.05$) attenuated the pressor and bradycardic responses caused by intra-RVLM NA (20 µg; $n = 8$) (Fig. 4.2C and D). The significant ($P < 0.05$) increase in LF/HF ratio, caused by intra-RVLM NA (indicative of increased sympathetic dominance) was abrogated by prior EP3R blockade (Fig. 4.3); neither EP3 blockade nor IsoNA had any effect on the measured variables (Data not shown). Moreover, there were no significant differences between the BP and HR values of all groups prior to drug or vehicle administration (Table 1).

4.6.4. EP3R Mediates the NA-Evoked Increase in Glutamate Levels.

Our previous in vivo and PC12 cell findings (Rezq and Abdel-Rahman, 2015) confirmed the contribution of L-glutamate release to the intra-RVLM NA-mediated pressor response. The purpose of this experiment was to investigate the role of EP3R in L-glutamate release and in the pressor response elicited by intra-RVLM NA or PGE2 (Fig. 4.2). NA (1 mM) or PGE2 (10 µM) significantly ($P < 0.05$) increased glutamate level in cultured PC12 cells, and such response was virtually abolished by prior incubation with the selective EP3R blocker L-798106 (10 µM) (Fig. 4.4).

4.6.5. Intra-RVLM GPR109A Activation Produces EP3R-Dependent Increase in c-Fos Expression in RVLM TH-ir Neurons.

In this experiment, we investigated whether GPR109A (NA)-evoked increase in c-Fos expression in RVLM TH-ir neurons (reflects sympathoexcitation) is EP3R-dependent. Immunofluorescence staining of RVLM sections taken from animals that received different treatments revealed that, compared to the vehicle, intra-RVLM NA (20 µg), but not IsoNA (20 µg), significantly ($P < 0.05$) increased c-Fos expression in the RVLM TH-ir neurons (Fig. 4.5). Further, prior RVLM EP3R blockade (L-798106; 0.1 nmol/100nl) abrogated the increase in c-Fos expression in the RVLM TH-ir neurons caused by intra-RVLM NA (20 µg) (Fig. 4.5D). The total numbers of TH-ir neurons in the control and treatment groups were similar (Fig. 4.5, lower panels).

4.6.6. EP3R Blockade Abrogated the Increases in RVLM ERK1/2 and nNOS Phosphorylation and NOX Activity and the Decrease in Catalase Activity Caused by Intra-RVLM NA.

NA (20 µg; $n = 5$), compared to its vehicle ($n = 6$), significantly ($P < 0.05$) increased RVLM ERK1/2 and nNOS phosphorylation (Fig. 6), NOX activity along with reducing catalase activity, and these responses were associated with increased RVLM ROS level (Fig. 4.7). These biochemical responses were mediated by NA activation of GPR109A because they were absent in IsoNA treated rats (Figs. 4.6 and 7), and were EP3R-dependent because they were abrogated by prior EP3R blockade with L-798106 (0.1 nmol/100nl) in NA-treated rats (Figs. 4.6 and 7).

4.6.7. Inhibition of RVLM nNOS Attenuated GPR109A-Mediated Oxidative Stress and Pressor Response.

The objective of this experiment was to establish a causal role for nNOS activation in central GPR109A-mediated RVLM oxidative stress and pressor response. Prior intra-RVLM injection of the selective nNOS inhibition NPLA (250 pmol) abrogated ($P<0.05$) the pressor and bradycardic effects (Fig. 4.8A-C) and the increases in nNOS phosphorylation (Fig. 4.8D), ROS (Fig. 4.8E) and NOX (Fig. 4.8F) as well as the reduction in catalase activity (Fig. 8G) caused by intra-RVLM NA (20 µg; n = 5). Notably, NPLA significantly ($P<0.05$) inhibited nNOS phosphorylation (Fig. 4.8E) and modestly ($P<0.05$) reduced ROS level (Fig. 4.8F) in the RVLM but had no effect on the other biochemical or cardiovascular variables measured in this experiment (Fig. 4.8).

4.6.8. Inhibition of nNOS Attenuated GPR109A-Mediated L-glutamate Release in PC12 cells and c-Fos Induction in RVLM.

Prior incubation of the selective nNOS inhibition NPLA (1 µM) abrogated ($P<0.05$) NA-mediated L-glutamate release in PC12 cells (Fig. 4.9A). Moreover, Prior intra-RVLM injection of NPLA (250 pmol) protected NA-treated rats from increased c-Fos expression, the marker of neuronal excitability (Fig. 4.9B).

Table 4. 1. MAP (mmHg) and HR (beats/min) values before pharmacological intervention.

Values of Mean Arterial Pressure (MAP, mmHg) and Heart Rate (HR, beats/min) at the end of pretreatment (time=30min) and immediately before treatment with the indicated intervention or its vehicle (ACSF).

Pretreatment/Treatment	Rats per group (n)	MAP (mmHg)	HR (beats/min)
ACSF	7	126.1 ± 5.501	341.7 ± 12.36
ACSF/Nicotinic acid	8	114.9 ± 5.266	366.5 ± 28.50
ACSF/PGE2	3	115.3 ± 5.365	415.4 ± 14.88
L-798106 /PGE2	3	124.0 ± 5.033	360.1 ± 4.167
L-798106 /Nicotinic acid	5	128.0 ± 7.406	335.0 ± 8.630
ACSF/NPLA	5	114.2 ± 2.46	347.8 ± 15
NPLA/NA	5	111.6 ± 4.65	326.9 ± 11.98

Figure 4.1. EP3R expression in the RVLM and PC12 cells and NA ability to increase PGE2 levels in both preparations

(A) Expression of EP3R (53-98 kDa) in the rat RVLM, PC12 cells or kidney (positive control); the wide range in molecular weight is ascribed to the different forms of the receptor (Osborne et al., 2009). The lower panel shows expression of EP3R (53-98 kDa) in the rat RVLM, PC12 cells or kidney (positive control). EP3R primary antibody was pre-incubated with its blocking peptide. Data are presented as integrated density ratio of GPR109A to the corresponding β-actin values (n = 4) and expressed as mean ± S.E.M. **(B)** Effect of NA (1 mM), or IsoNA (1 mM) on PGE2 levels (folds of control) in PC12 cells (n = 3 independent experiments). Measurements were done after 5 min incubation time. **(C)** RVLM PGE2 concentration (pg/ml) following intra-RVLM ACSF (100 nl; n = 6), NA (20 μg; n = 8) or IsoNA (20 μg; n = 5) injection. Data are expressed as mean ± S.E.M. *P < 0.05 vs. control or ACSF values; $^{\#}P$ < 0.05 vs. NA.

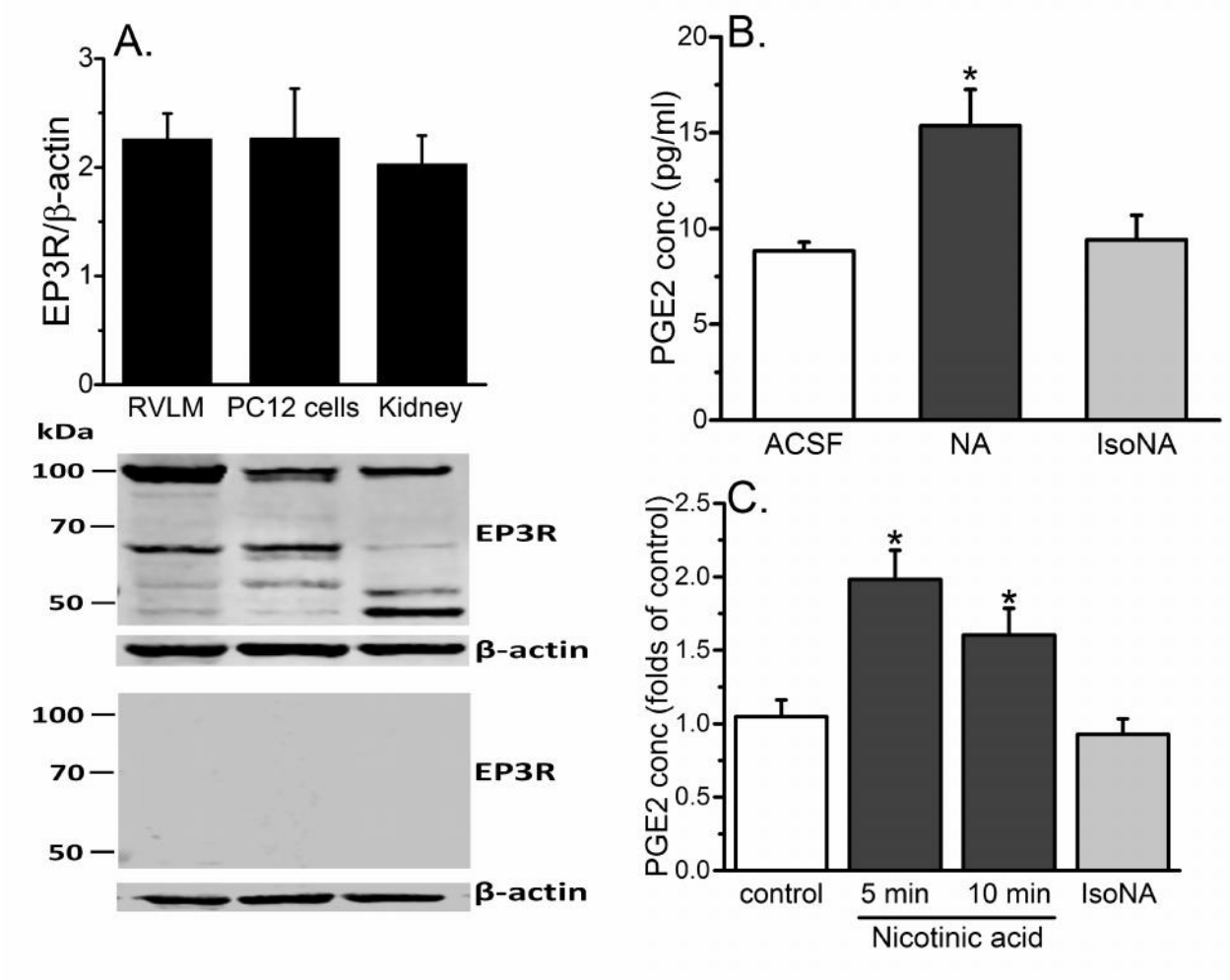
A.
EP3R/β-actin
RVLM
PC12 cells
Kidney
kDa
100
70
50
EP3R
β-actin
B.
PGE2 conc (pg/ml)
ACSF
NA
IsoNA
C.
PGE2 conc (folds of control)
control
5 min
10 min
IsoNA
Nicotinic acid

Figure 4.2. Effect of intra-RVLM NA or PGE2 on MAP and HR with or without EP3R blockade

Time-course changes in MAP and HR caused by intra-RVLM PGE2 (0.2 nmol, $n = 3$) **(A, B)** or NA (20 µg; $n = 8$) **(C, D),** compared with equal volume of ACSF, in conscious male rats pretreated, 10 min earlier, with ACSF (100 nl; $n = 8$) or EP3R blocker (L-798106, 0.1 nmol/100nl; $n = 3$-8). **(E, F)** The area under the curve (AUC) data generated from A and C, respectively for different treatments. Data from L-798106 treated rats, which were not significantly different from the control values, are not shown for clarity. Values are mean change from base line ± S.E.M. $^{*}P < 0.05$ vs. ACSF values; $^{\#}P < 0.05$ vs. NA. ACSF: artificial cerebrospinal fluid; BP: blood pressure; IsoNA: iso-nicotinic acid; RVLM: the rostral ventrolateral medulla.

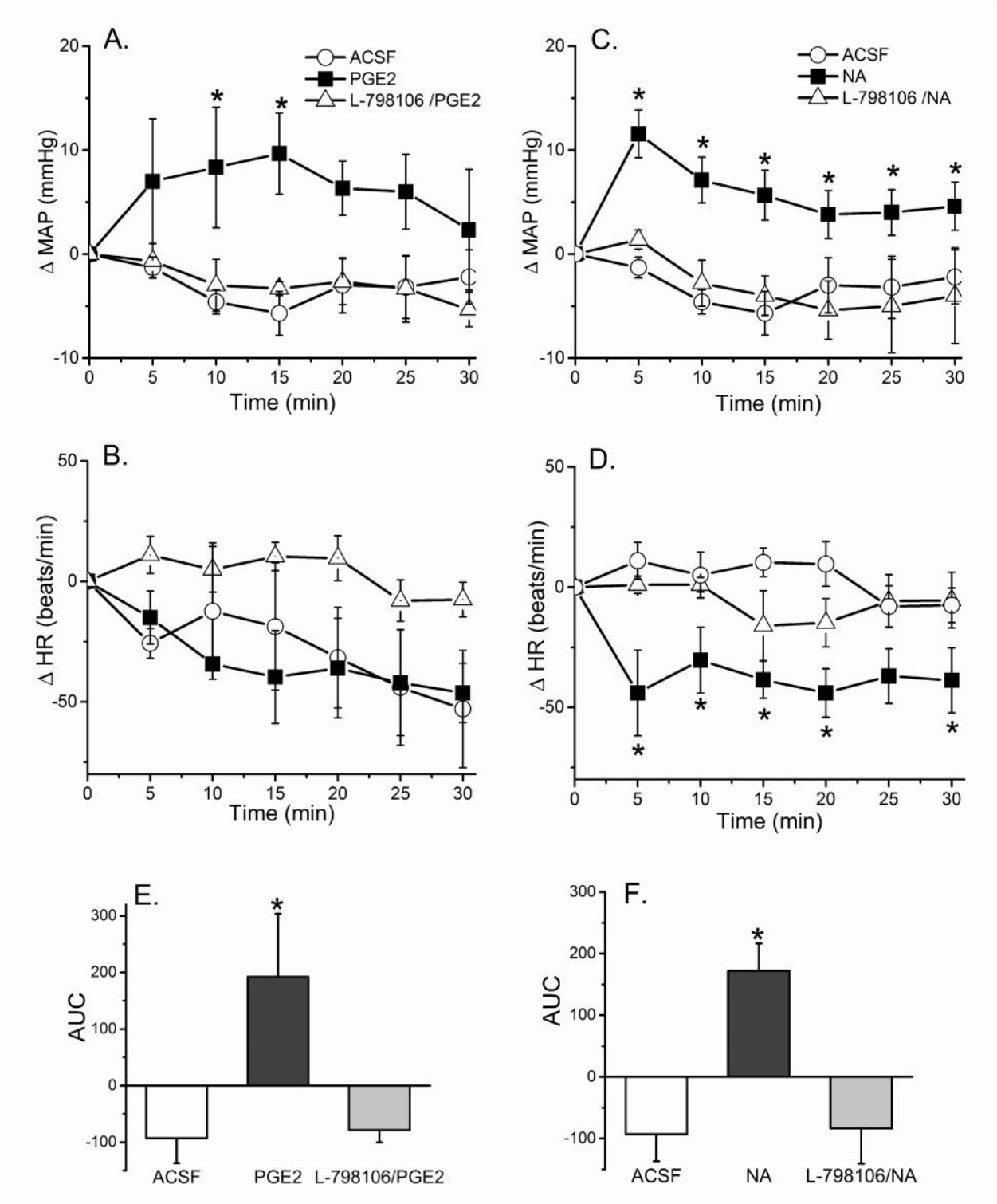
A.
ACSF
PGE2
L-798106 /PGE2
Δ MAP (mmHg)
Time (min)
C.
ACSF
NA
L-798106 /NA
Δ MAP (mmHg)
Time (min)
B.
Δ HR (beats/min)
Time (min)
D.
Δ HR (beats/min)
Time (min)
E.
AUC
ACSF
PGE2
L-798106/PGE2
F.
AUC
ACSF
NA
L-798106/NA

Figure 4.3. Autonomic changes elicited by intra-RVLM NA injection with and without prior EP3R blockade

Effect of intra-RVLM NA (20 µg; $n = 6$) or equal volume of ACSF (100 nl; $n = 6$) on: (**A**) low frequency (LF) component of spectral analysis of RRI (0.25 to 0.75 Hz), index of cardiac sympathetic tone; (**B**) High frequency (HF) component of the spectral analysis of RRI (0.75 to 3 Hz), index of cardiac vagal tone, and (**C**) LF_{RRI}/HF_{RRI} ratio as a measure of sympathovagal balance in conscious male rats pretreated, 10 min earlier, with ACSF (100 nl; $n = 6$) or EP3R blocker (L-798106, 0.1 nmol; $n = 5$). Data represent AUC values generated over the 30 min BP recording period. Values are mean ± S.E.M. $^{*}P < 0.05$ versus ACSF values; $^{\#}P < 0.05$ vs. NA.

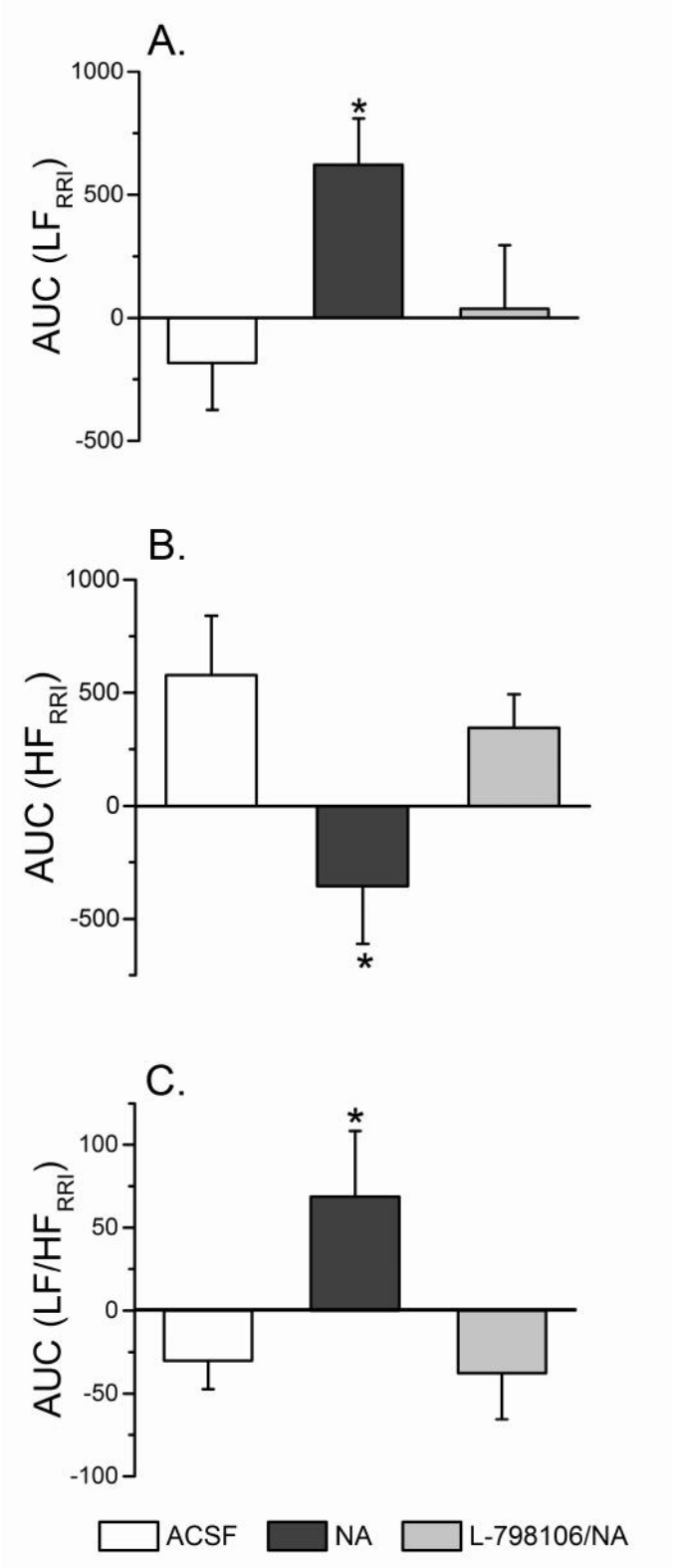
A.
1000
500
0
-500
AUC (LF RRI)
*
B.
1000
500
0
-500
AUC (HF RRI)
*
C.
100
50
0
-50
-100
AUC (LF/HF RRI)
*
ACSF
NA
L-798106/NA

Figure 4.4. Effect of intra-RVLM NA or PGE2 on glutamate release in PC12 cells (role of EP3R)

Effect of 1 min exposure of PC12 cells to PGE2 (10 μM) or NA (1 mM) on L-glutamate levels (folds increase of control) with or without 30 min prior incubation with the EP3R receptor antagonist L-798106 (10 μM). Data are expressed as mean ± S.E.M of 3 independent experiments. *$P < 0.05$ vs. control values; $^{\#}P < 0.05$ vs. NA; ^$P < 0.05$ vs. PGE2 values.

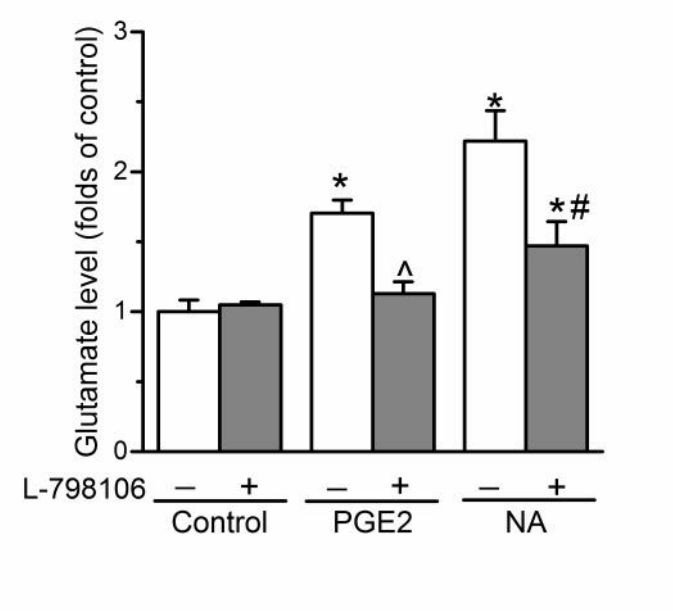
Glutamate level (folds of control)
3
2
1
0
*
*
*#
^
L-798106
–
+
–
+
–
+
Control
PGE2
NA

Figure 4.5. Effect of NA on c-Fos intensity and its co-localization with TH

Confocal dual-channel images showing TH-ir neurons (red) and c-Fos immunoreactive cell nuclei (green) in RVLM of rats treated as described under *Materials and Methods* with intra-RVLM ACSF **(A)**, 20 µg of isonicotinic (IsoNA**; B),** 20 µg of nicotinic acid **(**NA; **C)** or 0.1 nmol of the EP3R blocker L-798106 + 20 µg of NA **(D)**. In general, the 3 images for each section (A, B, C, or D) show the same field at different magnifications where the two smaller images show staining for different markers (e.g. A1 and A2) while the larger image (e.g. A) shows the merged staining for these two markers. The arrows illustrate co-labeled cells. Scale bar, 20 µm. c-Fos fluorescence intensity, number of TH-ir neurons, and percentage of TH-ir neurons colocalized with c-Fos in the RVLM of control rats and treated rats are shown below. Bar graphs represent mean ± S.E.M. of data obtained from four to six coronal brainstem sections/animal (n = 5-7 rats/group) by using one-way ANOVA followed by Bonferroni comparison test. *$P < 0.05$ vs. ACSF values; $^{\#}P < 0.05$ vs. NA.

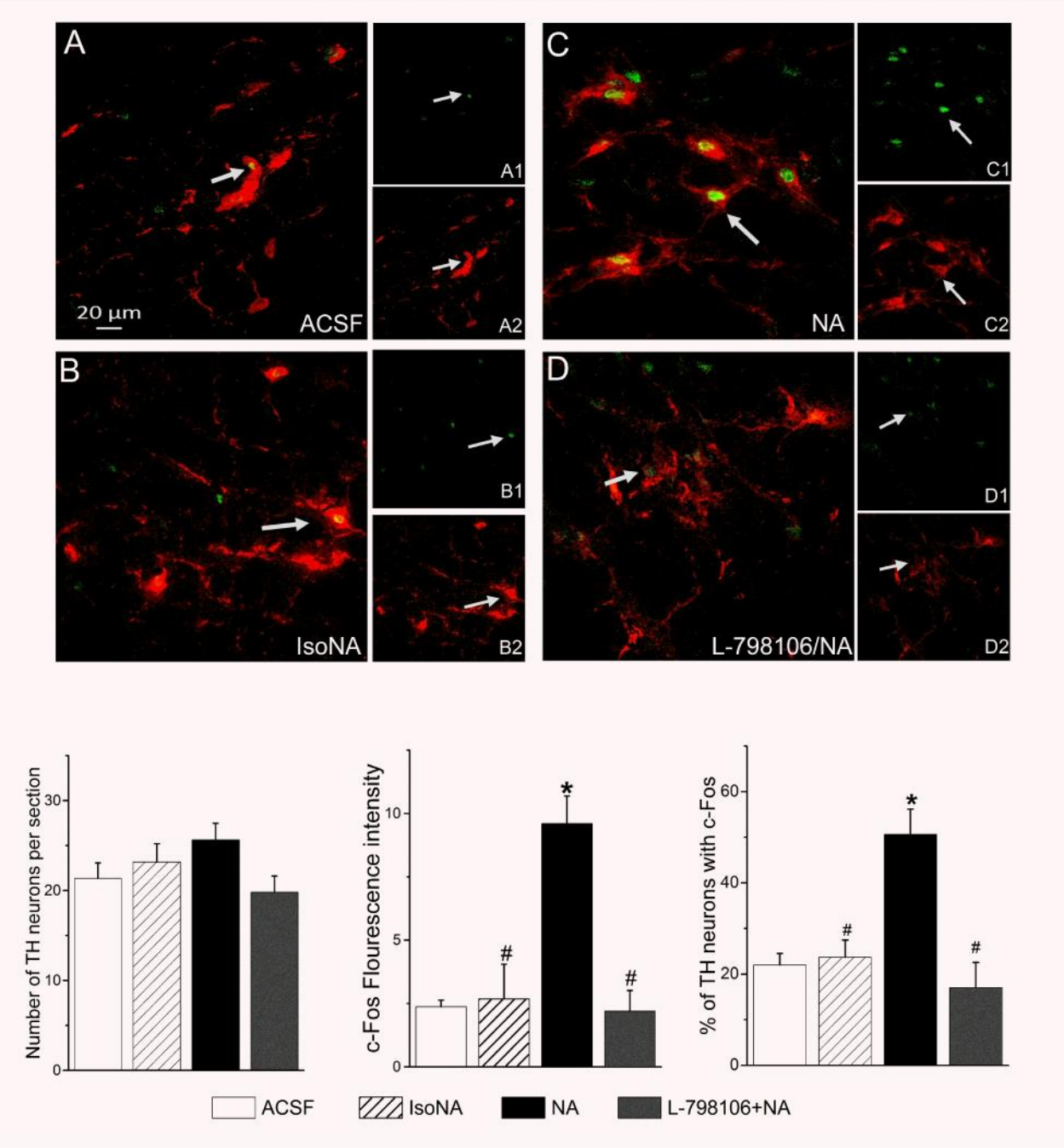
A
A1
A2
20 μm
ACSF
C
C1
C2
NA
B
B1
B2
IsoNA
D
D1
D2
L-798106/NA
Number of TH neurons per section
0
10
20
30
c-Fos Flourescence intensity
0
5
10
*
#
#
% of TH neurons with c-Fos
0
20
40
60
*
#
#
ACSF
IsoNA
NA
L-798106+NA

Figure 4.6. Effect of NA on pERK1/2 and p-nNOS levels

Changes in rat RVLM ERK1/2 **(A)** and nNOS **(B)** phosphorylation following intra-RVLM NA (20 μg) or ACSF in animals pretreated with ACSF or the EP3R antagonist L-798106 (0.1 nmol). Data are presented as integrated density ratio of phosphorylated (p-ERK1/2) or (p-nNOS) to the corresponding total (t-ERK1/2) or (t-nNOS) protein, respectively. Values are mean ± S.E.M. of 5–6 observations/group. *$p < 0.05$ versus vehicle values, $^{\#}P < 0.05$ vs. NA.

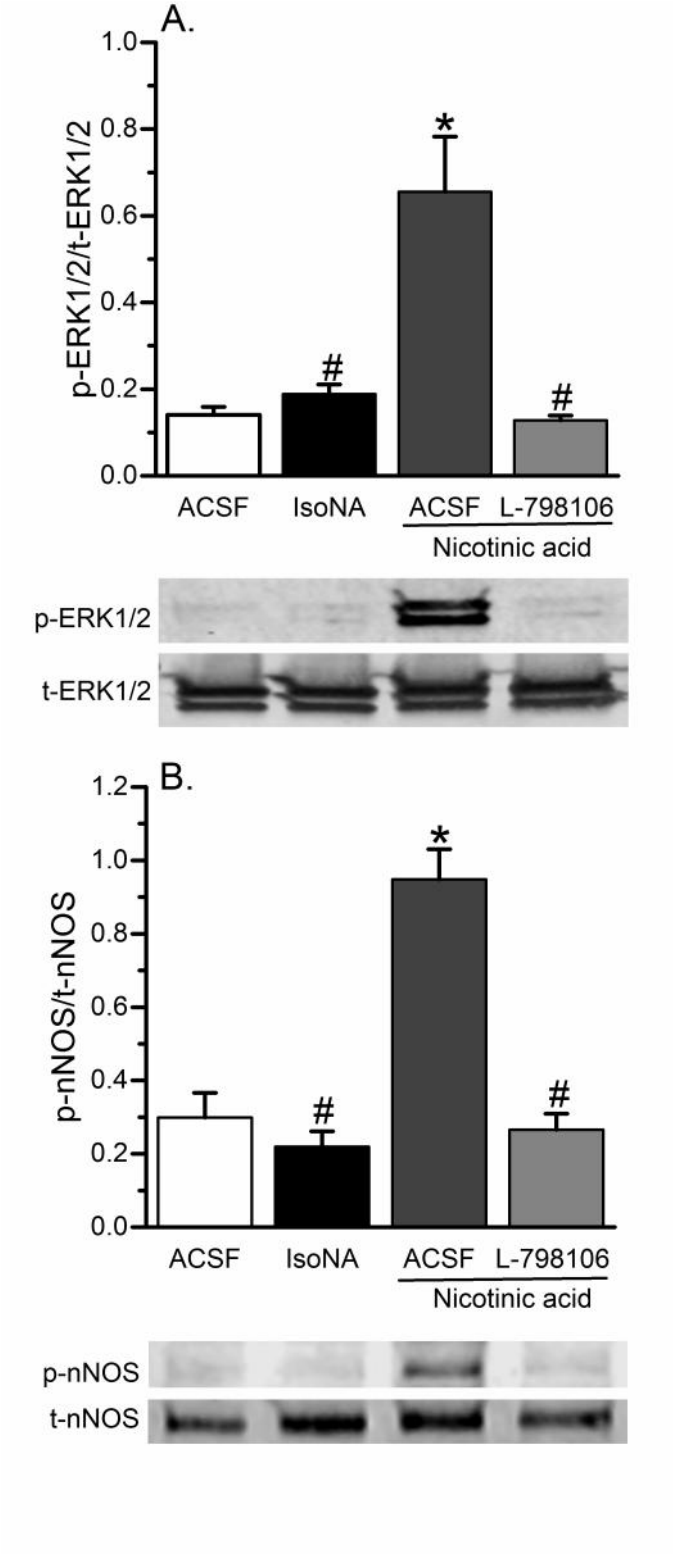
A.
p-ERK1/2/t-ERK1/2
1.0
0.8
0.6
0.4
0.2
0.0
*
#
#
ACSF
IsoNA
ACSF
L-798106
Nicotinic acid
p-ERK1/2
t-ERK1/2
B.
p-nNOS/t-nNOS
1.2
1.0
0.8
0.6
0.4
0.2
0.0
*
#
#
ACSF
IsoNA
ACSF
L-798106
Nicotinic acid
p-nNOS
t-nNOS

Figure 4.7. Effect of EP3R blockade on NA-mediated ROS generation and NOX and catalase activities in the RVLM.

(A) DCFH-DA measured ROS levels in terms of relative fluorescence units (RFU) of produced DCF in the RVLM (*n* = 5-6 rats) after ACSF (100nl), NA (20 μg), IsoNA (20 μg) or L-798106 (0.1 nmol)/ NA (20 μg). **(B)** Effect of ACSF (100nl), NA (20 μg), IsoNA (20 μg) or L-798106 (0.1 nmol)/NA (20 μg) on RVLM (*n* = 5-8 rats) NOX activity presented as the concentration of produced H2O2 (μM/μg protein). **(C)** Effect of ACSF (100nl), NA (20 μg), IsoNA (20 μg) or L-798106 (0.1 nmol)/ NA (20 μg) on RVLM (*n* = 4-6 rats) catalase activity (μmoles/μg protein/min). Values are mean ± S.E.M. **P* < 0.05 vs. ACSF values; $^{\#}P$ < 0.05 vs. NA. ACSF: artificial cerebrospinal fluid; IsoNA: iso-nicotinic acid; NA: nicotinic acid; RVLM: the rostral ventrolateral medulla.

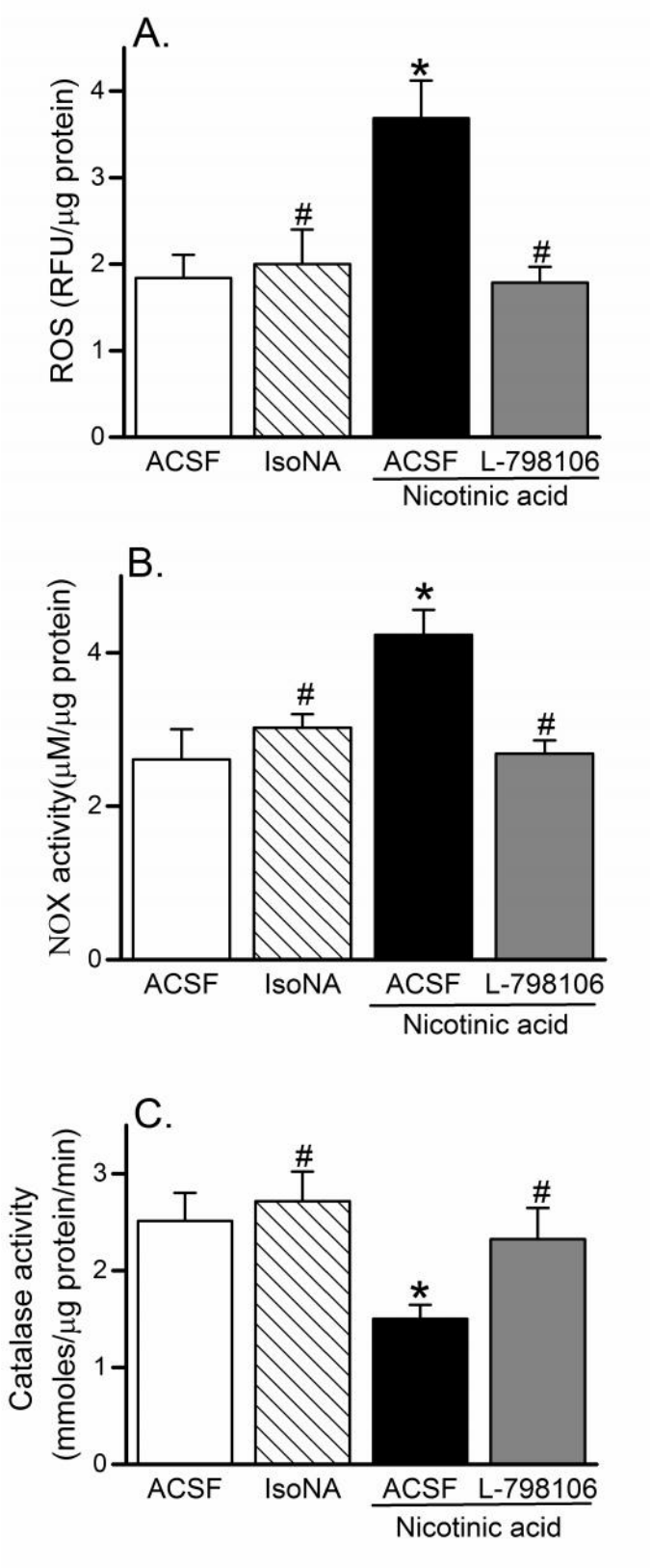
A.
ROS (RFU/μg protein)
0
1
2
3
4
*
#
#
ACSF
IsoNA
ACSF
L-798106
Nicotinic acid
B.
NOX activity(μM/μg protein)
0
2
4
*
#
#
ACSF
IsoNA
ACSF
L-798106
Nicotinic acid
C.
Catalase activity
(mmoles/μg protein/min)
0
1
2
3
#
*
#
ACSF
IsoNA
ACSF
L-798106
Nicotinic acid

Figure 4.8. Effect of intra-RVLM nNOS inhibition on GPR109A mediated pressor response and oxidative stress

Changes in **(A)** Mean arterial pressure (ΔMAP), and **(B)** Heart rate (ΔHR) following intra-RVLM microinjections of NA (20 μg) or equal volume of vehicle in conscious male SD rats pretreated, 30 min earlier, with NPLA (selective nNOS inhibitor; 250 pmol). Pretreatment with NPLA, virtually abolished the GPR109A (NA)-mediated pressor response. (**C)** Depict the area under the curve (AUC) data generated from the time-course values over the treatment (30 min) periods. (**D**) Inhibition of nNOS phosphorylation in ACSF and NA rats pretreated with NPLA (250 pmol). Effect of prior NPLA treatment (250 pmol) on ROS levels (**E**), NOX activity (**F**) or catalase activity (**G**) in rats pretreated with NA (20 μg) or equal volume of vehicle; n = 5 for all groups. **P* < 0.05 vs. ACSF (vehicle); #*P* < 0.05 vs. NA.

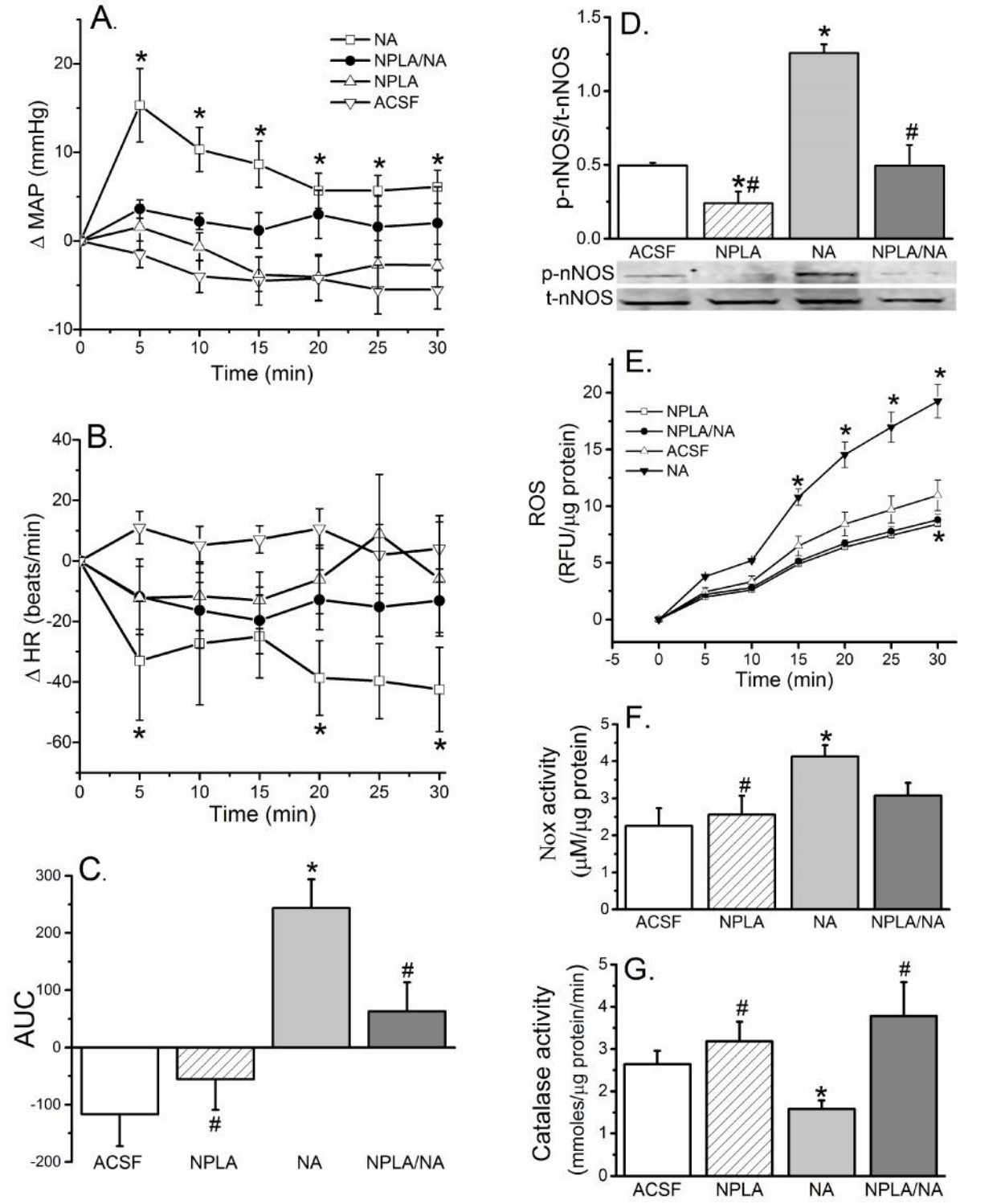
A.
NA
NPLA/NA
NPLA
ACSF
Δ MAP (mmHg)
Time (min)
B.
Δ HR (beats/min)
Time (min)
C.
AUC
ACSF
NPLA
NA
NPLA/NA
D.
p-nNOS/t-nNOS
p-nNOS
t-nNOS
E.
ROS
(RFU/μg protein)
Time (min)
F.
Nox activity
(μM/μg protein)
G.
Catalase activity
(mmoles/μg protein/min)

Figure 4.9. Effect of intra-RVLM nNOS inhibition on GPR109A mediated increase in L-glutamate release and c-Fos intensity.

(**A**) Effect of prior NPLA treatment (1μM) on NA-mediated L-glutamate release (1 min treatment) in cultured PC12 cells. (**B**) Effect of prior NPLA treatment (250 pmol) on c-Fos intensity in rats pretreated with NA (20 μg) or equal volume of vehicle; n = 5 for all groups. **P* < 0.05 vs. ACSF (vehicle); #*P* < 0.05 vs. NA.

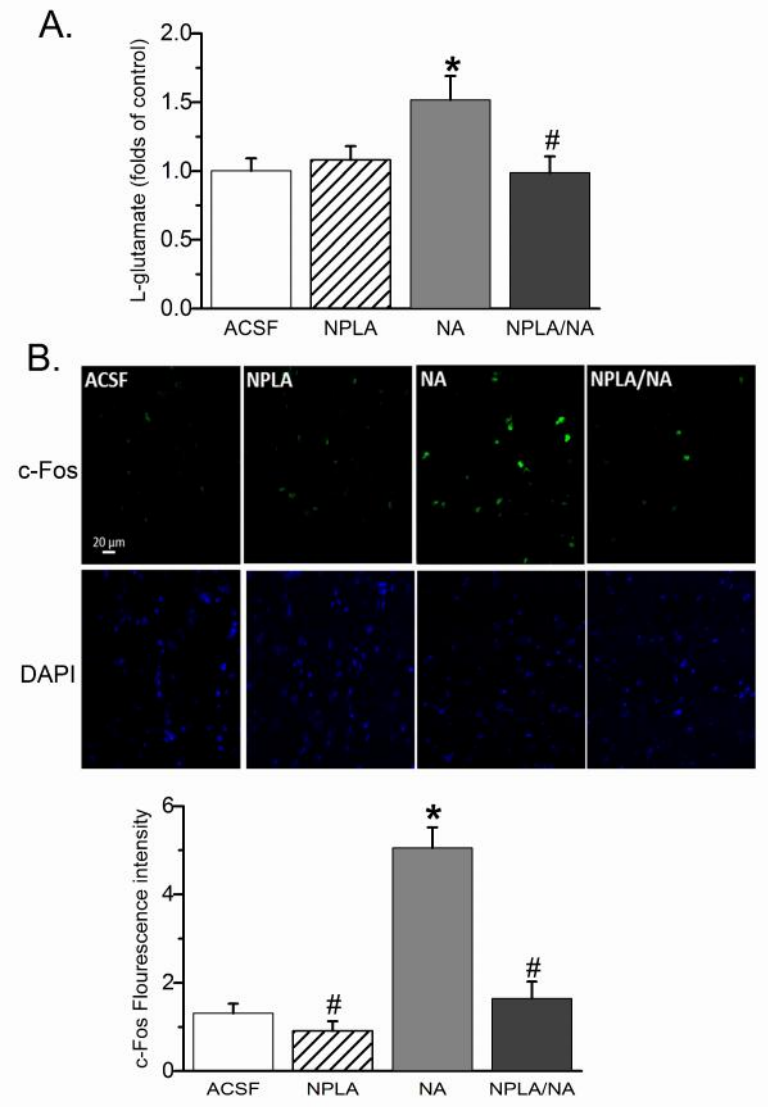
A.
L-glutamate (folds of control)
2.0
1.5
1.0
0.5
0.0
*
#
ACSF
NPLA
NA
NPLA/NA
B.
ACSF
NPLA
NA
NPLA/NA
c-Fos
20 μm
DAPI
c-Fos Flourescence intensity
6
4
2
0
*
#
#
ACSF
NPLA
NA
NPLA/NA

4.7. Discussion

In this study we tested the hypothesis that PGE2 (EP3R)-dependent elevations in mediators of oxidative stress and presympathetic neuronal activity play a pivotal role in RVLM GPR109A (NA)-mediated pressor response. Our most important findings are: (i) intra-RVLM NA or PGE2 caused a pressor response in conscious rats; (ii) NA elevated PGE2 (RVLM and PC12 cells), L-glutamate levels (PC12 cells), RVLM p-ERK1/2 and p-nNOS levels as well as RVLM TH-ir neurons excitation (c-Fos); (iii) NA induced RVLM oxidative stress due to increased NOX activity/ROS level and reduced catalase activity; (iv) EP3R blockade (L-798106) or nNOS inhibition (NPLA) attenuated the NA-evoked increases in BP and RVLM oxidative stress along with the associated biochemical responses. These findings establish a sympathoexcitatory role for PGE2-EP3R signaling in the RVLM, and present evidence for its contribution to the GPR109A-mediated RVLM oxidative stress and pressor response, at least partly, via nNOS activation.

NA, which serves as a GPR109A receptor ligand (Soga et al., 2003; Tunaru et al., 2003), produces a flushing reaction due to Ca^{2+}-dependent release of different PGs including PGE_2 (Benyo et al., 2005). Therefore, aspirin is usually prescribed for patients who receive NA for the treatment of hyperlipidemia (Andersson et al., 1977). We based our hypothesis on evidence that systemic NA reaches the brain in appreciable concentrations (Spector, 1979), the expression of the NA receptor, GPR109A, and its sympathoexcitatory function in the RVLM (Rezq and Abdel-Rahman, 2015), and on the ability of ICV or intra-PVN PGE2 to

increase sympathetic activity and BP (Ando et al., 1995; Ariumi et al., 2002; Murakami et al., 2002; Zhang et al., 2011).

In our recent study (Rezq and Abdel-Rahman, 2015), intra-RVLM NA produced a glutamate-dependent increase in BP that was associated with oxidative stress, but that study focused on the initial (1-5 min) pressor response. The purpose of the current study was to investigate whether PGs, particularly PGE2 release, contributes to longer lasting (30 min) pressor response caused by RVLM GPR109A activation given PGE2 ability to induce glutamate release (Bezzi et al., 1998; Wang et al., 2015).

While there is growing interest in the central effects of PGs, particularly the PGE2-mediated sympathoexcitation via EP3R activation (Ariumi et al., 2002; Zhang et al., 2011; Ando et al., 2015), the exact molecular mechanisms involved in this action are not clear. Equally important, the possibility has not been considered that PGE2-EP3R signaling is functional in the RVLM and contributes to the RVLM GPR109A-mediated pressor response. We reasoned that if PGE2 ability to increase NOX activity (Wang et al., 2013a), c-Fos expression and ERK1/2 pathway activation (Chuang et al., 2006) in different brain areas (Lacroix et al., 1996; Zhang et al., 2011), extends to the RVLM, may uncover a new role for PGE2 in the RVLM. Notably, these molecular mechanisms lead to sympathoexcitation and BP increase (Chalmers et al., 1994; Minson et al., 1994; Ibrahim and Abdel-Rahman, 2012; Chen et al., 2013). Therefore, we utilized a multilevel experimental approach to investigate these novel and interrelated possibilities.

In the absence of any data on the RVLM PGE2 or EP3R modulation of BP, it was important to obtain the first evidence that the EP3R is expressed in the RVLM as well as in the *in vitro* surrogate cell line, PC12 cells (Fig. 4.1A). Thereafter, we showed, for the first time, that the pressor response caused by PGE2 (0.2 nmol) microinjection into the hypothalamic pressor area (Zhang et al., 2011) is replicated in the RVLM, and is EP3R-dependent because it was abrogated by the selective EP3R antagonist L-798106 (0.1 nmol) (Fig. 4.2). Next, the significant (2-fold) elevations in PGE2 caused by NA in the RVLM and PC12 cells (Fig. 4.1C and D) presented direct link between RVLM GPR109A and local PGs. Two findings confirmed that the increase in RVLM PGE2 release was GPR109A-dependent and that the released PGE2 mediated the NA-evoked pressor response, at least partly, via local EP3R activation. First, the same intra-RVLM dose of the inactive NA isomer IsoNA failed to increase PGE2 release (Fig. 4.1). Second, intra-RVLM L-798106 abrogated the pressor response (time-course and AUC) caused by intra-RVLM NA (Fig. 4.2).

Whether L-glutamate release constitutes a biochemical link between NA and PGE2 deserved investigation because the GPR109A-dependent glutamate release, observed in PC12 cells, explains, at least partly, the pressor response caused by intra-RVLM NA in our recent study (Rezq and Abdel-Rahman, 2015). Here, we showed that NA increased PGE2 release in RVLM and in PC12 cells (Fig. 4.1), and increased glutamate release in PC12 cells via a PGE2-EP3R dependent mechanism (Fig. 4.4). These novel findings supported our hypothesis and further verified the relevance of the biochemical findings generated in PC12 cells in our present and recent studies (Rezq and Abdel-Rahman, 2015). The present findings

are consistent with PGE2 ability to: (i) Ca^{2+}-dependently increase glutamate levels in cultured astrocytes and neurons (Bezzi et al., 1998; Wang et al., 2015); (ii) enhance glutamatergic neurotransmission in primary micro-cultures of the rat hypothalamic structures (Simm et al., 2015); (iii) augment excitotoxicity produced by NMDA in mice (Iadecola et al., 2001); and (iv) augment glutamate induced excitotoxicity in hippocampal slices via EP3R activation (Ikeda-Matsuo, 2013).

The GPR109A expression in the RVLM TH-ir (presympathetic) neurons (Rezq and Abdel-Rahman, 2015) is functionally important because its activation significantly increased c-Fos expression, which reflects neuronal activity (Bullitt, 1990), in the same neuronal pool (Fig. 4.5C). These findings suggest sympathoexcitatory action for GPR109A, which is further supported by the spectral analysis findings in the same rats (Fig. 3). Importantly, the ability of local EP3R blockade to abrogate the NA-evoked increases in c-Fos expression in TH-ir neurons (Fig. 4.5D) and in sympathetic dominance (Fig. 4.3) implicates EP3R signaling in RVLM GPR109A-mediated sympathoexcitation. It was important, however, to determine the implicated molecular mechanisms in this neuronal response, particularly the oxidative stress in the RVLM.

A number of studies including ours directly linked RVLM ERK1/2 phosphorylation to central sympathoexcitation, at least partly, via activation of nNOS (Chan et al., 2010; Ibrahim and Abdel-Rahman, 2012) because nNOS-derived NO inhibits RVLM GABAergic neurotransmission and induces sympathoexcitation in conscious rats (Martins-Pinge et al., 2007; Ibrahim and Abdel-Rahman, 2011). Further, nNOS derived NO can contribute to ROS

generation by interacting with super oxide radicle to produce peroxynitrite (Beckman et al., 1990) and to L-glutamate release (McNaught and Brown, 1998; Bal-Price et al., 2002). The involvement of ERK1/2 pathway in PGE2-EP3R mediated signaling in other models (Chuang et al., 2006; Nicola et al., 2008) presented a rationale to investigate this pathway in the current study. We demonstrate substantial increases in local ERK1/2 and nNOS phosphorylation following intra-RVLM NA (Fig. 4.6). These neuronal responses paralleled the increase in RVLM TH neuronal activity (c-Fos; Fig. 5), and were all abrogated by local EP3R blockade. Further, prior nNOS inhibition (NPLA) abolished the NA-evoked nNOS phosphorylation and pressor response (Fig. 4.8) in rats and the increase in L-glutamate in PC12 cells (Fig.4.9). These findings suggest a pivotal role for a PGE2/EP3R-dependent increase in RVLM nNOS signaling in the GPR109A (NA)-mediated sympathoexcitation taking into consideration the ability of EP3R blockade to abrogate nNOS phosphorylation similar to NPLA (Fig. 4.6). These findings implicate PGE2/EP3 signaling in direct or indirect nNOS phosphorylation.

It is important to comment on increased RVLM ROS formation as a viable mechanistic link between the EP3R-dependent ERK1/2-nNOS activation and the sympathoexcitation caused by RVLM GPR109A activation. This notion is supported by the findings that high RVLM ROS level is associated with sympathoexcitation (increased c-Fos expression in TH-ir neurons) in this study (Fig. 4.5), and in reported studies that showed that NOX-derived superoxide anion activates ERK pathway with subsequent c-Fos induction and pressor response (Chan et al., 2005; Chan et al., 2007). These findings are consistent with local

PGE2 activation of NOX following central angiotensin II injection (Wang et al., 2013a). Our conclusion is bolstered by the ability of both selective nNOS inhibition (NPLA) and EP3R blockade (L-798106) to similarly abolish the increases in nNOS phosphorylation, c-Fos intensity, ROS level and NOX activity, and to restore the reduced catalase activity in NA-treated rats (Figs. 4.6, 7, 8 and 9) and to attenuate NA-mediated L-glutamate in cultured PC12 cells (Fig. 4.9).

In conclusion, this study provides evidence that PGE_2 activation of EP3R in the RVLM contributes to the GPR109A (NA)-mediated sympathoexcitation and pressor response via enhancing glutamatergic neurotransmission and oxidative stress. Further, we present novel findings on the expression of EP3R, and PGE2-EP3R signaling, in the RVLM as well as the molecular mechanisms for its sympathoexcitatory/pressor function acting alone or as a mediator of GPR109A (NA)-evoked pressor response (Fig. 4.10). The present pharmacologic and molecular findings may support a cardiovascular benefit for taking aspirin before NA in hyperlipidemic patients, and suggest a potential use for central EP3R blockers as antihypertensive medications.

Figure 4.10. Suggested mechanisms for the role of PGE2/EP3R in GPR109A-mediated pressor response.

Suggested mechanisms for the role of PGE2/EP3R in GPR109A-mediated pressor response caused by nicotinic acid (NA) microinjection into the RVLM. The sequence of events is based on the findings that: (i) Intra-RVLM GPR109A activation (NA) increased blood pressure/sympathetic activity in conscious freely moving rats (Figs. 2 and 3), and increased RVLM PGE2 (Fig. 1), c-Fos expression in TH-ir neurons (Fig. 5), p-ERK1/2 and p-nNOS levels (Fig. 6), and oxidative stress (Fig. 7); (ii) NA increased intracellular calcium levels in PC12 cells which exhibit a neuronal phenotype (Rezq and Abdel-Rahman, 2015) (iii) NA and PGE2 increased glutamate levels (Figs. 4) in PC12 cells; (iv) EP3R (L-798106) or nNOS blockade (NPLA) attenuated the RVLM GPR109A-mediated biochemical and pressor responses (see text for details).

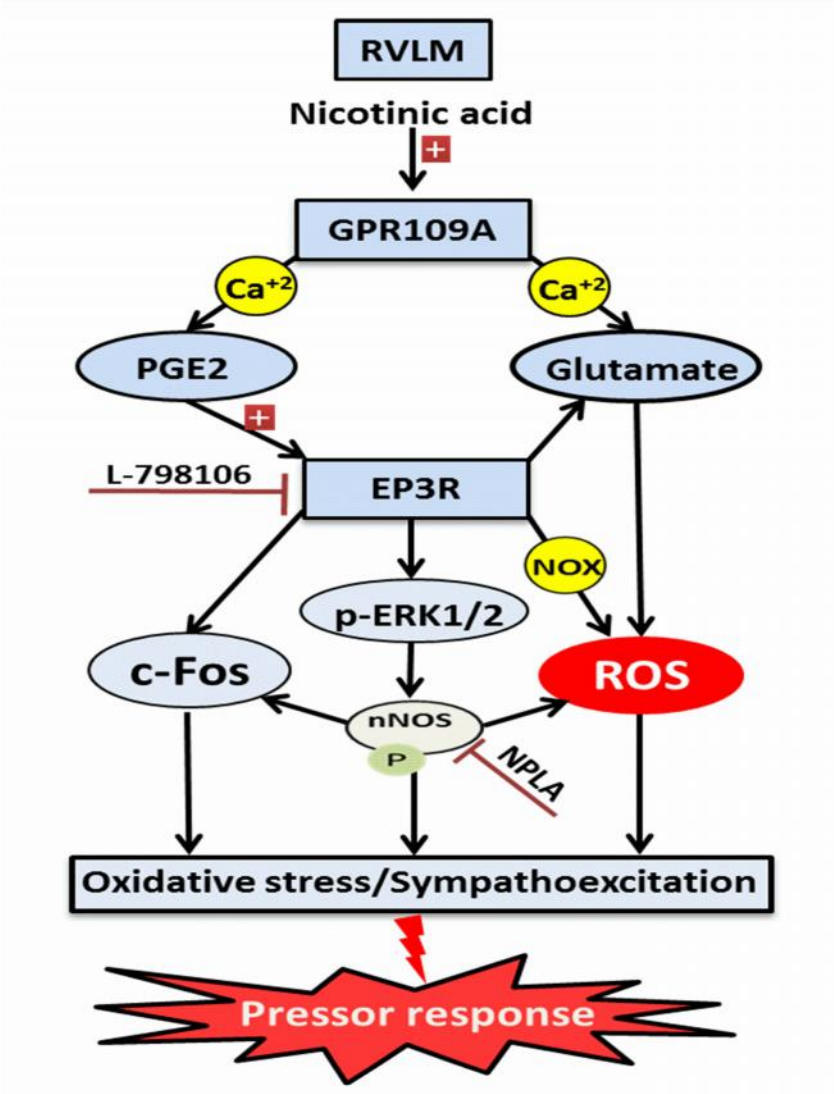
RVLM
Nicotinic acid
GPR109A
Ca+2
Ca+2
PGE2
Glutamate
L-798106
EP3R
NOX
p-ERK1/2
c-Fos
ROS
nNOS
P
NPLA
Oxidative stress/Sympathoexcitation
Pressor response

CHAPTER FIVE-GENERAL DISCUSSION AND SUMMARY

NA, a commonly used anti-hyperlipidemic drug, is known to produce a flushing reaction via activating GPR109A receptor to increase intracellular calcium levels and the release of different PGs including PGE2; the latter increases sympathetic activity and BP upon central activation of its receptor (EP3R) in hypothalamic nuclei (Ando et al., 1995; Ariumi et al., 2002; Murakami et al., 2002; Zhang et al., 2011). Additionally, both Ca^{2+}(Kish and Ueda, 1991; Berridge, 1998; Sudhof, 2004) and PGE2 (Bezzi et al., 1998; Wang et al., 2015) induce the release of the sympathoexcitatory amino acid L- glutamate. The ability of NA to reach the brain in appreciable concentrations following peripheral administration raised the possible contribution of central GPR109A to cardiovascular regulation. The main goal of the current study was to elucidate the role of GPR109A in central regulation of BP, and uncovering the contribution of both l-glutamate and PGE2 to this role. As there are no previous reports on central expression of GPR109A in the RVLM, the main cardiovascular regulating nucleus in the brain stem, we demonstrated the expression of the receptor in this neuronal pool as well as in PC12 cells using western blot (Fig. 3.1). Equally important, this was followed by elucidating the spatial distribution of GPR109A relative to different cell types (glial and neuronal), giving special attention to TH-ir neurons (Figs. 3.1 and 3.2), which regulate the sympathetic activity (Guyenet, 2006a; Kumagai et al., 2012). Our findings indicated a sharp robust increase in BP and a decrease in HR following intra-RVLM injection of NA. The similarities between this response and the response elicited by intra-RVLM L-glutamate (via NMDAR), inferred contribution of the latter to NA-evoked pressor response. To investigate this interesting postulate, it was important to utilize pharmacological interventions that target different glutamate receptors.

Subsequent *ex vivo* and cell culture studies using PC12 cells elucidated the mechanisms implicated in the central GPR109A-evoked pressor response in SD rats. In pursuit of this goal, we characterized the centrally-elicited hemodynamic effects of GPR109A in conscious SD rats. Intra-RVLM administration of GPR109A dose-dependently increased MAP and decreased HR, suggesting a role of GPR109A in central BP regulation (Fig. 3.3). Interestingly, similar onset and pattern were shared between the pressor responses elicited by intra-RVLM NA or L-glutamate (Fig. 3.3A), and the latter replicated the findings in reported studies including ours (Bachelard et al., 1990; Mao and Abdel-Rahman, 1994). These findings raised a potential link between NA and L-glutamate, the main cardiovascular excitatory amino acid. This notion was supported by the findings that the NA-evoked pressor response was abolished by prior NMDAR (AP5), but not with non-NMDAR (CNQX), blockade, and was exacerbated with prior glutamate uptake inhibition (PDC) (Fig. 3.4). While the rapid onset of the pressor response (Fig. 3.3A) precluded investigation of NA effect on RVLM L-glutamate release, we adopted direct biochemical measurements in PC12 cells to support L-glutamate involvement in the NA-evoked cardiovascular responses. The ability of NA to increase Ca^{2+} levels in cultured PC12 cells, which is consistent with other findings showing that NA (10 µM-3 mM) mediates a GPR109A dependent increase in intracellular Ca^{2+} levels in macrophages and epidermal Langerhans cells (Benyo et al., 2005; Benyo et al., 2006; Vanhorn et al., 2012; Gaidarov et al., 2013), is important because Ca^{2+} triggers L-glutamate release (Kish and Ueda, 1991; Berridge, 1998; Sudhof, 2004) and GPR109A-mdiated PGs release (Benyo et al., 2005). It is imperative, nonetheless, to note that these cardiovascular responses were mediated via NA activation of RVLM GPR109A because the inactive NA isomer, IsoNA (similar dose in vivo and concentration *in vitro*), failed

to produce similar cardiovascular and biochemical effects (Fig. 3.4, A and B). Next, we targeted ROS as the main molecular mechanism that underlies L-glutamate mediated sympathoexcitation (Albrecht et al., 2010) to support our L-glutamate hypothesis. *Ex vivo* studies on RVLM tissues revealed higher ROS level in NA-treated rats, which was attenuated by prior NMDAR blockade (AP5), and exacerbated by glutamate uptake inhibition (PDC). These biochemical responses paralleled the changes in NA-evoked pressor response in these treatment groups (Figs. 3.4 and 5). Moreover, *in vitro* studies in PC12 cells demonstrated that NA (1 mM) and L-glutamate, in a concentration (100 nM) similar to that released by NA (1 mM), produced comparable increases in oxidative stress, an effect that was abrogated with prior NMDAR blockade (Fig. 3.7). The above-mentioned effects are mediated via GPR109A activation because the use of the inactive isomer, IsoNA failed to produce hemodynamic or biochemical changes that are significantly different from untreated controls (Figs. 3.5,6 and 7). Equally important, NA failed to increase Ca^{2+} or glutamate levels in PC12 cells following siRNA-evoked GPR109A knockdown (Fig. 3.8).

In the second part of this research project, we aimed to investigate whether PGs, in particular PGE2, which is reported among other PGs to elicit a sympathoexcitatory response when injected centrally specifically via activating EP3R, is involved in NA-mediated pressor response at least partially via enhancing L-glutamate release. We elucidated the ability of NA to increase PGE2 release in both RVLM and PC12 cells. Although EP3R is expressed in other brain areas (Kotani et al., 1995), there is no evidence on the expression or function of EP3R in the RVLM. Further, the effect of local PGE2 in the RVLM on BP was not reported before. Here, we

demonstrated, for the first time, EP3R expression in the RVLM and in PC12 cells. Next, we demonstrated the effect of locally injecting PGE2 in the RVLM on BP and HR. Further, we investigated the effect of the selective EP3R blockade, the subtype of PGE2 receptors we hypothesized that it mediates the PGE2-evoked sympathoexcitatory activity, based on reported findings in other brain areas (Ariumi et al., 2002; Zhang et al., 2011). As first step, the current findings demonstrated the expression of EP3R in both the RVLM and PC12 cells (Fig. 4.1). Intra-RVLM PGE2 increased BP that was abolished with prior EP3R blockade, which also attenuated NA-mediated pressor response (Fig. 4.2) and adverse autonomic changes (Fig. 4.3). These in vivo findings extend the sympathoexcitatory role of PGE2/EP3R, described in hypothalamic nuclei (Ando et al., 1995; Ariumi et al., 2002; Murakami et al., 2002; Zhang et al., 2011), to the RVLM. Subsequent molecular studies indicated that the increase in L-glutamate in cultured PC12 cells was mediated, at least partially, by locally released PGE2 via EP3R because selective EP3R blockade attenuated this effect (Fig. 4.4). This finding is consistent with reported findings on the ability of: (i) PGE2 to increase both L-glutamate level and glutamatergic neurotransmission in cultured neurons and mice (Bezzi et al., 1998; Iadecola et al., 2001; Simm et al., 2015; Wang et al., 2015) (Iadecola et al., 2001), and (ii) EP3R antagonism to attenuate glutamate induced excitotoxicity in hippocampal slices (Ikeda-Matsuo, 2013). Another evidence for the role of EP3R in PGE2-mediated sympathoexcitation is the ability of its antagonist to attenuate the intra-RVLM neuronal reactivity (c-Fos expression) elicited by intra-RVLM PGE2 (Fig. 4.5).

The next step was to investigate molecular mechanisms involved in the pressor response elicited by intra-RVLM NA as a downstream of PGE2 release. We reasoned that PGE2 ability to increase NOX activity (Wang et al., 2013a), c-Fos expression in different brain areas involved in cardiovascular and autonomic regulation (Lacroix et al., 1996; Zhang et al., 2011), and ERK1/2 pathway activation (Chuang et al., 2006) are sufficient molecular mechanisms for central PGE2-evoked pressor response because these biochemical responses lead to sympathoexcitation and BP increase (Chalmers et al., 1994; Minson et al., 1994; Ibrahim and Abdel-Rahman, 2012; Chen et al., 2013). Therefore, we utilized a multilevel experimental approach to investigate these novel and interrelated possibilities. In our model, NA increased c-Fos expression, ERK1/2 and nNOS phosphorylation and oxidative stress (elevated ROS levels, increased NOX activity and decreased catalase activity). The previously mentioned effects were all blocked by prior EP3R blockade, suggesting that: (i) locally released PGE2 in the RVLM mediates these effects, which ultimately leads to the pressor response elicited by NA; and (ii) EP3R among other PGE2 receptors is pivotal for PGE2-evoked sympathoexcitatory actions in the RVLM.

We tested the hypothesis that nNOS activation (increased NO generation), at least partly via ERK1/2 activation, plays important role in the EP3R-dependent pressor response caused by intra-RVLM NA for the following reasons. First, reported studies including ours showed that the RVLM ERK1/2-nNOS pathway is implicated in sympathoexcitation (Martins-Pinge et al., 2007; Chan et al., 2010; Ibrahim and Abdel-Rahman, 2011; Ibrahim and Abdel-Rahman, 2012). Second, this signaling pathway is implicated in the PGE2-EP3R mediated effects in other model systems (Chuang et al., 2006; Nicola et al., 2008), and in L-glutamate mediated neurotoxicity

(Garthwaite et al., 1988; Dawson et al., 1993). Third, NA-mediated pressor response was associated with higher p-nNOS level in our model system (Figs. 4.6) that was decreased with prior EP3R blockade. Based on biochemical findings that supported our hypothesis, we extended our in vivo studies (Fig. 4.8) to establish biological relevance for this signaling pathway by investigating the effect of local selective nNOS blockade (NPLA) on biochemical events in the RVLM and the pressor response caused by intra-RVLM NA. We showed that NPLA abrogated NA-evoked increase in L-glutamate in PC12 cells and the following neurochemical responses in the RVLM: c-Fos expression and oxidative stress (increased ROS and NOX activity and decreased catalase activity). Equally important, nNOS inhibition in the RVLM abolished the pressor responses caused by intra RVLM NA, which suggested a viable mechanistic link between the EP3R-dependent ERK1/2 activation and the sympathoexcitation caused by RVLM GPR109A activation. This notion is supported by the findings that high RVLM ROS level is associated with sympathoexcitation (increased c-Fos expression in TH-ir neurons) in this study (Fig. 4.5), and in reported studies that showed that NOX-derived superoxide anion activates ERK pathway with subsequent c-Fos induction and pressor response (Chan et al., 2005; Chan et al., 2007). Although, others implicated RVLM ERK1/2-nNOS activation in hypotensive responses (El-Mas et al., 2009; Kastenmayer et al., 2012) (Kagiyama et al., 1997), which raises the possibility that GPR109A-mediated increase in NO levels could ultimately oppose the pressor effect of intra-RVLM NA. We found that selective nNOS blockade (NPLA) significantly attenuated NA-elicited pressor response and oxidative stress (Fig. 4.8), which rules out this possibility in our model system. Further, similar to EP3R blockade, NPLA abrogated NA-mediated increase in L-glutamate (PC12 cells) and RVLM c-Fos expression (Fig. 4.9) lending

more support to our hypothesis and agrees with reported ability of NO to increase L-glutamate release (McNaught and Brown, 1998; Bal-Price et al., 2002) and c-Fos expression (Chan et al., 2004). Collectively, this part of the study suggested that PGE2 is critical for the glutamate-mediated pressor response elicited by NA directly by enhancing glutamate release (Fig. 4.4) or indirectly by triggering signaling pathways that contribute to this sympathoexcitatory response, in particular the ERK1/2-nNOS signaling pathway with its associated oxidative stress.

In summary, the present study presents the first evidence for GPR109A expression in the RVLM, and its mediation of sympathoexcitation and elevation of BP via L-glutamate/NMDAR-dependent mechanisms (Fig. 3.9). Additionally, this study provides evidence that PGE_2 activation of EP3R in the RVLM contributes to the GPR109A (NA)-mediated sympathoexcitation and pressor response via enhancing glutamatergic neurotransmission and oxidative stress. Further, we present novel findings on the expression of EP3R in the RVLM as well as the implicated molecular mechanisms of its sympathoexcitatory/pressor function (Fig. 4.9). Moreover, the present findings might have pathophysiological ramifications, particularly in hypertension for three reasons. First, there is a clear link between an exacerbated RVLM neuronal oxidative stress and the elevated BP in hypertension (Wu et al., 2014). Second, compared to normotensive controls, activation of RVLM NMDAR causes greater elevation in BP in spontaneously hypertensive rats (Lin et al., 1995). Third, the present findings may support a cardiovascular benefit for taking aspirin before NA in hyperlipidemic patients, and suggest a potential use for central EP3R blockers as antihypertensive medications. Collectively, the

present findings, along with these reported studies, highlight central GPR109A as well as EP3R as molecular targets for the development of novel antihypertensive medications.

LIMITATIONS

1. The L-glutamate, a major player of NA pressor response, release was only assessed *in vitro* in cultured PC12 cells. This alternative approach was adopted because the rapid onset (1 min) of the L-glutamate-dependent pressor response elicited by NA precluded in vivo measurement of L-glutamate even by microdialysis (Wang et al., 2005). The microdialysis probe size is relatively big for small area like the RVLM and the 15-min time intervals needed for dialysate collection, also precluded the use of that technique in our studies.
2. PC12 cells are derived from a transplantable rat adrenal medulla pheochromocytoma cells. Importantly, PC12 cells respond to nerve growth factor (NGF) by converting to sympathetic-neuron-like phenotype (Greene and Rein, 1977; Greene, 1978). Further, PC12 cells are tyrosine hydroxylase expressing cells. Based on these characteristics, these cells have been used in many reported studies including ours to conduct *in vitro* studies that are not feasible in the RVLM in vivo (Separovic et al., 1997; Zhang and Abdel-Rahman, 2005; Zhang and Abdel-Rahman, 2008) due to time or tissue limitations such as calcium, glutamate and NO measurements. Nonetheless, PC12 cells have their own limitations as there is no guarantee that the exact phenotype that those cells will acquire upon differentiation will mimic that of RVLM neurons. Therefore, a primary RVLM neuronal cell culture would be a better future approach. GPR109A is known to be expressed in microglia (Penberthy, 2009), which might offer the use of microglial cell line as another alternative model system for our *in vitro* studies.

3. PGE2, which is known among other PGs to be sympathoexcitatory, can act through a number of receptors including EP1, EP2, EP3, and EP4 receptors (Narumiya et al., 1999). Although EP3R mediates the central cardiovascular excitatory effects and renal sympathetic nerve activity of PGE2 in other studies (Ariumi et al., 2002; Zhang et al., 2011) and that similar results were obtained in the current study, our conclusion will be bolstered by investigating the role of other PGs known to be released by NA in the periphery as well as other prostanoid receptors subtypes. Nonetheless, the present findings are the first to implicate PGE2/EP3R signaling in the RVLM in sympathoexcitation and as intermediary neurochemical mechanism for GPR109A (NA)-evoked pressor response.
4. The effect of ERK1/2-nNOS signaling on NA-mediated pressor response was based on the ability of NA to enhance both ERK1/2 and nNOS phosphorylation, compared to the control group. While we presented pharmacological (NPLA) and biochemical (inhibition of nNOS phosphorylation) that supported a causal role for nNOS phosphorylation in the NA-mediated pressor response, it might be important to show that the latter was secondary to ERK1/2 activation by pharmacologically inhibiting the latter in the RVLM. Notably, our previous studies established such link in the RVLM of conscious rats (Ibrahim and Abdel-Rahman, 2012).

FUTURE DIRECTIONS

The present findings suggest a novel role for brainstem PGE2-EP3R signaling in the central GPR109A-evoked pressor response. Importantly, the findings are the first to suggest a sympathoexcitatory role for PGE2 in the RVLM, the major cardiovascular regulating nucleus in the brain stem. Further, the study provides a novel insight into the suggested mechanisms that are involved in PGE2 sympathoexcitatory actions, mainly through ERK1/2-nNOS phosphorylation. In support of these findings, future studies are needed to elucidate the role of PGE2 relative to other PGs (for example PGD2 and PGI2) and the role of EP3R relative to other prostanoid receptors (EP1, EP2 or EP4). Our preliminary experiments in PC12 cells revealed that upon using the concentration range applied throughout the study, both NA (1 mM) and PGE2 (10 µM) induced mild decrease in cell viability following 24 hrs incubation and this effect was also abolished with prior EP3R blockade (L-798106, 10µM) (Fig. 5.1). Future mechanistic studies are warranted to elucidate the PGE2-mediated neurotoxic effect (via EP3R) using serial dilutions of PGE2 in cultured PC12 cells as well as conducting *ex vivo* studies following longer time window after intra-RVLM PGE2 (24-48 hrs after treatment). Such studies will advance our knowledge of the role of PGs in the neural control of BP, in particular in conditions of systemic inflammation or disease states that are associated with pressor responses and neurotoxicity/sympathoexcitation such as cerebral stroke. Future clinical/epidemiological studies are needed to evaluate the benefit for the concurrent use of small doses of aspirin to confer cardiovascular protection against an overlooked central sympathoexcitation that potentially occurs in patients who receive NA for the treatment of dyslipidemia. Finally, future studies are needed in models of experimental

hypertension to test the hypothesis that EP3R signaling in the RVLM is hyperactive and to examine the potential therapeutic value for central EP3R blockade in hypertension.

Figure 5.1. NA induces apoptosis in PC12 cells via EP3R

(A) Effect of NA (100 µM, 1mM and 10mM), or IsoNA (10mM) on PC12 cell viability. Measurements were done 24 hrs incubation time using MTS assay. Data representing folds of vehicle treated cells and presented as mean ± S.E.M. **(B)** Effect of 24 hrs exposure of PC12 cells to NA (1mM) or PGE2 (10 µM) on cell viability (folds increase of control) with or without 30 min prior incubation with the selective EP3R blocker, L-798106 (0.1 nmol). Data are expressed as mean ± S.E.M. *$P < 0.05$ vs. control values; $^{\#}P < 0.05$ vs. NA; $^{\wedge}P < 0.05$ vs. PGE2.

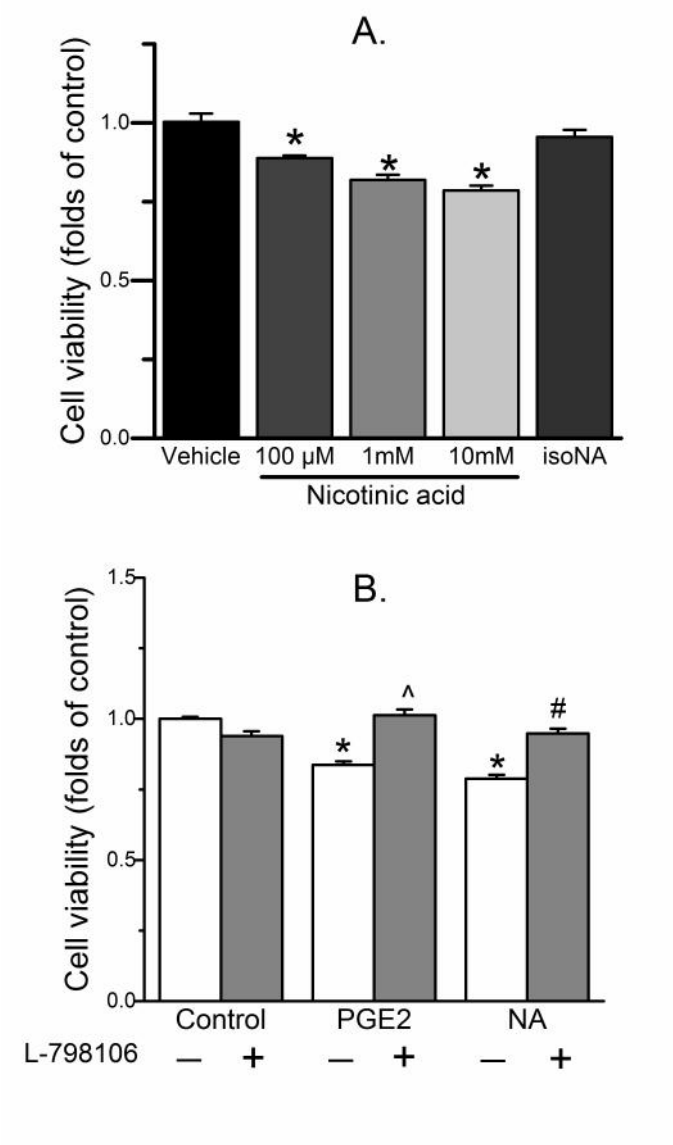
A.
Cell viability (folds of control)
1.0
0.5
0.0
*
*
*
Vehicle
100 μM
1mM
10mM
isoNA
Nicotinic acid
B.
Cell viability (folds of control)
1.5
1.0
0.5
0.0
*
^
*
#
Control
PGE2
NA
L-798106
—
+
—
+
—
+

REFERENCE LIST

(1975) Clofibrate and niacin in coronary heart disease. *Jama* **231**:360-381.

Akki A, Zhang M, Murdoch C, Brewer A and Shah AM (2009) NADPH oxidase signaling and cardiac myocyte function. *Journal of Molecular and Cellular Cardiology* **47**:15-22.

Albrecht P, Lewerenz J, Dittmer S, Noack R, Maher P and Methner A (2010) Mechanisms of oxidative glutamate toxicity: the glutamate/cystine antiporter system xc- as a neuroprotective drug target. *CNS & neurological disorders drug targets* **9**:373-382.

Andersson RG, Aberg G, Brattsand R, Ericsson E and Lundholm L (1977) Studies on the mechanism of flush induced by nicotinic acid. *Acta pharmacologica et toxicologica* **41**:1-10.

Ando K, Kondo F, Yamaguchi N, Tachi M, Fukayama M, Yoshikawa K, Gosho M, Fujiwara Y and Okada S (2015) Centrally administered isoproterenol induces sympathetic outflow via brain prostaglandin E2-mediated mechanisms in rats. *Autonomic neuroscience : basic & clinical* **189**:1-7.

Ando T, Ichijo T, Katafuchi T and Hori T (1995) Intracerebroventricular injection of prostaglandin E2 increases splenic sympathetic nerve activity in rats. *The American journal of physiology* **269**:R662-668.

Ariumi H, Takano Y, Masumi A, Takahashi S, Hirabara Y, Honda K, Saito R and Kamiya HO (2002) Roles of the central prostaglandin EP3 receptors in cardiovascular regulation in rats. *Neuroscience letters* **324**:61-64.

Bachelard H, Gardiner SM and Bennett T (1990) Cardiovascular responses elicited by chemical stimulation of the rostral ventrolateral medulla in conscious, unrestrained rats. *J Auton Nerv Syst* **31**:185-190.

Bal-Price A, Moneer Z and Brown GC (2002) Nitric oxide induces rapid, calcium-dependent release of vesicular glutamate and ATP from cultured rat astrocytes. *Glia* **40**:312-323.

Bazil MK and Gordon FJ (1993) Sympathoexcitation from the rostral ventrolateral medulla is mediated by spinal NMDA receptors. *Brain research bulletin* **31**:273-278.

Beckman JS, Beckman TW, Chen J, Marshall PA and Freeman BA (1990) Apparent hydroxyl radical production by peroxynitrite: implications for endothelial injury from nitric oxide and superoxide. *Proceedings of the National Academy of Sciences of the United States of America* **87**:1620-1624.

Bedard K and Krause K-H (2007) The NOX Family of ROS-Generating NADPH Oxidases: Physiology and Pathophysiology. *Physiological Reviews* **87**:245-313.

Benyo Z, Gille A, Bennett CL, Clausen BE and Offermanns S (2006) Nicotinic acid-induced flushing is mediated by activation of epidermal langerhans cells. *Molecular pharmacology* **70**:1844-1849.

Benyo Z, Gille A, Kero J, Csiky M, Suchankova MC, Nusing RM, Moers A, Pfeffer K and Offermanns S (2005) GPR109A (PUMA-G/HM74A) mediates nicotinic acid-induced flushing. *The Journal of clinical investigation* **115**:3634-3640.

Berridge MJ (1998) Neuronal calcium signaling. *Neuron* **21**:13-26.

Bezzi P, Carmignoto G, Pasti L, Vesce S, Rossi D, Rizzini BL, Pozzan T and Volterra A (1998) Prostaglandins stimulate calcium-dependent glutamate release in astrocytes. *Nature* **391**:281-285.

Bindokas VP, Jordan J, Lee CC and Miller RJ (1996) Superoxide production in rat hippocampal neurons: selective imaging with hydroethidine. *The Journal of neuroscience : the official journal of the Society for Neuroscience* **16**:1324-1336.

Blad CC, Ahmed K, AP IJ and Offermanns S (2011) Biological and pharmacological roles of HCA receptors. *Adv Pharmacol* **62**:219-250.

Brown BG, Zhao XQ, Chait A, Fisher LD, Cheung MC, Morse JS, Dowdy AA, Marino EK, Bolson EL, Alaupovic P, Frohlich J and Albers JJ (2001) Simvastatin and niacin, antioxidant vitamins, or the combination for the prevention of coronary disease. *The New England journal of medicine* **345**:1583-1592.

Bullitt E (1990) Expression of c-fos-like protein as a marker for neuronal activity following noxious stimulation in the rat. *The Journal of comparative neurology* **296**:517-530.

Canner PL, Berge KG, Wenger NK, Stamler J, Friedman L, Prineas RJ and Friedewald W (1986) Fifteen year mortality in Coronary Drug Project patients: long-term benefit with niacin. *Journal of the American College of Cardiology* **8**:1245-1255.

Carlson LA (2005) Nicotinic acid: the broad-spectrum lipid drug. A 50th anniversary review. *Journal of internal medicine* **258**:94-114.

Chalmers J, Arnolda L, Llewellyn-Smith I, Minson J, Pilowsky P and Suzuki S (1994) Central neurons and neurotransmitters in the control of blood pressure. *Clinical and experimental pharmacology & physiology* **21**:819-829.

Chan SH, Chang KF, Ou CC and Chan JY (2004) Nitric oxide regulates c-fos expression in nucleus tractus solitarii induced by baroreceptor activation via cGMP-dependent protein kinase and cAMP response element-binding protein phosphorylation. *Molecular pharmacology* **65**:319-325.

Chan SH, Hsu KS, Huang CC, Wang LL, Ou CC and Chan JY (2005) NADPH oxidase-derived superoxide anion mediates angiotensin II-induced pressor effect via activation of p38 mitogen-activated protein kinase in the rostral ventrolateral medulla. *Circulation research* **97**:772-780.

Chan SH, Sun EY and Chang AY (2010) Extracellular signal-regulated kinase 1/2 plays a pro-life role in experimental brain stem death via MAPK signal-interacting kinase at rostral ventrolateral medulla. *Journal of biomedical science* **17**:17.

Chan SH, Wang LL and Chan JY (2003) Differential engagements of glutamate and GABA receptors in cardiovascular actions of endogenous nNOS or iNOS at rostral ventrolateral medulla of rats. *British journal of pharmacology* **138**:584-593.

Chan SH, Wang LL, Tseng HL and Chan JY (2007) Upregulation of AT1 receptor gene on activation of protein kinase Cbeta/nicotinamide adenine dinucleotide diphosphate oxidase/ERK1/2/c-fos signaling cascade mediates long-term pressor effect of angiotensin II in rostral ventrolateral medulla. *Journal of hypertension* **25**:1845-1861.

Chan SHH, Tai M-H, Li C-Y and Chan JYH (2006) Reduction in molecular synthesis or enzyme activity of superoxide dismutases and catalase contributes to oxidative stress and neurogenic hypertension in spontaneously hypertensive rats. *Free Radical Biology and Medicine* **40**:2028-2039.

Chapp AD, Gui L, Huber MJ, Liu J, Larson RA, Zhu J, Carter JR and Chen QH (2014) Sympathoexcitation and pressor responses induced by ethanol in the central nucleus of amygdala involves activation of NMDA receptors in rats. *American journal of physiology Heart and circulatory physiology* **307**:H701-709.

Chen J, Xia C, Wang J, Jiang M, Zhang H, Zhang C, Zhu M, Shen L and Zhu D (2013) The effect of orexin-A on cardiac dysfunction mediated by NADPH oxidase-derived superoxide anion in ventrolateral medulla. *PloS one* **8**:e69840.

Chuang PC, Sun HS, Chen TM and Tsai SJ (2006) Prostaglandin E2 induces fibroblast growth factor 9 via EP3-dependent protein kinase Cdelta and Elk-1 signaling. *Molecular and cellular biology* **26**:8281-8292.

Ciriello J, Caverson MM and Polosa C (1986) Function of the ventrolateral medulla in the control of the circulation. *Brain research* **396**:359-391.

Cortese-Krott MM, Rodriguez-Mateos A, Kuhnle GG, Brown G, Feelisch M and Kelm M (2012) A multilevel analytical approach for detection and visualization of intracellular NO production and nitrosation events using diaminofluoresceins. *Free radical biology & medicine* **53**:2146-2158.

Dampney RA (1994) Functional organization of central pathways regulating the cardiovascular system. *Physiological Reviews* **74**:323-364.

Dampney RA, Coleman MJ, Fontes MA, Hirooka Y, Horiuchi J, Li YW, Polson JW, Potts PD and Tagawa T (2002) Central mechanisms underlying short- and long-term regulation of the cardiovascular system. *Clinical and experimental pharmacology & physiology* **29**:261-268.

Dampney RA, Czachurski J, Dembowsky K, Goodchild AK and Seller H (1987) Afferent connections and spinal projections of the pressor region in the rostral ventrolateral medulla of the cat. *Journal of the Autonomic Nervous System* **20**:73-86.

Dawson VL, Dawson TM, Bartley DA, Uhl GR and Snyder SH (1993) Mechanisms of nitric oxide-mediated neurotoxicity in primary brain cultures. *The Journal of neuroscience : the official journal of the Society for Neuroscience* **13**:2651-2661.

DePuy SD, Stornetta RL, Bochorishvili G, Deisseroth K, Witten I, Coates M and Guyenet PG (2013) Glutamatergic neurotransmission between the C1 neurons and the parasympathetic preganglionic neurons of the dorsal motor nucleus of the vagus. *The*

Journal of neuroscience : the official journal of the Society for Neuroscience **33**:1486-1497.

Dieterich S, Bieligk U, Beulich K, Hasenfuss G and Prestle J (2000) Gene expression of antioxidative enzymes in the human heart: increased expression of catalase in the end-stage failing heart. *Circulation* **101**:33-39.

Digby JE, Lee JM and Choudhury RP (2009) Nicotinic acid and the prevention of coronary artery disease. *Current opinion in lipidology* **20**:321-326.

Digby JE, McNeill E, Dyar OJ, Lam V, Greaves DR and Choudhury RP (2010) Anti-inflammatory effects of nicotinic acid in adipocytes demonstrated by suppression of fractalkine, RANTES, and MCP-1 and upregulation of adiponectin. *Atherosclerosis* **209**:89-95.

Dingledine R, Borges K, Bowie D and Traynelis SF (1999) The glutamate receptor ion channels. *Pharmacological reviews* **51**:7-61.

Drake TJ, Jezzini S, Lovell P, Moroz LL and Tan W (2005) Single cell glutamate analysis in Aplysia sensory neurons. *Journal of neuroscience methods* **144**:73-77.

Eklund B, Kaijser L, Nowak J and Wennmalm A (1979) Prostaglandins contribute to the vasodilation induced by nicotinic acid. *Prostaglandins* **17**:821-830.

El-Mas MM, Fan M and Abdel-Rahman AA (2009) Facilitation of Myocardial PI3K/Akt/nNOS Signaling Contributes to Ethanol-Evoked Hypotension in Female Rats. *Alcoholism: Clinical and Experimental Research* **33**:1158-1168.

Farlow DM, Goodchild AK and Dampney RA (1984) Evidence that vasomotor neurons in the rostral ventrolateral medulla project to the spinal sympathetic outflow via the dorsomedial pressor area. *Brain research* **298**:313-320.

Filpa V, Carpanese E, Marchet S, Prandoni V, Moro E, Lecchini S, Frigo G, Giaroni C and Crema F (2015) Interaction between NMDA glutamatergic and nitrergic enteric pathways during in vitro ischemia and reperfusion. *European journal of pharmacology* **750**:123-131.

Fisher JP and Paton JF (2012) The sympathetic nervous system and blood pressure in humans: implications for hypertension. *Journal of human hypertension* **26**:463-475.

Frey RS, Ushio-Fukai M and Malik AB (2009) NADPH oxidase-dependent signaling in endothelial cells: role in physiology and pathophysiology. *Antioxidants & redox signaling* **11**:791-810.

Gabor A and Leenen FH (2012) Central neuromodulatory pathways regulating sympathetic activity in hypertension. *J Appl Physiol (1985)* **113**:1294-1303.

Gaidarov I, Chen X, Anthony T, Maciejewski-Lenoir D, Liaw C and Unett DJ (2013) Differential tissue and ligand-dependent signaling of GPR109A receptor: implications for anti-atherosclerotic therapeutic potential. *Cellular signalling* **25**:2003-2016.

Ganji SH, Qin S, Zhang L, Kamanna VS and Kashyap ML (2009) Niacin inhibits vascular oxidative stress, redox-sensitive genes, and monocyte adhesion to human aortic endothelial cells. *Atherosclerosis* **202**:68-75.

Garthwaite J, Charles SL and Chess-Williams R (1988) Endothelium-derived relaxing factor release on activation of NMDA receptors suggests role as intercellular messenger in the brain. *Nature* **336**:385-388.

Greene LA (1978) Nerve growth factor prevents the death and stimulates the neuronal differentiation of clonal PC12 pheochromocytoma cells in serum-free medium. *The Journal of cell biology* **78**:747-755.

Greene LA and Rein G (1977) Release of (3H)norepinephrine from a clonal line of pheochromocytoma cells (PC12) by nicotinic cholinergic stimulation. *Brain research* **138**:521-528.

Griendling KK, Sorescu D and Ushio-Fukai M (2000) NAD(P)H Oxidase : Role in Cardiovascular Biology and Disease. *Circulation research* **86**:494-501.

Grynkiewicz G, Poenie M and Tsien RY (1985) A new generation of Ca2+ indicators with greatly improved fluorescence properties. *The Journal of biological chemistry* **260**:3440-3450.

Guemez-Gamboa A, Estrada-Sanchez AM, Montiel T, Paramo B, Massieu L and Moran J (2011) Activation of NOX2 by the stimulation of ionotropic and metabotropic glutamate receptors contributes to glutamate neurotoxicity in vivo through the production of reactive oxygen species and calpain activation. *Journal of neuropathology and experimental neurology* **70**:1020-1035.

Guyenet PG (2006a) The sympathetic control of blood pressure. *Nature reviews Neuroscience* **7**:335-346.

Guyenet PG (2006b) The sympathetic control of blood pressure. *Nat Rev Neurosci* **7**:335-346.

Guyenet PG, Haselton JR and Sun MK (1989) Sympathoexcitatory neurons of the rostroventrolateral medulla and the origin of the sympathetic vasomotor tone. *Progress in Brain Research* **81**:105-116.

Hanson J, Gille A, Zwykiel S, Lukasova M, Clausen BE, Ahmed K, Tunaru S, Wirth A and Offermanns S (2010) Nicotinic acid- and monomethyl fumarate-induced flushing involves GPR109A expressed by keratinocytes and COX-2-dependent prostanoid formation in mice. *The Journal of clinical investigation* **120**:2910-2919.

Hokfelt T., Johansson O. and M. G (1984) Central catecholamine neurons as revealed by immunohistochemsitry with special reference to adrenaline neurons. *Classical Transmitters in the CNS*:157-276.

Huang PH, Lin CP, Wang CH, Chiang CH, Tsai HY, Chen JS, Lin FY, Leu HB, Wu TC, Chen JW and Lin SJ (2012) Niacin improves ischemia-induced neovascularization in diabetic mice by enhancement of endothelial progenitor cell functions independent of changes in plasma lipids. *Angiogenesis* **15**:377-389.

Iadecola C, Niwa K, Nogawa S, Zhao X, Nagayama M, Araki E, Morham S and Ross ME (2001) Reduced susceptibility to ischemic brain injury and N-methyl-D-aspartate-mediated neurotoxicity in cyclooxygenase-2-deficient mice. *Proceedings of the National Academy of Sciences of the United States of America* **98**:1294-1299.

Ibrahim BM and Abdel-Rahman AA (2011) Role of brainstem GABAergic signaling in central cannabinoid receptor evoked sympathoexcitation and pressor responses in conscious rats. *Brain research* **1414**:1-9.

Ibrahim BM and Abdel-Rahman AA (2012) Enhancement of rostral ventrolateral medulla neuronal nitric-oxide synthase-nitric-oxide signaling mediates the central cannabinoid receptor 1-evoked pressor response in conscious rats. *The Journal of pharmacology and experimental therapeutics* **341**:579-586.

Ibrahim BM and Abdel-Rahman AA (2015) A pivotal role for enhanced brainstem Orexin receptor 1 signaling in the central cannabinoid receptor 1-mediated pressor response in conscious rats. *Brain research* **1622**:51-63.

Ikeda-Matsuo Y (2013) The role of prostaglandin E2 in stroke-reperfusion injury. *Yakugaku zasshi : Journal of the Pharmaceutical Society of Japan* **133**:947-954.

Ito S, Hiratsuka M, Komatsu K, Tsukamoto K, Kanmatsuse K and Sved AF (2003) Ventrolateral medulla AT1 receptors support arterial pressure in Dahl salt-sensitive rats. *Hypertension* **41**:744-750.

Iwata J, Chida K and LeDoux JE (1987) Cardiovascular responses elicited by stimulation of neurons in the central amygdaloid nucleus in awake but not anesthetized rats resemble conditioned emotional responses. *Brain research* **418**:183-188.

Kagiyama S, Tsuchihashi T, Abe I and Fujishima M (1997) Cardiovascular effects of nitric oxide in the rostral ventrolateral medulla of rats. *Brain research* **757**:155-158.

Kastenmayer RJ, Moore RM, Bright AL, Torres-Cruz R and Elkins WR (2012) Select Agent and Toxin Regulations: Beyond the Eighth Edition of the Guide for the Care and Use of Laboratory Animals. *J Am Assoc Lab Anim* **51**:333-338.

Kish PE and Ueda T (1991) Calcium-dependent release of accumulated glutamate from synaptic vesicles within permeabilized nerve terminals. *Neuroscience letters* **122**:179-182.

Kishi T, Hirooka Y, Sakai K, Shigematsu H, Shimokawa H and Takeshita A (2001) Overexpression of eNOS in the RVLM Causes Hypotension and Bradycardia Via GABA Release. *Hypertension* **38**:896-901.

Kishi T, Hirooka Y, Shimokawa H, Takeshita A and Sunagawa K (2008) Atorvastatin reduces oxidative stress in the rostral ventrolateral medulla of stroke-prone spontaneously hypertensive rats. *Clin Exp Hypertens* **30**:3-11.

Koga Y, Hirooka Y, Araki S, Nozoe M, Kishi T and Sunagawa K (2008) High salt intake enhances blood pressure increase during development of hypertension via oxidative stress in rostral ventrolateral medulla of spontaneously hypertensive rats. *Hypertension research : official journal of the Japanese Society of Hypertension* **31**:2075-2083.

Kotani M, Tanaka I, Ogawa Y, Usui T, Mori K, Ichikawa A, Narumiya S, Yoshimi T and Nakao K (1995) Molecular cloning and expression of multiple isoforms of human prostaglandin E receptor EP3 subtype generated by alternative messenger RNA splicing: multiple second messenger systems and tissue-specific distributions. *Molecular pharmacology* **48**:869-879.

Kubo T, Amano M and Asari T (1993) N-methyl-D-aspartate receptors but not non-N-methyl-D-aspartate receptors mediate hypertension induced by carotid body chemoreceptor stimulation in the rostral ventrolateral medulla of the rat. *Neuroscience letters* **164**:113-116.

Kumagai H, Oshima N, Matsuura T, Iigaya K, Imai M, Onimaru H, Sakata K, Osaka M, Onami T, Takimoto C, Kamayachi T, Itoh H and Saruta T (2012) Importance of rostral ventrolateral medulla neurons in determining efferent sympathetic nerve activity and blood pressure. *Hypertension research : official journal of the Japanese Society of Hypertension* **35**:132-141.

La Favor JD, Anderson EJ, Dawkins JT, Hickner RC and Wingard CJ (2013) Exercise prevents Western diet-associated erectile dysfunction and coronary artery endothelial dysfunction: response to acute apocynin and sepiapterin treatment. *American journal of physiology Regulatory, integrative and comparative physiology* **305**:R423-434.

Lacroix S, Vallieres L and Rivest S (1996) C-fos mRNA pattern and corticotropin-releasing factor neuronal activity throughout the brain of rats injected centrally with a prostaglandin of E2 type. *Journal of neuroimmunology* **70**:163-179.

Li G, Deng X, Wu C, Zhou Q, Chen L, Shi Y, Huang H and Zhou N (2011) Distinct kinetic and spatial patterns of protein kinase C (PKC)- and epidermal growth factor receptor (EGFR)-dependent activation of extracellular signal-regulated kinases 1 and 2 by human nicotinic acid receptor GPR109A. *The Journal of biological chemistry* **286**:31199-31212.

Lin JC, Tsao WL and Wang Y (1995) Cardiovascular effects of NMDA in the RVLM of spontaneously hypertensive rats. *Brain research bulletin* **37**:289-294.

Lin LL, Lin AY and Knopf JL (1992) Cytosolic phospholipase A2 is coupled to hormonally regulated release of arachidonic acid. *Proceedings of the National Academy of Sciences of the United States of America* **89**:6147-6151.

Lipton SA and Rosenberg PA (1994) Excitatory amino acids as a final common pathway for neurologic disorders. *The New England journal of medicine* **330**:613-622.

Maciejewski-Lenoir D, Richman JG, Hakak Y, Gaidarov I, Behan DP and Connolly DT (2006) Langerhans cells release prostaglandin D2 in response to nicotinic acid. *The Journal of investigative dermatology* **126**:2637-2646.

Mahboubi K, Witman-Jones T, Adamus JE, Letsinger JT, Whitehouse D, Moorman AR, Sawicki D, Bergenhem N and Ross SA (2006) Triglyceride modulation by acifran analogs: activity towards the niacin high and low affinity G protein-coupled receptors HM74A and HM74. *Biochemical and biophysical research communications* **340**:482-490.

Malliani A, Pagani M, Lombardi F and Cerutti S (1991) Cardiovascular neural regulation explored in the frequency domain. *Circulation* **84**:482-492.

Mao L and Abdel-Rahman AA (1994) Inhibition of glutamate uptake in the rostral ventrolateral medulla enhances baroreflex-mediated bradycardia in conscious rats. *Brain research* **654**:343-348.

Martins-Pinge MC, Araujo GC and Lopes OU (1999) Nitric oxide-dependent guanylyl cyclase participates in the glutamatergic neurotransmission within the rostral ventrolateral medulla of awake rats. *Hypertension* **34**:748-751.

Martins-Pinge MC, Garcia MR, Zoccal DB, Crestani CC and Pinge-Filho P (2007) Differential influence of iNOS and nNOS inhibitors on rostral ventrolateral medullary mediated cardiovascular control in conscious rats. *Autonomic neuroscience : basic & clinical* **131**:65-69.

McGee MA and Abdel-Rahman AA (2012) Enhanced vascular neuronal nitric-oxide synthase-derived nitric-oxide production underlies the pressor response caused by peripheral N-methyl-D-aspartate receptor activation in conscious rats. *The Journal of pharmacology and experimental therapeutics* **342**:461-471.

McNaught KS and Brown GC (1998) Nitric oxide causes glutamate release from brain synaptosomes. *Journal of neurochemistry* **70**:1541-1546.

Medina-Ceja L, Pardo-Pena K, Morales-Villagran A, Ortega-Ibarra J and Lopez-Perez S (2015) Increase in the extracellular glutamate level during seizures and electrical stimulation determined using a high temporal resolution technique. *BMC neuroscience* **16**:11.

Minson JB, Llewellyn-Smith IJ, Arnolda LF, Pilowsky PM, Oliver JR and Chalmers JP (1994) Disinhibition of the rostral ventral medulla increases blood pressure and Fos expression in bulbospinal neurons. *Brain research* **646**:44-52.

Montague PR, Gancayco CD, Winn MJ, Marchase RB and Friedlander MJ (1994) Role of NO production in NMDA receptor-mediated neurotransmitter release in cerebral cortex. *Science* **263**:973-977.

Montiel T, Camacho A, Estrada-Sanchez AM and Massieu L (2005) Differential effects of the substrate inhibitor l-trans-pyrrolidine-2,4-dicarboxylate (PDC) and the non-substrate inhibitor DL-threo-beta-benzyloxyaspartate (DL-TBOA) of glutamate transporters on neuronal damage and extracellular amino acid levels in rat brain in vivo. *Neuroscience* **133**:667-678.

Morgan JI and Curran T (1991) Stimulus-transcription coupling in the nervous system: involvement of the inducible proto-oncogenes fos and jun. *Annual review of neuroscience* **14**:421-451.

Morrow JD, Parsons WG, 3rd and Roberts LJ, 2nd (1989) Release of markedly increased quantities of prostaglandin D2 in vivo in humans following the administration of nicotinic acid. *Prostaglandins* **38**:263-274.

Murakami Y, Okada S, Nishihara M and Yokotani K (2002) Roles of brain prostaglandin E2 and thromboxane A2 in the activation of the central sympatho-adrenomedullary outflow in rats. *European journal of pharmacology* **452**:289-294.

Narumiya S, Sugimoto Y and Ushikubi F (1999) Prostanoid receptors: structures, properties, and functions. *Physiol Rev* **79**:1193-1226.

Nassar NN, Li G, Strat AL and Abdel-Rahman AA (2011) Enhanced hemeoxygenase activity in the rostral ventrolateral medulla mediates exaggerated hemin-evoked hypotension in the spontaneously hypertensive rat. *The Journal of pharmacology and experimental therapeutics* **339**:267-274.

Nicola C, Chirpac A, Lala PK and Chakraborty C (2008) Roles of Rho guanosine 5'-triphosphatase A, Rho kinases, and extracellular signal regulated kinase (1/2) in prostaglandin E2-mediated migration of first-trimester human extravillous trophoblast. *Endocrinology* **149**:1243-1251.

Nishihara M, Hirooka Y, Matsukawa R, Kishi T and Sunagawa K (2012) Oxidative stress in the rostral ventrolateral medulla modulates excitatory and inhibitory inputs in spontaneously hypertensive rats. *Journal of hypertension* **30**:97-106.

Okouchi M, Okayama N and Aw TY (2005) Differential susceptibility of naive and differentiated PC-12 cells to methylglyoxal-induced apoptosis: influence of cellular redox. *Current neurovascular research* **2**:13-22.

Osborne NN, Li GY, Ji D, Andrade da Costa BL, Fawcett RJ, Kang KD and Rittenhouse KD (2009) Expression of prostaglandin PGE2 receptors under conditions of aging and stress and the protective effect of the EP2 agonist butaprost on retinal ischemia. *Investigative ophthalmology & visual science* **50**:3238-3248.

Paolini JF, Mitchel YB, Reyes R, Kher U, Lai E, Watson DJ, Norquist JM, Meehan AG, Bays HE, Davidson M and Ballantyne CM (2008) Effects of laropiprant on nicotinic acid-

induced flushing in patients with dyslipidemia. *The American journal of cardiology* **101**:625-630.

Parati G, Frattola A, Di Rienzo M, Castiglioni P, Pedotti A and Mancia G (1995) Effects of aging on 24-h dynamic baroreceptor control of heart rate in ambulant subjects. *The American journal of physiology* **268**:H1606-1612.

Paxinos G and Watson C (2005) *The rat brain in stereotaxic coordinates*. Elsevier Academic Press, Amsterdam ; Boston.

Paxinos G, Watson CR and Emson PC (1980) AChE-stained horizontal sections of the rat brain in stereotaxic coordinates. *Journal of neuroscience methods* **3**:129-149.

Penberthy WT (2009) Nicotinic acid-mediated activation of both membrane and nuclear receptors towards therapeutic glucocorticoid mimetics for treating multiple sclerosis. *PPAR research* **2009**:853707.

Penugonda S, Mare S, Goldstein G, Banks WA and Ercal N (2005) Effects of N-acetylcysteine amide (NACA), a novel thiol antioxidant against glutamate-induced cytotoxicity in neuronal cell line PC12. *Brain research* **1056**:132-138.

Penumarti A and Abdel-Rahman AA (2014) The novel endocannabinoid receptor GPR18 is expressed in the rostral ventrolateral medulla and exerts tonic restraining influence on blood pressure. *The Journal of pharmacology and experimental therapeutics* **349**:29-38.

Pepponi R, Ferrante A, Ferretti R, Martire A and Popoli P (2009) Region-specific neuroprotective effect of ZM 241385 towards glutamate uptake inhibition in cultured neurons. *European journal of pharmacology* **617**:28-32.

Pischon T, Girman CJ, Hotamisligil GS, Rifai N, Hu FB and Rimm EB (2004) Plasma adiponectin levels and risk of myocardial infarction in men. *Jama* **291**:1730-1737.

Plaisance EP, Lukasova M, Offermanns S, Zhang Y, Cao G and Judd RL (2009) Niacin stimulates adiponectin secretion through the GPR109A receptor. *American journal of physiology Endocrinology and metabolism* **296**:E549-558.

Platt SR (2007) The role of glutamate in central nervous system health and disease--a review. *Vet J* **173**:278-286.

Reigada D, Lu W and Mitchell CH (2006) Glutamate acts at NMDA receptors on fresh bovine and on cultured human retinal pigment epithelial cells to trigger release of ATP. *The Journal of physiology* **575**:707-720.

Rezq S and Abdel-Rahman AA (2015) Central GPR109A activation Mediates Glutamate-Dependent Pressor Response in Conscious Rats. *The Journal of pharmacology and experimental therapeutics*.

Robinson KM, Janes MS, Pehar M, Monette JS, Ross MF, Hagen TM, Murphy MP and Beckman JS (2006) Selective fluorescent imaging of superoxide in vivo using ethidium-

based probes. *Proceedings of the National Academy of Sciences of the United States of America* **103**:15038-15043.

Schulze MB, Shai I, Rimm EB, Li T, Rifai N and Hu FB (2005) Adiponectin and future coronary heart disease events among men with type 2 diabetes. *Diabetes* **54**:534-539.

Separovic D, Kester M, Haxhiu MA and Ernsberger P (1997) Activation of phosphatidylcholine-selective phospholipase C by I1-imidazoline receptors in PC12 cells and rostral ventrolateral medulla. *Brain research* **749**:335-339.

Shaltout HA and Abdel-Rahman AA (2005) Mechanism of fatty acids induced suppression of cardiovascular reflexes in rats. *The Journal of pharmacology and experimental therapeutics* **314**:1328-1337.

Simm B, Ott D, Pollatzek E, Murgott J, Gerstberger R, Rummel C and Roth J (2015) Effects of prostaglandin E on cells cultured from the rat organum vasculosum laminae terminalis and median preoptic nucleus. *Neuroscience* **313**:23-35.

Soga T, Kamohara M, Takasaki J, Matsumoto S, Saito T, Ohishi T, Hiyama H, Matsuo A, Matsushime H and Furuichi K (2003) Molecular identification of nicotinic acid receptor. *Biochemical and biophysical research communications* **303**:364-369.

Soudijn W, van Wijngaarden I and Ijzerman AP (2007) Nicotinic acid receptor subtypes and their ligands. *Medicinal research reviews* **27**:417-433.

Southam E, East SJ and Garthwaite J (1991) Excitatory amino acid receptors coupled to the nitric oxide/cyclic GMP pathway in rat cerebellum during development. *Journal of neurochemistry* **56**:2072-2081.

Spector R (1979) Niacin and niacinamide transport in the central nervous system. In vivo studies. *Journal of neurochemistry* **33**:895-904.

Sudhof TC (2004) The synaptic vesicle cycle. *Annual review of neuroscience* **27**:509-547.

Sved A, Ito S and Sved J (2003) Brainstem mechanisms of hypertension: Role of the rostral ventrolateral medulla. *Current Hypertension Reports* **5**:262-268.

Taggart AK, Kero J, Gan X, Cai TQ, Cheng K, Ippolito M, Ren N, Kaplan R, Wu K, Wu TJ, Jin L, Liaw C, Chen R, Richman J, Connolly D, Offermanns S, Wright SD and Waters MG (2005) (D)-beta-Hydroxybutyrate inhibits adipocyte lipolysis via the nicotinic acid receptor PUMA-G. *The Journal of biological chemistry* **280**:26649-26652.

Tang Y, Zhou L, Gunnet JW, Wines PG, Cryan EV and Demarest KT (2006) Enhancement of arachidonic acid signaling pathway by nicotinic acid receptor HM74A. *Biochemical and biophysical research communications* **345**:29-37.

Tavintharan S, Lim SC and Sum CF (2009) Effects of niacin on cell adhesion and early atherogenesis: biochemical and functional findings in endothelial cells. *Basic & clinical pharmacology & toxicology* **104**:206-210.

Tingley FD, 3rd and Arneric SP (1990) Evidence for clonidine presynaptically modulating amino acid release in the rostral ventral medulla: role in hypertension. *Brain research* **537**:175-181.

Tunaru S, Kero J, Schaub A, Wufka C, Blaukat A, Pfeffer K and Offermanns S (2003) PUMA-G and HM74 are receptors for nicotinic acid and mediate its anti-lipolytic effect. *Nature medicine* **9**:352-355.

Vanhorn J, Altenburg JD, Harvey KA, Xu Z, Kovacs RJ and Siddiqui RA (2012) Attenuation of niacin-induced prostaglandin D(2) generation by omega-3 fatty acids in THP-1 macrophages and Langerhans dendritic cells. *Journal of inflammation research* **5**:37-50.

Walters RW, Shukla AK, Kovacs JJ, Violin JD, DeWire SM, Lam CM, Chen JR, Muehlbauer MJ, Whalen EJ and Lefkowitz RJ (2009) beta-Arrestin1 mediates nicotinic acid-induced flushing, but not its antilipolytic effect, in mice. *The Journal of clinical investigation* **119**:1312-1321.

Wang D, Wang P, Jiang J, Lv Q, Zeng X and Hong Y (2015) Activation of Mas Oncogene-Related G Protein-Coupled Receptors Inhibits Neurochemical Alterations in the Spinal Dorsal Horn and Dorsal Root Ganglia Associated with Inflammatory Pain in Rats. *The Journal of pharmacology and experimental therapeutics* **354**:431-439.

Wang G, Sarkar P, Peterson JR, Anrather J, Pierce JP, Moore JM, Feng J, Zhou P, Milner TA, Pickel VM, Iadecola C and Davisson RL (2013a) COX-1-derived PGE2 and PGE2 type 1 receptors are vital for angiotensin II-induced formation of reactive oxygen species and

Ca(2+) influx in the subfornical organ. *American journal of physiology Heart and circulatory physiology* **305**:H1451-1461.

Wang J, Peng YJ and Zhu DN (2005) Amino acids modulate the hypotensive effect of angiotensin-(1-7) at the caudal ventrolateral medulla in rats. *Regulatory peptides* **129**:1-7.

Wang WZ, Wang LG, Gao L and Wang W (2007) Contribution of AMPA/kainate receptors in the rostral ventrolateral medulla to the hypotensive and sympathoinhibitory effects of clonidine. *American journal of physiology Regulatory, integrative and comparative physiology* **293**:R1232-1238.

Wang X and Abdel-Rahman AA (2005) Effect of chronic ethanol administration on hepatic eNOS activity and its association with caveolin-1 and calmodulin in female rats. *American journal of physiology Gastrointestinal and liver physiology* **289**:G579-585.

Wang Z, Wei X, Liu K, Zhang X, Yang F, Zhang H, He Y, Zhu T, Li F, Shi W, Zhang Y, Xu H, Liu J and Yi F (2013b) NOX2 deficiency ameliorates cerebral injury through reduction of complexin II-mediated glutamate excitotoxicity in experimental stroke. *Free radical biology & medicine* **65**:942-951.

Whitney EJ, Krasuski RA, Personius BE, Michalek JE, Maranian AM, Kolasa MW, Monick E, Brown BG and Gotto AM, Jr. (2005) A randomized trial of a strategy for increasing high-density lipoprotein cholesterol levels: effects on progression of coronary heart disease and clinical events. *Annals of internal medicine* **142**:95-104.

Wise A, Foord SM, Fraser NJ, Barnes AA, Elshourbagy N, Eilert M, Ignar DM, Murdock PR, Steplewski K, Green A, Brown AJ, Dowell SJ, Szekeres PG, Hassall DG, Marshall FH, Wilson S and Pike NB (2003) Molecular identification of high and low affinity receptors for nicotinic acid. *The Journal of biological chemistry* **278**:9869-9874.

Wu BJ, Chen K, Barter PJ and Rye KA (2012) Niacin inhibits vascular inflammation via the induction of heme oxygenase-1. *Circulation* **125**:150-158.

Wu KL, Chao YM, Tsay SJ, Chen CH, Chan SH, Dovinova I and Chan JY (2014) Role of nitric oxide synthase uncoupling at rostral ventrolateral medulla in redox-sensitive hypertension associated with metabolic syndrome. *Hypertension* **64**:815-824.

Yang EJ, Kim GS, Jun M and Song KS (2014) Kaempferol attenuates the glutamate-induced oxidative stress in mouse-derived hippocampal neuronal HT22 cells. *Food & function* **7**:1395-1402.

Yoshitaka H (2008) Role of reactive oxygen species in brainstem in neural mechanisms of hypertension. *Autonomic Neuroscience* **142**:20-24.

Zanzinger J (2002) Mechanisms of action of nitric oxide in the brain stem: role of oxidative stress. *Autonomic neuroscience : basic & clinical* **98**:24-27.

Zhang J and Abdel-Rahman AA (2002a) The hypotensive action of rilmenidine is dependent on functional N-methyl-D-aspartate receptor in the rostral ventrolateral medulla of conscious

spontaneously hypertensive rats. *The Journal of pharmacology and experimental therapeutics* **303**:204-210.

Zhang J and Abdel-Rahman AA (2002b) The Hypotensive Action of Rilmenidine is Dependent on FunctionalN-Methyl-d-aspartate Receptor in the Rostral Ventrolateral Medulla of Conscious Spontaneously Hypertensive Rats. *Journal of Pharmacology and Experimental Therapeutics* **303**:204-210.

Zhang J and Abdel-Rahman AA (2005) Mitogen-activated protein kinase phosphorylation in the rostral ventrolateral medulla plays a key role in imidazoline (i1)-receptor-mediated hypotension. *The Journal of pharmacology and experimental therapeutics* **314**:945-952.

Zhang J and Abdel-Rahman AA (2008) Inhibition of nischarin expression attenuates rilmenidine-evoked hypotension and phosphorylated extracellular signal-regulated kinase 1/2 production in the rostral ventrolateral medulla of rats. *The Journal of pharmacology and experimental therapeutics* **324**:72-78.

Zhang J, El-Mas MM and Abdel-Rahman AA (2001) Imidazoline I(1) receptor-induced activation of phosphatidylcholine-specific phospholipase C elicits mitogen-activated protein kinase phosphorylation in PC12 cells. *European journal of pharmacology* **415**:117-125.

Zhang Y, Schmidt RJ, Foxworthy P, Emkey R, Oler JK, Large TH, Wang H, Su EW, Mosior MK, Eacho PI and Cao G (2005) Niacin mediates lipolysis in adipose tissue through its

G-protein coupled receptor HM74A. *Biochemical and biophysical research communications* **334**:729-732.

Zhang ZH, Yu Y, Wei SG, Nakamura Y, Nakamura K and Felder RB (2011) EP(3) receptors mediate PGE(2)-induced hypothalamic paraventricular nucleus excitation and sympathetic activation. *American journal of physiology Heart and circulatory physiology* **301**:H1559-1569.

Zimmerman MC, Lazartigues E, Sharma RV and Davisson RL (2004) Hypertension caused by angiotensin II infusion involves increased superoxide production in the central nervous system. *Circulation research* **95**:210-216.

Zucker IH and Gao L (2005) The regulation of sympathetic nerve activity by angiotensin II involves reactive oxygen species and MAPK. *Circulation research* **97**:737-739.

APPENDIX

ANIMAL CARE AND USE COMMITTEE APPROVAL LETTER

East Carolina University

'mal Care and Commitee
212 Ed Warren Life Sciences Building
East Carolina University
Greenville, NC 27834

252-744-2436 office
252-744-2355 fax

June 24, 2013

Abdel Abdel-Rahman, Ph.D.
Department of Pharmacology
Brody 6S-10
ECU School of Medicine

Dear Dr. Abdel-Rahman:

Your Animal Use Protocol entitled, "Mechanisms of Estrogen-Dependent Cardiovascular Effects of Alcohol" (AUP #W237) was reviewed by this institution's Animal Care and Use Committee on 6/24/13. The following action was taken by the Committee:

"Approved as submitted"

Please contact Dale Aycock at 744-2997 prior to hazard use

A copy is enclosed for your laboratory files. Please be reminded that all animal procedures must be conducted as described in the approved Animal Use Protocol. Modifications of these procedures cannot be performed without prior approval of the ACUC. The Animal Welfare Act and Public Health Service Guidelines require the ACUC to suspend activities not in accordance with approved procedures and report such activities to the responsible University Official (Vice Chancellor for Health Sciences or Vice Chancellor for Academic Affairs) and appropriate federal Agencies.

Sincerely yours,

Susan McRae, Ph.D.
Chair, Animal Care and Use Committee

SM/jd

enclosure